

# UNESCO-IHE INSTITUTE FOR WATER EDUCATION



## Potassium recovery from source separated urine

**Davis M. Murunga**

MSc Thesis (ES-EST 11.29)  
April 2011



# **Potassium recovery from source separated urine**

Master of Science Thesis  
by  
**Davis M. Murunga**

Supervisors  
**Prof. Piet Lens (UNESCO-IHE)**  
**Dr. Mariska Ronteltap (UNESCO-IHE)**

Examination committee  
**Prof. Piet Lens (UNESCO-IHE)**  
**Dr. Mariska Ronteltap (UNESCO-IHE)**  
**Philipp Kuntke (Wetsus Institute)**

This research is done for the partial fulfilment of requirements for the Master of Science degree at the UNESCO-IHE Institute for Water Education, Delft, the Netherlands

**Delft**  
**April 2011**

The findings, interpretations and conclusions expressed in this study do neither necessarily reflect the views of the UNESCO-IHE Institute for Water Education, nor of the individual members of the MSc committee, nor of their respective employers.

## **DEDICATION**

This thesis is dedicated to all scientists with the interest in sustainable management of waste resources

## Abstract

Potassium is a significant natural resource required by plants and animals. Its extraction has possible adverse environmental effects. Human urine is a key potassium source and source separation could significantly improve waste water effluent quality. In domestic waste water, potassium is 60% of urine.

The main objective was to determine the potassium recovery potential from recipes of artificial human urine that is assumed to have undergone four treatment processes, namely; hydrolysis, sharon-anammox, nitrification and struvite precipitation.

This was achieved through use of two techniques; adsorption and precipitation. Zeolites were used as adsorbents in each of the solutions from the four treatment processes. For precipitation experiments, magnesium and potassium were added in equal ratios to potassium in the respective solution in order to precipitate potassium struvite. The precipitation experiments were also simulated by PHREEQC (Version 2) model to determine the key species involved in each of the treatment stream during precipitation process.

In precipitation, the sharon-anammox stream gave the overall highest recovery of potassium, with at least 55% recovery for all its sub-stream experiments. The struvite and hydrolysis streams gave the lowest potassium recovery, with hydrolysis stream having an average of 44% while struvite had an average of 46%.

Similarly, in adsorption experiments, sharon-anammox stream had the best output. Using Langmuir adsorption model in experiment 3, it had an equilibrium adsorption constant ( $b$ ) value of 72.22 litres per gram, with monolayer adsorption capacity ( $q_m$ ) of 0.0086 grams per gram of zeolite ( $R^2=0.703$ ). More so, with Freundlich model the stream it had an adsorption capacity ( $K$ ) of 0.0095 ( $R^2= 0.63$ ). The value of the Freundlich parameter,  $n$  which was computed as 7.41 was found to be between 1 and 10 which indicates a favourable adsorption.

*Keywords:* recovery, adsorption, precipitation

## **Acknowledgements**

I wish to thank the almighty God for the opportunity to undertake this work.

I would also thank my supervisors; Prof. Piet Lens, Dr.Mariska Ronteltap and Philipp Kuntke for the guidance and support during this research period .I also want to extend my gratitude to Wetsus Institute for allowing me to carry out my experiments and analysis in their facilities.

I also would like to thank the entire community of UNESCO-IHE for the support accorded to me during this research period.

## TABLE OF CONTENTS

Abstract.....	i
Acknowledgements .....	ii
List of Abbreviations .....	vi
<b>1.0 INTRODUCTION.....</b>	<b>1</b>
1.1 Background information.....	1
1.2 Problem statement .....	2
1.3 Justification of the study.....	2
1.4 Objectives .....	3
1.5 Research questions .....	3
1.6 Significance of the research.....	3
1.7 Scope of this research .....	4
<b>2.0 LITERATURE REVIEW.....</b>	<b>5</b>
2.1 Introduction .....	5
2.2 Potassium.....	5
2.3 Human Urine .....	6
2.4. Potassium struvite precipitation from urine .....	8
2.4.1 Factors affecting struvite precipitation .....	9
2.4.2 Sources of struvite components .....	10
2.4.3 Crystallization.....	10
2.4.4 Conditional solubility .....	15
2.5 Treatment processes for source separated urine .....	16
The struvite stream has no big difference in ammonia concentration from the hydrolysis stream as only about 3% of ammonium is removed (Maurer, <i>et al.</i> , 2006).....	20
2.6 Adsorption .....	20
<b>3.0 MATERIALS AND METHODS .....</b>	<b>27</b>
3.1) Derivation of Synthetic urine recipes.....	27
3.2) Adsorption experiments .....	30
3.3 Precipitation experiments .....	34
<b>4.0 RESULTS AND DISCUSSION .....</b>	<b>38</b>
4.2. Adsorption results.....	39
4.1.1 Results for batch adsorption experiments (1) using zeolites (2-3.15mm)....	39
4.1.2 Results for batch adsorption experiment (2) using zeolites (1-1.2mm) .....	39
4.1.3 Results for adsorption batch experiment (3).....	40
4.2 Precipitation results .....	40
4.3 Analysis and Discussion.....	43
4.3.1 Batch adsorption experiment (2) using zeolites (1-1.2 mm) .....	43
4.3.2 Batch adsorption for experiment (3) using zeolites (2-3.15mm).....	47
4.3.3 Precipitation.....	50
4.3.4 Summary of discussion.....	58
4.3.4.5 <i>Comparison of Sodium and Potassium adsorption in the Batch adsorption experiment (3) for 2-3.15 mm zeolites</i> .....	60
4.3.5 Limitations encountered in the experiments.....	61
<b>5.0 RECOMMENDATIONS AND CONCLUSION.....</b>	<b>62</b>

<b>REFERENCE .....</b>	<b>64</b>
<b>APPENDICES .....</b>	<b>70</b>
Appendix 1 .....	70
Appendix 2 Langmuir and Freundlich components for batch adsorption experiments (2) using zeolites (1-1.2mm).....	70
Hydrolysis.....	71
Sharon-anammox.....	71
Nitrification .....	72
Struvite .....	73
Appendix 3 Langmuir and Freundlich components for batch adsorption experiments (3) using zeolites (2-3.15mm).....	74
Sharon-anammox.....	74
Nitrification .....	75
Hydrolysis.....	76
Struvite .....	76
Appendix 4 The Kinetic results of urine streams for batch adsorption experiment (1) using Zeolites (2-3.15mm) .....	78
Appendix 5 The comparison of changes in concentration of potassium with sodium in the batch experiment 3 for (2-3.15 mm zeolites).....	80
Appendix 6 Codes used in the synthetic urine treatment schemes.....	81
Appendix 7 The stoichiometric equations from Griffith et al., (1976) recipe.....	81
Appendix 8 EDX Analysis Tables.....	84

**LIST OF FIGURES**

Figure 2.1 Crystal structure of Potassium struvite .....	8
Figure 2.2 The influence of supersaturation on nucleation and growth. ....	11
Figure 2.3 A process scheme for nucleation and crystal growth.....	13
Figure 2.4: The adsorption mechanism .....	21
Figure 2.5 SEM EDX Analysis of Untreated zeolite .....	25
Figure 2.6 SEM EDX Analysis of treated zeolite .....	26
Figure 3.1 Derived treatment scheme of urine .....	28
Figure 3.2 Zeolites (2-3.15) mm.....	31
Figure 3.3 Zeolites (1-1.2) mm.....	31
Figure 3.4 Batch adsorption set up .....	32
Figure 3.5 Atomic emission spectrometer (Model: Perkin-Elmer AAnalyst 200).....	34
Figure 3.6 Precipitation set-up.....	35
Figure 3.7 IC Machine (Model: Dionex ICS-1000 ION Chromatography system).....	36
Figure 4.1 Adsorption kinetics for experiment 2 with zeolites (1-1.2mm) .....	45
Figure 4.2 The Langmuir and Freundlich isotherm for experiment 2 (with 1-1.2 mm zeolites).....	46
Figure 4.3 The Langmuir isotherms for experiment 3 (using 2-3.15 mm of zeolite).....	49
Figure 4.4 The Freundlich isotherms for experiment 3 (using 1-1.2 mm of zeolite) .....	50
Figure 4.5 The concentration of potassium, phosphates and magnesium in the nitrification filtrate stream .....	51
Figure 4.6 The concentration of nitrates in the filtrate of nitrification stream .....	52

Figure 4.7 The concentration of potassium, phosphates, and magnesium in the filtrate	53
Figure 4.8 The concentration of phosphates, magnesium and potassium in precipitation filtrate .....	55
Figure 4.9 The concentration of potassium, phosphates and magnesium in the filtrate.	57
Figure 5.1 Proposed scheme for adsorption and precipitation .....	63

## LIST OF TABLES

Table 2.1 Characteristics of atoms and ions of Group 1A elements .....	6
Table 2.2: Reference values for fresh and stored urine. ....	6
Table 2.3 Thermodynamic equilibria and their governing equations.....	14
Table 2.4 Complexes of Phosphate species in hydrolyzed urine .....	17
Table 2.5 Parameters of aerobic and anaerobic ammonia oxidation.....	19
Table 2. 6: Type of isotherm and favorability of adsorption processes for various $R_L$ values. ....	23
Table 3.1 The formulation of synthetic urine by Griffith et al. (1976) .....	27
Table 3.2 Summary of chemicals used and their concentrations .....	30
Table 3.3 The pH of diluted synthetic urine streams.....	33
Table 3.4 Characteristics of prepared synthetic urine streams .....	34
Table 3.5 The ratios of magnesium chloride and sodium mono phosphate used for precipitation experiments in the four streams .....	37
Table 4.1 The summary of expected concentrations of individual ions that are actively involved in the four treatment processes.....	38
Table 4.2 Percentage adsorption and desorption for 10 g zeolite mass(1-1.2 mm) in experiment 2.....	39
Table 4.3 Potassium recovery from batch adsorption experiment (3) using zeolites of sizes 2-3.15 mm .....	40
Table 4.4 The concentrations of potassium, phosphates and magnesium in the filtrates	41
Table 4.5 The nitrate concentration recovery from nitrification stream.....	42
Table 4.6 Combined Langmuir and Freundlich isotherms for experiments (1),(2) and (3) .....	43
Table 4.7 The pH and Electrical conductivity of the solution streams.....	51
Table 4.8 Changes in concentration of Potassium and Sodium during the adsorption in experiment 3 with zeolites (2-3.15mm) .....	61

## List of Abbreviations

AES	Atomic emission spectrometer
UNDP	United Nations Development Programme
UNEP	United Nations Environmental Programme
IFA	International Fertilizer Industry
ANAMMOX	Anaerobic ammonia oxidation
MAP	Magnesium ammonium phosphate
ICP	Inductively Coupled Plasma
WHO	World Health Organisation
FAO	Food and Agriculture organisation

# 1.0 INTRODUCTION

## 1.1 Background information

Among the key target of millennium development goals (1) and (7), are to eradicate extreme hunger , integrate sustainable development into country policies and to reverse the loss of environmental resource(UNDP,2010).In addition, besides the economic turmoil that has hit many developing and some developed nations, the demand for food and clean water is increasingly growing(FAO,2009).

Therefore, the scale of natural resource consumption, such as minerals and agricultural land, makes environmental impact an increasingly important issue against which human activities must be gained(UNEP;IFA,2001).This further initiated sustainable development as a concepts suggested by UNEP and IFA (2001) to be addressed in enhancing the efficient use of natural resources. This concept integrates economic, environmental and social considerations with the aim of improving lives of present generation while ensuring the future generations have adequate resources (UNEP; IFA, 2001).

Sustainable development requires maintenance, rational use and enhancement of natural resources, which also considers balancing the interests of ecology, economy and social justice (Wellmer and Becker-Platen, 2002).According to Roosa (2008), there is credible evidence that natural resources, such as phosphorus, are limited and can become exhausted. He further says that environmental, scientific and governmental entities are now focusing on understanding of environmental processes and their sustainability impact.

A key pillar in sustainable development is the development of Agenda 21 which stipulates attention to demand for natural resources generated by unsustainable consumption and efficient use of those resources, consistent with the goal of minimizing depletion and reducing pollution (United Nations, 2002).

Similarly, according to the *Kentucky energy watch (2006)*, the environmental concerns are significantly linked to sustainable development. This clearly reflects the need to reuse and recycle natural resources for the benefit of the environment.

In particular cases, more focus has been given to reduction of nutrient losses from soils in the agricultural sector, as opposed to recycling of nutrients excreted as urine. Recycling safely of urine can improve agricultural production through production of fertilizer (struvite). However, most farmers in the developing countries are unaware of possibilities of re-use of human excreta (Sustainable sanitation practice, 2010).

Recently, the production of struvite from urine commenced and currently research is progressing on the same. Wilsenach *et al.* (2007) reports that two forms of struvite can be successfully formed; magnesium ammonium phosphate and magnesium potassium phosphate. The latter is considered as a valuable source for potassium recovery.

Potassium is significant natural resource which is required by plants and cannot be substituted (Wellmer and Becker-platen, 2002).It is an essential element for sustenance of fundamental cell functions in Plants and animals. It regulates the opening and closing of stomata in plants, which is a process driven by the osmotic potential and turgor of the guard cells .To add on, potassium, contributes to the plant tissue structure through its effect on turgor and cell extension (Rangel, 2008).

Moreover, other key roles of Potassium in plants are in the uptake of nitrogenous compounds and in photosynthesis (Rangel, 2008). In line with this, Rangel (2008) proposes a balanced uptake of potassium for maintenance and development.

In the context of ecological sanitation it is safe to recover nutrients from human excreta, and recycle them back into the environment in productive systems. This is because human excreta contain valuable resources for food production. (Esrey *et al.*, 2001)

The separate collection of the urine can enhance a favourable treatment method to the specific composition and need for treatment (Vinnerås, 2001), which depends upon the use of the treated material, as well as the need to protect the environment from pollution. More studies shows that urine contains most of the plant nutrients in household waste. Thus, in source separating systems, the less polluted and nutrient-rich urine can be sanitized by a relatively simple and inexpensive treatment, such as storage, to ensure safe sanitation (Schönning and Stenstrom, 2004; WHO, 2006).

## **1.2 Problem statement**

Potassium bearing rocks are mined from salt lakes, brines and underground ore deposits (Eatock, 1985). These extraction activities have possible adverse environmental effects which greatly depend on the type of ore, the land profile, ecosystem and prevailing climatic conditions (UNEP and IFA, 2001).

Extraction activities affect the growth of local biodiversity due to excavation of large pits and therefore have an impact on the landscape.

Mining also affects water resources by contamination through salt release from ore, the weathering of ores, and slurry brine release. Also, there will be a risk of overconsumption of the ground water resources hence lowering the surrounding ground water table. Another possible key impact is air pollution where dust particulates are generated through the blasting and excavation methods of extraction (UNEP; IFA, 2001).

On a different perspective, it has been reported, that human urine contains higher concentrations of sodium chloride, urea, phosphate and potassium, and trace elements of calcium, sulphate and magnesium (Larsen and Gujer, 1996). The authors further elaborates that less than 1% volume of municipal water constitutes urine, but this contributes to about 90% of Potassium in waste water. Moreover, Wilsenach and Van Loosdrecht (2003) suggested that source separation of urine could significantly improve effluent quality, reduce energy and investment costs and enhance effective recovery and circulation of nutrients.

Finally, considering disposal of untreated urine may pose greater health risks than its re-use such that nutrients in urine can contaminate both surface and groundwater (Esrey *et al.*, 2001), it is clear that resource recovery is essential in reduction of pollution and enclosing the nutrient cycle loop.

## **1.3 Justification of the study**

The fate of potassium is mostly not involved in debate on minerals because; it is not considered a pollutant in surface waters, and the perceived scarcity of potassium is less severe than that of phosphate (Henze *et al.*, 1997).

Contrary to this, Ganrot *et al.* (2007), argues that sustainable development in wastewater management includes not only nutrient recovery, but also recycling of recovered nutrients.

Moreover, municipal wastewater is a major source for key agricultural nutrients; nitrogen, phosphorus and potassium, and holds about 50-90% of the said elements (Maurer *et al.*, 2003).

Ganrot *et al.* (2007) also, quantifies Potassium to be 60% of urine in domestic waste water. Besides that, the author further says that, resource recovery is more efficient in urine separating systems than conventional systems. Similarly, Lind *et al.* (2001) says that urine separation ideas have been proposed for achievement of maximum recovery of nutrients. Concentrated streams are favorable because of lower pathogen survival rate (Hoglund, 2001), and reduction of costs in the need for advanced nutrient removal from waste water (Wilsenach *et al.*, 2007).

It is in this view that this study is intended to undertake a research of recovery of potassium from source separated urine.

#### **1.4 Objectives**

This research will aim at potassium recovery from urine after four treatment processes, namely, storage, anammox, nitrification, and struvite precipitation.

The main objectives of this study are;

- To determine composition recipes of synthetic urine after four different treatment processes
- To find out the potassium recovery potential of the composition from derived recipes.

The specific objectives are;

- To determine the ionic composition of the synthetic urine after the four treatment processes
- To determine the physico-chemical parameters of the treated synthetic urine.
- To determine the constituent ionic species from recovered potassium struvite.
- To evaluate the potassium recovery potential using adsorption and precipitation techniques

#### **1.5 Research questions**

In order to achieve the above mentioned objectives, the following research questions were formulated;

- What are the ionic compositions of synthetic urine after the four treatment processes?
- What are the physico-chemical conditions of each treated synthetic urine process?
- Which recovery techniques are applicable to potassium recovery from synthetic urine?
- In which form is potassium recoverable from urine after the four processes?

#### **1.6 Significance of the research**

This research will be a contribution to sources of knowledge and information as a base for reference or development on potassium recovery research.

### **1.7 Scope of this research**

This research will focus on potential strategies on Potassium struvite recovery from synthetic urine and possibly human urine.

## 2.0 LITERATURE REVIEW

This chapter provides a general review of literature on potassium, human urine and the treatment processes and mechanisms in potassium recovery.

### 2.1 Introduction

In source-separated urine, precipitation is the only process that may significantly affect the potassium concentration. Potassium is known to be incorporated in struvite as well as in hydroxyapatite (Udert *et al*, 2006).

However, in source-separated urine the molar concentration of ammonia and ammonium is nearly fivefold higher than the potassium concentration. Therefore, a possible assumption would be only a relatively small amount of ammonium is replaced by potassium. In the completely hypothetical case that all ammonium in struvite would be substituted by potassium, the loss of soluble potassium would be less than 7% (Udert *et al*, 2006).

### 2.2 Potassium

Potassium is a silvery white metal with a cut surface is oxidized in dry air forming a dark grey superoxide. It belongs to the alkali metals. It is the eighth most abundant element and occurs as salt deposits formed by evaporation of ancient lakes and sea bed. Its main minerals are carnallite ( $\text{KMgCl}_3 \cdot 6\text{H}_2\text{O}$ ), Polyhalite ( $\text{K}_2\text{MgCa}_2[\text{SO}_4]_4 \cdot 2\text{H}_2\text{O}$ ), Langbeinite ( $\text{K}_2\text{Mg}_2[\text{SO}_4]_3$ ), Kainite ( $\text{KMg}[\text{ClSO}_4]_4 \cdot 11\text{H}_2\text{O}$ ) (Ferro and Saccone, 2008).

The atomic number and mass for potassium are 19 and 40 respectively. Its ion has a valency of 1, and oxidation state of 1. Its atomic structure is  $[\text{Ar}]4s^1$ . It has a specific density of  $0.862 \text{ g/cm}^3$ ; Melting point of  $63.25^\circ\text{C}$ , and boiling point of  $760^\circ\text{C}$  (Krebs, 2006).

The reactivity of potassium is owed to the greater distance between its nuclei and the outer valence electrons, and hence it combines readily with many elements. More so, the salts of quaternary ammonium cations, such as the ammonium ion, exhibit similar characteristics to heavier alkali metals. It follows that the properties of ammonium salts are similar to corresponding potassium salts (King, 1995).

The main difference between ammonium chemistry and that of the alkali metal salts is the relative ease with which ammonium decomposes to release ammonia. This is possible by warming aqueous solutions with alkali (Massey, 2000).

The alkali metals completely ionize in aqueous solution forming few stable complexes in aqueous media.

The variations in their properties are apparent in their solid state. Some typical properties change in the order;

$\text{Li} > \text{Na} > \text{K} > \text{Rb} > \text{Cs}$ .

This includes ease of thermal decomposition of compounds containing polyatomic anions, such as carbonates, hydroxides and nitrates (Massey, 2000).

Sodium ions are relatively in high concentrations in urine. This, apart from the high concentrations of ammonium ions, clearly interferes with the adsorption process of the

zeolite, behaving as a competitor (Dorfner, 1991). It is known that the presence of sodium ion can decrease the capacity of the zeolite by up to 50 % (Cooney and Booker, 1999). The atomic and ionic radii of sodium are smaller than that of Potassium and it could gain more access to the adsorption sites through the apertures (House and House, 2010).

**Table 2.1 Characteristics of atoms and ions of Group 1A elements**

Metal	Radii of atom(Pm)	Radii of ion(Pm)	M-M bond energy (Kj/mole)	-ΔHydration (Kj/mole)
Sodium (Na)	186	95	73	406
Potassium(K)	227	133	49.9	418

Source: House and House (2010)

## 2.3 Human Urine

Human excreta consist of faeces and urine which are waste products of the normal biological metabolism. The characteristics of urine depend on the health conditions of the person excreting it and the consumption patterns (Lentner *et al.*, 1981).

.Lind *et al.* ,(2000), elaborated on the composition of human urine as a complex aqueous solution containing urea as a dominant compound, apart from sodium chloride, and potassium, calcium, sulphate and phosphate . More so, Potassium exists in urine as an ionic component ( $K^+$ ).

The following table shows the concentrations of different constituents in fresh urine from literature values compiled from various sources by Udert *et al.* (2006).

**Table 2.2: Reference values for fresh and stored urine.**

The concentrations in fresh urine are literature values compiled from various sources. The concentrations in stored urine are simulated values.

	Units	Fresh urine			Stored urine
		Average	CV%	Data range	
Total nitrogen	[gN/m <sup>3</sup> ]	9200	20	-	9200
Total Ammonia	[gN/m <sup>3</sup> ]	480	29	-	8100
Ammonia NH <sub>3</sub>	[gN/m <sup>3</sup> ]	0.3	-	-	2700
Urea	[gN/m <sup>3</sup> ]	7700	20	-	0
Total phosphate	[gP/m <sup>3</sup> ]	740	14	-	540
Calcium	[g/m <sup>3</sup> ]	190	22	-	0
Magnesium	[g/m <sup>3</sup> ]	100	21	-	0

Potassium	[g/m <sup>3</sup> ]	2200	-	1300-3100	2200
Total carbonate	[gC/m <sup>3</sup> ]	0	-	-	3200
Sulphate	[gSO <sub>4</sub> /m <sup>3</sup> ]	1500	29	-	1500
Chloride	[g/m <sup>3</sup> ]	3800	-	2300-7700	3800
Sodium	[g/m <sup>3</sup> ]	2600	-	1800 - 5800	2600
pH		6.2	8	-	9.1
Alkalinity	[mM]	22	-	-	490
COD	[gO <sub>2</sub> /m <sup>3</sup> ]	10000	4000	-	10000
Volume	(lt)	1.25	0.61	-	1.25

Source: Udert *et al.*, (2006)

The potassium concentrations in the above table 1 are considerably high enough as compared to calcium and magnesium. This provides an opportunity for sustainable management of nutrients from source separated urine (Maurer *et al.*, 2003).

The quality of Urine as a fertilizer also has to be examined. It has several disadvantages such; strong smell, large storage space, bulky to transport, volatilization of ammonia, and presence of contaminants. By source separation of urine, these problems can be dealt with by enhancing better technologies for nutrient removal such as nitrification (Maurer *et al.*, 2006).

On the other hand, struvite is odourless, dense, compact, convenient to transport and it is consistent in nutrient content (Wilsenach, *et al.*, 2007). Natural zeolites have been used for adsorption and extraction of ammonium from municipal and agricultural waste streams. More so, the zeolites have a higher selectivity for potassium than ammonium (Ames, 1960), and hence provide a convenient option for potassium recovery.

In source separated urine therefore, potassium could be recovered after treatment of urine to acceptable quality for recovery. In this study, the four streams identified were designed through a representative synthetic urine recipe developed by Griffith *et al.* (1976).

Griffith's recipe (Table 3.1) is predominantly used by researchers. It is based on recommendable work of Robertson *et al.* (1968) who derived using data from 60 healthy and 60 stone affected men to determine the representative values (Tilley, 2006).

In this recipe, the phosphate concentration was increased by 50% to be more representative of recent studies (Wilsenach *et al.*, 2007).

Ganrot *et al.* (2005) reported that almost 22-64% of potassium can be recovered in struvite MAP. The author further says that struvite MAP is not a pure end member. This could offer several advantages including possibility of recovering many essential elements from urine. However, struvite (MAP) is a product which recovers a small fraction of the ammonium and a larger fraction of the phosphates in solid form (Maurer *et al.*, 2006). This requires a large amount of phosphorus and magnesium resources in order to also increase recovery of ammonium.

The three other treatment processes; nitrification, sharon-anammox and hydrolysis are largely aided by micro-organisms. Nitrification was among the conventional biological nutrient removal processes aimed at elimination of nitrogen in low strength wastewaters. The sharon-anammox is a more recent innovation for achieving improved nitrogen removal from waste streams (Ahn, 2006).

The hydrolysis on the other hand, is a treatment process that occurs voluntarily once fresh urine gets in contact with air and proceeds to completion (Liu *et al.*, 2008)

## 2.4. Potassium struvite precipitation from urine

Potassium struvite mineral has been discovered at two different localities. First, at Lengebach in Binntal, Switzerland in a dolomitic rock of Triassic age. The second locality is Rossblei, Schladminger tavern in Austria in an abandoned galena mine. It occurs as aggregates which represent close intergrowths of fine grained potassium struvite (Graeser *et al.*, 2008).

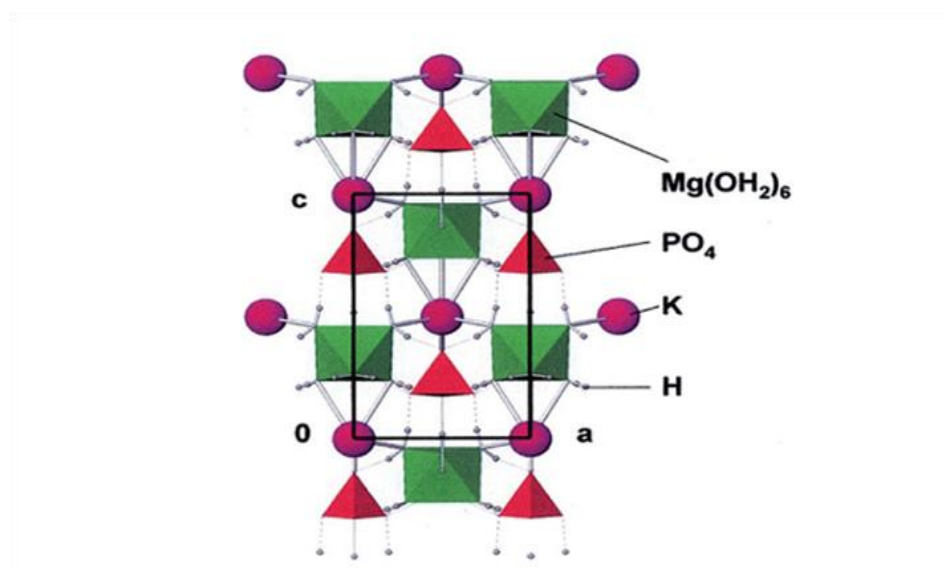
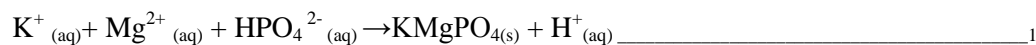


**Figure 2.1 Crystal structure of Potassium struvite**

*Source: Graeser et al. (2008)*

Wilsenach *et al.*, (2007) reported the molar ratio  $\text{NH}_4^+$ : K: P: Mg in urine as 260: 13: 16: 1. The authors, further suggest that complete ammonium oxidation, or nitrogen removal from urine, potassium struvite could be precipitated. Moreover, the authors reported pH differences between ammonium struvite and potassium struvite. For potassium struvite, the pH decreased with increasing phosphate removal while for Ammonium struvite the pH increased with increasing phosphate removal. They authors attributed this reaction according to the following equation, where hydrogen ions are produced thereby reducing the pH;



Crystallization is frequently used separation process especially in the organic chemical industry. The crystallization system is fed with a solution from which the solute is precipitated (Rousseau, 1987).

## 2.4.1 Factors affecting struvite precipitation

### 2.4.1.1 pH

This is an important factor that influences the solubility and supersaturation. Generally, pH increases, reduces the solubility of struvite. It therefore controls greatly the rate of precipitation. Several authors have studied the crystallization range of struvite. Bouropoulos and Koutsoukos (2000), found out a range of pH between 9 and 10, with the optimum being 9.5.

The pH also is determined by concentration of constituent elements. Ammonia forms an equilibrium with ammonium ions which acts as a buffer capacity that controls the pH, with  $pK_A$  of 9.3 (Ronteltap *et al.*, 2007).

Stratful *et al* (2001), found that at pH levels, below 10, the struvite yields were affected. This is because gradual reduction of pH as struvite forms. Despite that, the authors report that pH 7.5 marked the onset of struvite precipitation, and as it increased to 8.5, 92% of magnesium and 85% of phosphorus were recovered.

### 2.4.1.2 Supersaturation ratio

Supersaturation influences the ionic activity of a solution. Le Corre (2006) reported that at fixed pH, the super saturation level of solution affect the crystallization process, specifically the induction time. Furthermore, it also influences the rate of formation of struvite crystals.

Bouropoulos and Koutsoukos (2000) added on, that, spontaneous formation of struvite in supersaturated solutions suggests the influence of solution supersaturation apart from the solution pH.

### 2.4.1.3 Temperature

Temperature as a factor has lower impact than pH and supersaturation. It increases the solubility of struvite and affects the crystal growth and morphology (Le Corre, 2006).

### 2.4.1.4 Mixing energy/turbulence

Turbulence is also a factor that can affect precipitation. High turbulence can cause, increase in pH because of carbon dioxide liberation (Le Corre, 2006).

Ohlinger *et al.* (1999) demonstrated the influence of different mixing energy on struvite crystal size and shape. The authors found high growth rates in high mixing zones in their experiments.

### 2.4.1.5 Presence of foreign ions

A solution with impurities could cause the blocking of potential crystal growth sites, which inhibits crystal growth (Jones, 2002). It has also been reported that the presence of calcium and carbonate species, could influence the growth of struvite which can in turn increase the induction time (Koutsoukos *et al.*, 2003).

The precipitation process could possibly be affected by other ion interactions depending with the relative concentrations. Interactions of other ions in solution lead to an increase in solubility. In determination of the ionic strength, Davies approximation of Debye-Hückel equation is normally used for the calculation of activity coefficients (Doyle and Parsons, 2002).

Magnesium ions form complexes (hydro complexes and magnesium phosphate complexes) which always remain in solution and are responsible for reducing the struvite formation potential.

On the other hand, Sodium hydrogen diphosphate and sodium polyphosphate are known to be potential inhibitors of struvite formation by seizing the magnesium making it unavailable for struvite precipitation. (Doyle and Parsons, 2002)

## **2.4.2 Sources of struvite components**

The increasing scarcity of non-renewable resources such as phosphorus, their recovery will be an important consideration for the future generations. The key inputs are phosphorus and magnesium. There are alternative possible sources for phosphorus and magnesium which can be of use for struvite recovery:

### **2.4.2.1 Phosphorus**

The phosphorus in urine offers an opportunity for recovery. Phosphorus can be sourced in domestic sewage, phosphorus is in the form of bio-available orthophosphates (phosphates, monohydrogen phosphates, and dihydrogen phosphates) (Doyle and Parsons, 2002). Balmer (2004) also suggests that toilet wastes, urine, wastewater sludge, incinerated sludge, and wastewater have been examined as potential phosphorus sources.

### **2.4.2.2 Magnesium**

There are possible alternative non-commercial sources from hard water environment, the coastal and sea waters. The clay minerals can also be another which is capable of releasing part of their structural components. More so, some industrial discharges contain some magnesium sources. But this is a viable option if the magnesium can be feasibly separated for re-use (Doyle and Parsons, 2002).

## **2.4.3 Crystallization**

The crystal size distributions are influenced by nucleation and growth. The main factor behind them is supersaturation, whereby in some cases both nucleation and growth do occur as a resulting in competition for available solute (Rousseau, 1987).

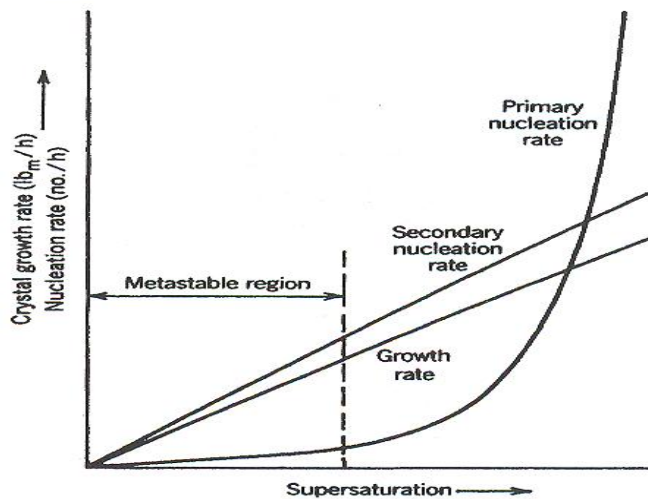


**Figure 2.2**The influence of supersaturation on nucleation and growth.

Source: Rousseau, R.W. (1987)

In figure 1, the growth rate and secondary nucleation kinetics are linear functions of supersaturation. Primary nucleation has a high order dependence on supersaturation. Supersaturation describes a state of a solution where the solute concentration is higher than the equilibrium concentration.

This process normally leads to precipitation. Potassium struvite contains three ions and its solute concentration is defined by Ion activity product (IAP) (Galbraith and Schneider, 2009).

$$IAP = \{Mg^{2+}\}\{K^+\}\{PO_4^{3-}\} \dots \dots \dots 2$$

The system is supersaturated if the Ion activity product (IAP) is higher than the minimum solubility product ( $K_{so}$ ). This may result to nucleation and growth which returns the system to equilibrium.

### 2.4.3.1 Nucleation

This is defined as the formation of a solid phase from liquid phase. In this case new crystal formation results from the transfer of solute from liquid to solid phase. The mechanisms involved are primary and secondary nucleation (Rousseau, 1987).

Struvite precipitation can be categorized into; nucleation and growth. Nucleation involves formation of crystal embryos by constituent ions, whereas growth follows nucleation until equilibrium is achieved (Doyle and Parsons, 2002). Nucleation is a transition stages from which spontaneous growth of new centres originate. This results in material deposit on the nuclei forming large crystals through a process known as ripening (Stumm and Morgan, 1996).

The process is controlled by temperature, supersaturation degree, pH, and availability of other influencing ions in the solution. However its solubility decreases with increase in

temperature, and also pH, which in turn increases precipitation potential (Doyle and Parsons, 2002).

### Primary nucleation

This is based on both homogeneous and heterogeneous mechanisms which results to crystal formation in sequences that combine constituent units which form a crystal. One important aspect of this mechanism is that the existing crystals in the unit are not involved in the nucleation process. The nucleation process in homogenous mechanism is spontaneous and is as a result of supersaturation, while for heterogeneous is stimulated by foreign matter in a super saturated liquid. Both the homogenous and heterogeneous mechanisms require super saturation conditions (Rousseau, 1987).

The mechanism of primary nucleation is expressed as;

$$B^0 = A \exp. \left[ - \frac{(16\pi\sigma^3 v^2)}{(3K^3 T^3 s^2)} \right]$$

Where  $B^0$  is the nucleation rate,  $K$  is the Boltzmann constant,  $\sigma$  is surface energy per unit area,  $v$  the molar volume,  $A$  is a constant, and  $s$  is the supersaturation. More so, supersaturation can be defined in several ways (Rousseau, 1987);

- The difference between the solute and equilibrium concentrations,  $C - C^*$
- The difference between the system temperature and the temperature at equilibrium,  $T - T^*$
- The ratio of the solute concentration and the equilibrium concentration,  $C / C^*$
- The ratio of the difference between the solute concentration and equilibrium concentration to the equilibrium concentration,  $s = (C - C^*)/C^*$ .

The key variables affecting primary nucleation rate are energy  $\sigma$ , Temperature  $T$ , and super saturation  $s$ .

### Secondary nucleation

This involves the formation of ne crystals due to the presence of solute crystals. A number of mechanisms are involved here which include initial breeding, contact nucleation and shear breeding. Initial breeding occurs accordingly as seed crystals are immersed in a supersaturated solution. Contact nucleation is formed by either collision of crystals with each other, the crystallizer internals, the circulation pump, or with an agitator. Lastly, for sheer breeding, this results when crystal precursors are carried by supersaturated solutions as they flow on a crystal surface (Rousseau, 1987).

## Struvite Nucleation

The free ions that interact to form struvite are subject to a range of speciations that are pH dependant. The equilibria between various dissolved species in solution form the basis for all subsequent thermodynamics calculations and measurements (Mullin, 1993).

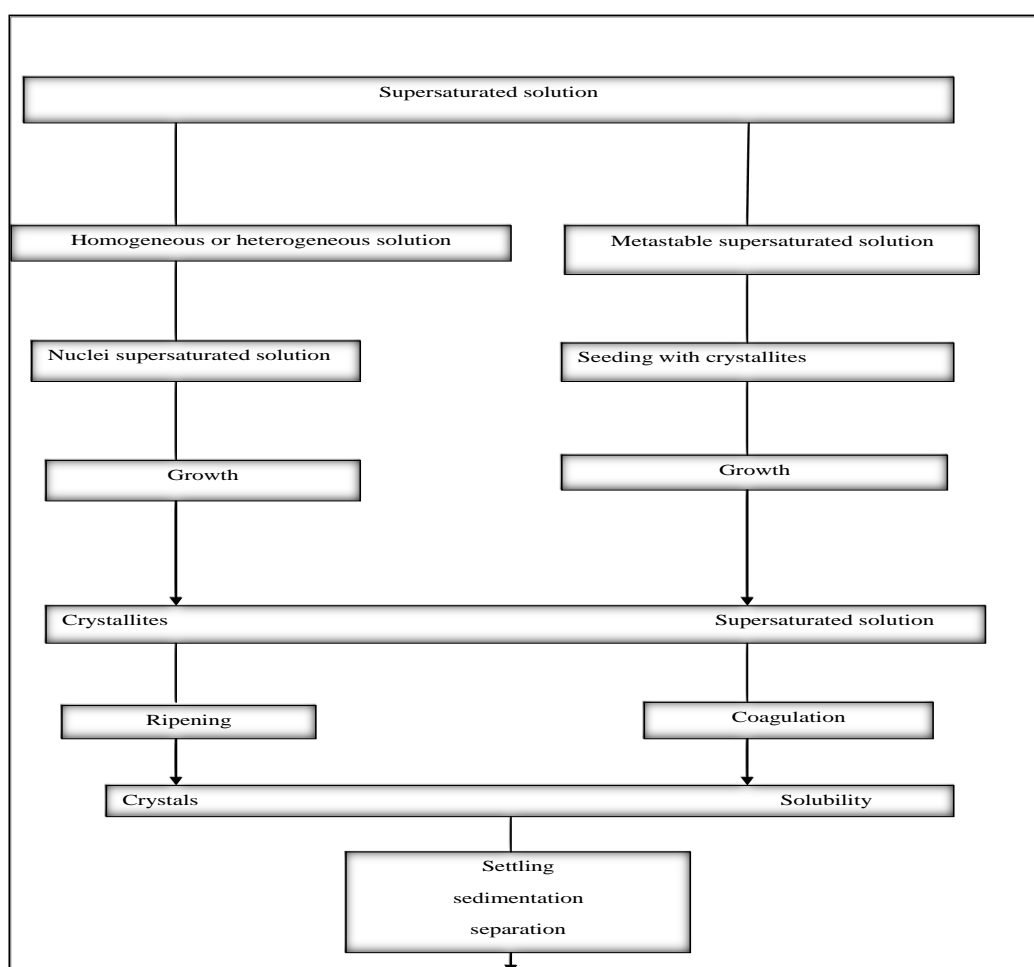


Figure 2.3 A process scheme for nucleation and crystal growth

Source: Stumm and Morgan (1996)

Ohlinger *et al.*(1998), identified major species involved in struvite nucleation process, which include  $\text{HPO}_4^{2-}$ ,  $\text{H}_2\text{PO}_4^-$ ,  $\text{H}_3\text{PO}_4$ ,  $\text{MgPO}_4^-$ ,  $\text{MgHPO}_4$ ,  $\text{MgH}_2\text{PO}_4^+$ ,  $\text{MgOH}^+$ ,  $\text{NH}_4^+$ , and  $\text{H}_2\text{O}$ .

**Table 2.3 Thermodynamic equilibria and their governing equations**

<i>Compound</i>	<i>Equilibrium equation</i>	<i>Equilibrium Constant(Ki)</i>	<i>Reference</i>
HPO <sub>4</sub> <sup>2-</sup>	$\frac{\{H^+\}\{PO_4^{3-}\}}{\{HPO_4^{2-}\}}$	10 <sup>-12.35</sup>	(Morel and Hering, 1993)
H <sub>2</sub> PO <sub>4</sub> <sup>-</sup>	$\frac{\{H^+\}\{HPO_4^{2-}\}}{\{H_2PO_4^-\}}$	10 <sup>-7.20</sup>	(Morel and Hering, 1993)
H <sub>3</sub> PO <sub>4</sub>	$\frac{\{H^+\}\{H_2PO_4^-\}}{\{H_3PO_4\}}$	10 <sup>-2.15</sup>	(Martell and Smith, 1989)
MgPO <sub>4</sub> <sup>-</sup>	$\frac{\{Mg^{2+}\}\{PO_4^{3-}\}}{\{MgPO_4^-\}}$	10 <sup>-4.80</sup>	(Martell and Smith, 1989)
MgHPO <sub>4</sub>	$\frac{\{Mg^{2+}\}\{HPO_4^{2-}\}}{\{MgHPO_4\}}$	10 <sup>-2.91</sup>	(Martell and Smith, 1989)
MgH <sub>2</sub> PO <sub>4</sub> <sup>+</sup>	$\frac{\{Mg^{2+}\}\{H_2PO_4^{3-}\}}{\{MgH_2PO_4^+\}}$	10 <sup>-0.45</sup>	(Martell and Smith, 1989)
MgOH <sup>+</sup>	$\frac{\{Mg^{2+}\}\{OH^-\}}{\{MgOH^+\}}$	10 <sup>-2.56</sup>	(Childs,1970)
NH <sub>4</sub> <sup>+</sup>	$\frac{\{H^+\}\{NH_3\}}{\{NH_4^+\}}$	10 <sup>-9.25</sup>	(Taylor <i>et al.</i> ,1963)
H <sub>2</sub> O	$\frac{\{H^+\}\{OH^-\}}{\{H_2O\}}$	10 <sup>-14</sup>	(Harris,2003)

Source: Galbraith and Schneider, 2009

The calculation of activity coefficients are normally done in determining various equilibria. The calculations can be done using the following formulas

$$I = 1/2 \sum C_i Z_i^2 \quad \text{4}$$

$$-\log \gamma_i = AZ_i^2 \left( \left[ \frac{\sqrt{I}}{1+\sqrt{I}} \right] - 0.3I \right) \quad \text{5}$$

$$\{i\} = \gamma_i C_i \quad \text{6}$$

Where I is the Ionic strength, C<sub>i</sub> is the concentration of species i, Z<sub>i</sub> is valency of species i, γ<sub>i</sub> is activity coefficient of species i, and A is Debye-Huckel constant (Mullin, 2003).

A computer program is normally used to solve the equations (4,5 and 6). A common package to be used in this research is PHREEQC. This program calculates concentration of all species in solution using a database of equilibrium information and initial setting of the system (Bhuyian *et al.*,2008).

### 2.4.3.2 Crystal growth

The crystals form by deposition of precipitate constituent ions into the nuclei (Snoeyink and Jenkins, 1980).

Crystal growth is the process where crystal embryos interact together to form crystals of detectable size. The growth rate is governed by mass transfer and surface integration processes. The mass transfer process involves the transportation of particles from solution to crystal surfaces by either diffusion, convection, or their combination. The surface reaction which involves surface integration leads to incorporation of material into the crystal lattice (Le Corre, 2006).

### 2.4.4 Conditional solubility

Solubility is a key issue in struvite precipitation. Struvite precipitation which is determined by the solution pH, super saturation degree, presence of foreign ions and temperature occurs when the constituent ions surpass the solubility product. Solubility product ( $K_{sp}$ ) fits well with very soluble solution because it does not consider the ionic activity, ionic strength and the pH of solution (Doyle and Parsons, 2002).

Undiluted stored urine has a consistent composition with respect to pH and ionic strength, and its complexity is well suited with a conditional solubility product (Ronteltap *et al.*, 2007).

A conditional solubility product depends on solution conditions other than presence of a common ion. It is used in determination of precipitates' solubility of ions which interact with solution constituents through various reactions. This includes complexation and hydrolysis (Snoeyink and Jenkins, 1980).

The conditional solubility product can be determined from the ionic activities and strengths of constituent ions in solution:

$$\text{Conditional solubility product} = \frac{K_{sp}KMgPO_4}{\alpha K\alpha M\alpha P} \text{-----} 7$$

Where  $\alpha$  is the fraction of magnesium, potassium and phosphate that form potassium struvite.

The product of the fraction of each constituent ion forms an ion activity product (IAP). The total ionic strength of solution is a key factor that directly affects each ion's activity. The conditional solubility product ( $K_{so}$ ) can be derived from solubility product ( $K_{sp}$ ) by dividing it with ion activity potential (IAP) (Doyle and Parsons, 2002)

Supersaturation ratio can be obtained by dividing the conditional solubility product by the product of constituent ions in the solution. When the ion activity product (IAP) is greater than conditional solubility product ( $K_{so}$ ), the solution will thus be supersaturated and hence the struvite precipitation will occur, until equilibrium is achieved again. (Doyle and Parsons, 2002)

These calculations can be simulated using thermodynamic solvers such as the PHREEQC model. The PHREEQC is a program is based on an ion-association aqueous model with capabilities for calculating speciation and saturation-index values; batch-reaction and one-dimensional (1D) transport calculations involving reversible reactions. This includes aqueous, gas, solid-solution, mineral, and ion-exchange equilibria, and irreversible reactions (Parkhurst and Appelo, 1999).

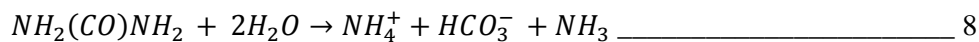
## 2.5 Treatment processes for source separated urine

Separation of urine at the source provides opportunities for nutrient recovery and recycling from concentrated nutrient solutions (Wilsenach and Van Loosdrecht, 2003). The complexity of urine allows several technologies to be applied for treatment. For potassium recovery, some of the possible technologies to be applied are storage, struvite (MAP) recovery, Anammox and nitrification.

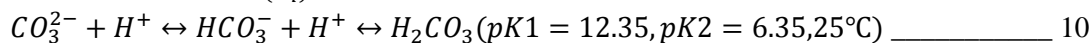
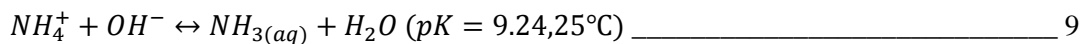
### 2.5.1 Storage (Hydrolysis)

This is a potential process for reduction of pathogens. It retains approximately 99% of carbon, nitrogen and 80% of phosphorus. The effectiveness of this process depends mainly on the temperature, pH and storage time (Maurer et al, 2006).

The hydrolysis of urea releases ammonium and bicarbonate, according to equation below;



Ammonium ions, ammonia, carbonate and bicarbonate ions are responsible for the pH increase. They exist in the equilibria of ammonia and carbonate ions respectively (Liu *et al.*, 2008);



According to Mobley and Hausinger (1999), there should be complete hydrolysis in this reaction before precipitation takes place. The authors further say that the process is facilitated by urease enzyme from eucaryotic and procaryotic bacteria. They are commonly found in aquatic environments and human intestines (Mobley and Hausinger, 1999).

According to Udert *et al.* (2003a), this process can take 24 hours if urease is added in urine with proper mixing at 25°C. Hydrolysis process does not affect the concentration of potassium from the fresh urine.

Similarly, according to simulated values of stored urine, all the calcium and magnesium are precipitated into hydroxylapatite and struvite respectively Udert *et al.* (2003a). The different precipitates of calcium, ammonium and phosphates are shown in Table 2.4

Depending on the conditions, hydroxylapatite (equation 11) will either evolve from amorphous calcium phosphate or octacalcium phosphate or nucleate directly from solution (Abbona, 1996).



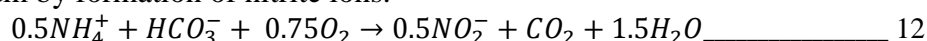
**Table 2.4 Complexes of Phosphate species in hydrolyzed urine**

Species	Chemical formula	Conditions for formation	Ref
Dicalcium phosphate dihydrate	$CaHPO_4 \cdot 2H_2O$	In slightly acidic conditions	Regy <i>et al.</i> (2001)
Amorphous calcium phosphate	$Ca_3(PO_4)_2$	pH range 7-9	
Octacalcium phosphate	$Ca_8H_2(PO_4)_6 \cdot 2.5H_2O$		
Hydroxylapatite	$Ca_5(PO_4)_3OH$		
Struvite(Magnesium ammonium phosphate)	$MgNH_4PO_4 \cdot 6H_2O$	pH>8.5	Stratful <i>et al.</i> (2001)

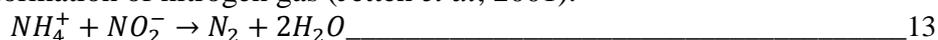
### 2.5.2 Sharon-Anammox process

Among the novel processes for nitrogen removal to be developed, is the combined SHARON-Anammox process (van Dongen *et al.*, 2001).

This combination is capable of 90% removal of nitrogen from ammonium rich solution (Young-Ho A., 2006). The Anammox process targets wastewater that contains much ammonium and little organic material. The SHARON process is capable of removing ammonium by formation of nitrite ions.



These nitrite ions are then used as the electron acceptors for the anammox process, which leads to formation of nitrogen gas (Jetten *et al.*, 2001).

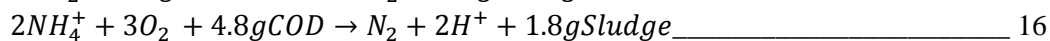


Benefits of the combined SHARON-Anammox process compared to the SHARON process with denitrification are the reduction by 50% of the aeration costs, since only half of the Total ammonium nitrogen(TAN )is converted, the omission of the need for additional COD source, the virtual absence of sludge production and the possibility to obtain low nitrogen effluent concentrations through the subsequent autotrophic Anammox process. The latter has been an inspiring starting point for the development of more sustainable municipal wastewater treatment systems (Jetten *et al.*, 1997).

### 2.5.2.1 Sharon process

This process was developed for the removal of ammonia through the formation of nitrite (Hellenga *et al.*, 1998). This process is characterized by both heterotrophic denitrification and autotrophic nitrification. This process lowers the pH and hence methanol is always added to stabilize the pH, to balance off the acidifying effect.

Equations 11, 12 and 13 below represent the Sharon reactions



Partial nitrification techniques, such as the continuously aerated SHARON process, have examined as very promising for improved sustainability of wastewater treatment (Abeling and Seyfried, 1992). The conventional process for nitrogen removal in wastewaters is achieved using nitrification/denitrification. In such systems, nitrifying bacteria oxidize ammonium to nitrate under oxic conditions, and nitrate is subsequently or simultaneously reduced to dinitrogen gas, under anoxic conditions.

### 2.5.2.2 Anaerobic ammonia oxidization (Anammox)

Anammox is a biological process in which ammonium is directly converted to dinitrogen gas with nitrite as the electron acceptor under anoxic conditions. The Anammox process is carried out by the chemolithoautotrophic bacteria of the order *planctomycetales*. These bacteria are unique in that they are able to consume ammonia in the absence of oxygen (Young-Ho, 2006).

Anammox is energetically more favourable than normal oxic nitrification. Anammox requires ammonium and nitrite as substrates in the ratio of approximately one to one Jetten, *et al.*, (2001).

The oxidation process follows equation 14;



The nature of the process was verified and nitrite was confirmed to be the preferred electron acceptor, with, hydroxylamine and hydrazine as the intermediate products (Jetten *et al.*, 1998).

This process is relatively new and promising alternative to conventional Nitrogen removal process. The application of Anammox to Nitrogen removal would lead to a significant reduction of costs for aeration (Jetten *et al.*, 2001)

Jetten, *et al.*, (2001) suggests that the application of the anammox process to nitrogen removal, would lead to cost reduction to about 90%. The author further elaborates that the process is suitable for wastewaters with a higher concentration of ammonium and little concentration of organic matter. In addition to that, this process will enrich the natural nitrogen cycle (Dong and Tollner, 2003).

**Table 2.5 Parameters of aerobic and anaerobic ammonia oxidation**

<i>Parameter</i>	<i>Nitrification</i> $NH_4^+ + O_2^- \rightarrow NO_2^-$	<i>Anammox</i> $NH_4^+ + NO_2^- \rightarrow N_2$	<i>Unit</i>
Free energy	-275	-357	kJ/mol
Biomass yield	0.08	0.07	Mol/molC
Aerobic rate	200-600	0	Nmol/min/mg protein
Anaerobic rate	2	60	Nmol/min/mg protein
Growth rate	0.04	0.003	/h
Doubling time	0.73	10.6	days
Ks $NH_4^+$	5-2600	5	$\mu$ M
Ks $NO_2^-$	N/A	<5	$\mu$ M
Ks $O_2$	10-50	N/A	$\mu$ M
pH range	Variable	6.7-8.3	
Temperature range	$\leq 42$	20-43	$^{\circ}$ C

N/A- Not applicable; Ks- affinity constant  
Source: Jetten, *et al.*,( 2001) and Ahn(2006)

### 2.5.4 Nitrification

This is a process of biological oxidation of ammonia to nitrite and thereafter, to the nitrate form. It involves chemolithoautotrophic oxidation of ammonia to nitrate under aerobic conditions in two stages. Two major species of organism responsible for the processes in these stages are the autotrophic bacteria *Nitrosomonas* and *Nitrobacter* (Surampalli, *et al.*, 1997). The first stage uses ionized ammonia as the energy source .

The first process involves the conversion of ammonia into nitrite by *Nitrosomonas* bacteria, as shown in equation 15. (Gerardi, 2006)



The second process involves the oxidation of the nitrite to nitrate by *Nitrobacter* bacteria as shown in equation 16 (Gerardi, 2006);



This process involves nitrifying bacteria which oxidize ionized ammonia and nitrite to obtain energy for their cellular metabolism. The bicarbonate alkalinity supplies the carbon needed for the process (Gerardi, 2006).

The process of nitrification lowers the pH from the production of nitrous acid. Since urine does not have adequate buffer capacity, nitrification only oxidizes half the ammonium, until the process halts due to low pH. The product that is formed is ammonium nitrite or nitrate at approximately 1:1 composition (Maurer *et al.*, 2006).

In urine treatment, apart from stabilizing the ammonia, nitrification is also known to degrade micro pollutants (Pronk and Kone, 2009). The authors further suggested a combination of sand bed nitrification with solar evaporation as a sustainable low cost application in removing micro pollutants.

### 2.5.5 Magnesium Struvite Precipitation

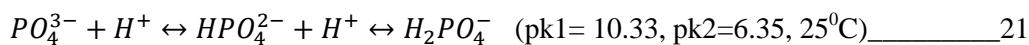
The pH of hydrolysis is optimal for struvite precipitation (Buchanan *et al.*, 1994).

This has been an attractive product because it bears two fertilizer ingredients in solid form and it can also be used as slow releasing fertilizer. In hydrolyzed urine, the precipitation is triggered by presence of magnesium (Maurer, *et al.*, 2006).

After urea is completely hydrolyzed to ammonium ions, struvite precipitation reaction begins to occur according to the equation below (Liu, *et al.*, 2008) ;



Similarly, the phosphate ions would achieve chemical equilibrium due to the pH increase as follows;



The struvite stream has no big difference in ammonia concentration from the hydrolysis stream as only about 3% of ammonium is removed (Maurer, *et al.*, 2006).

## 2.6 Adsorption

Adsorption is the enrichment of material, or the increase in the density of the fluid in the vicinity of an interface or enrichment of one or more of the components between two bulk phases (Rouquerol *et al.*, 1999).

This is basically a mass transfer operation whereby one constituent is transferred from one phase to the other (Asano *et al.*, 2007). It is defined as a process that enhances enrichment of gaseous or dissolved substances on the boundary surface of a solid as shown in figure 1 below (Wypych, 2001). Sundstrom and Klei (1979) also defined it as the accumulation of a substance at the interphase between two phases. These surfaces bear active sites that binding forces between individual atoms in the solid structure are partly saturated by neighbouring atoms

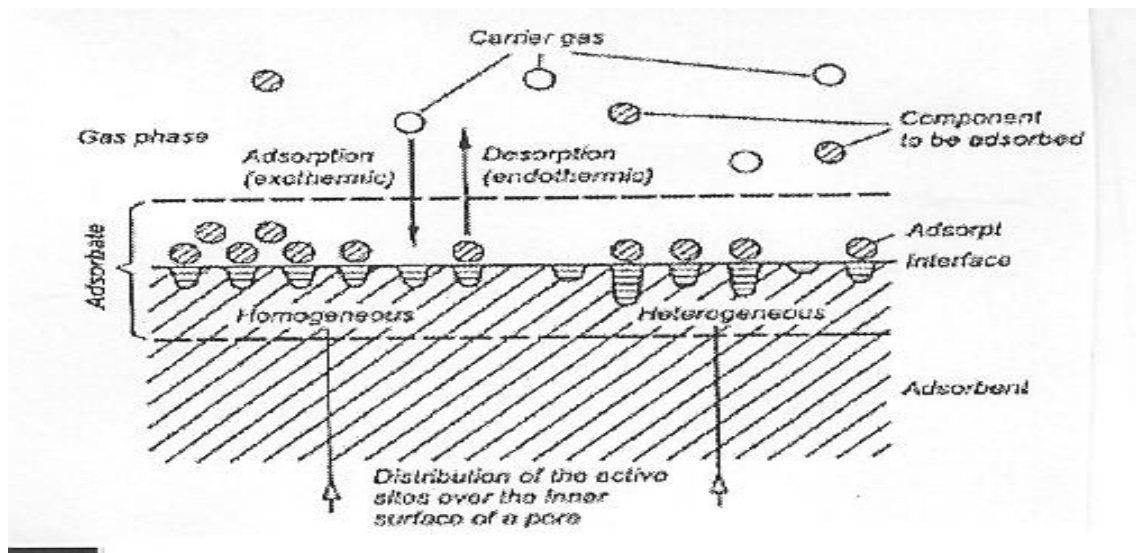


**Figure 2.4: The adsorption mechanism**

Source: Wypych G. (2001)

The adsorbate is the substance undergoing removal from one phase to the other on the interface and it accumulates on the adsorbent. The adsorption process involves four steps;

- Bulk solution transport
- Film diffusion transport
- Pore and surface transport
- Adsorption

In adsorption step, the adsorbed material is attached to the adsorbent at appropriate adsorption site (Snoeyink and Summers, 1999). The equilibrium capacity of the adsorbent is achieved when the adsorption rate equals the desorption rate (Asano *et al.*, 2007).

### 2.6.1 Adsorption Isotherms

The distribution of solutes between two key phases of liquid and solid are described using isotherms. Adsorption capacity largely depends from the size and structure of its inner surface area for a defined component. It is normally represented as a function of the component concentration (C) for the equilibrium conditions at constant temperature, referred to as adsorption isotherm (Wypych, 2001). The adsorption isotherms are used to determine the theoretical adsorption capacity for a given adsorbent. (Asano *et al.*, 2007) Adsorption Kinetics is determined by the diffusion rate through the pore structure. The ratio of pore diameter to the radius of adsorbed molecule and other characteristics of the adsorbed component govern the diffusion coefficient. Moreover, adsorption rate is governed by diffusion resistance. The adsorbent bears a large surface area due to its porosity, and hence readily allows pore diffusion. This results in loss of Kinetic energy by the molecules due to the physical adherence to the surface (Wypych, 2001).

The other key factors that determine the kinetics are; the nature of adsorbate in terms of solubility, the relative concentrations of adsorbent in the solute, the adsorptive forces and molecular sizes. Also, adsorption decreases with increasing ionization since it is affected by the pH and adsorption of an ionized species changes (Sundstrom and Klei, 1979)

### 2.6.1.1 Freundlich isotherm

This is based on assumption of heterogeneous adsorption on the surface which comprises of varied classes of adsorption sites and energies (Sharma, 2001).

This is mostly applicable in dilute solutions especially over small concentration changes. Its frequently used to the adsorption of impurities from a liquid solution onto activated carbon (Sundstrom *et al.*, 1979)

The equation is defined as follows (Asano *et al.*, 2007);

$$\frac{x}{m} = q_e = K_f C_e^{1/n} \quad \text{22}$$

Where  $x/m$  is mass of adsorbate adsorbed per unit mass of adsorbent after equilibrium;  $K_f$  is Freundlich capacity factor [(mg adsorbate / g zeolite)\*(Litre of solution/mg adsorbate)<sup>1/n</sup>],  $1/n$  is the Freundlich intensity parameter;  $C_e$  is the equilibrium concentration of adsorbate after absorption has occurred; and  $q_e$  is the adsorbent phase concentration after equilibrium, mg adsorbate/g adsorbent

The higher the value of  $K$  the higher the adsorption capacity and the lower the value of  $1/n$ , the stronger is the adsorption bond (Sharma, 2001).

The constants are determined by plotting the  $\log(x/m)$  versus  $\log C_e$  as follows;

$$\text{Log } \frac{x}{m} = \text{Log } K_f + \frac{1}{n} \text{Log } C_e \quad \text{23}$$

### 2.6.1.2 Langmuir Isotherm

This isotherm describes an adsorbate-adsorbent system where the extent of adsorbent coverage is limited to one molecular layer. The isotherm, which was proposed by Langmuir (1918) is more appropriate for chemisorptions and is obeyed at moderately low coverages (Crittenden and Thomas 1998).

Moreover, the author further says, the isotherm is formulated on the basis of dynamic equilibrium between the adsorbed phase and the gaseous or vapor phase. It was proposed that the rate, at which adsorbent gas molecules strike a surface of an adsorbent, is proportional to the product of the partial pressure ( $P$ ) of the gas, and the fraction  $(1-\theta)$  of surface remaining uncovered by adsorbates which are then available as adsorption sites. Therefore, the fractional surface coverage is directly proportional to the rate of desorption, implying that rates of adsorption and desorption are equal at equilibrium (Crittenden and Thomas 1998);

$$K_a P(1-\theta) = K_d \theta \quad \text{24}$$

Where  $K_a$  and  $K_d$  are respective rate constants for adsorption and desorption. This equation can be expressed as;

$$\theta = \frac{q}{q_e} = \frac{bP}{1 + bP}, \text{ where } b = \frac{K_a}{K_d} \quad \text{25}$$

The main equation is expressed as follows (Asano *et al.* 2007);

$$\frac{x}{m} = q = \frac{q_m b C_e}{(1 + b C_e)} \quad \text{26}$$

Where  $q$  - quantity of solute adsorbed per unit weight of adsorbent= $x/m$  (g/g)

b - Langmuir isotherm constant  
 $q_m$  -the maximum monolayer adsorption capacity  
 $C_e$ - equilibrium concentration (g/l)

For the Langmuir constants, the higher the value of  $q_m$  the higher the adsorption capacity (Sharma, 2001).

On linearization, the equation will be of the form;

$$\frac{1}{q} = \frac{1}{q_m} + \frac{1}{C_e q_e b} \quad \text{27}$$

The dimensionless constant  $R_L$ , termed the separation factor or equilibrium parameter, was determined from the Langmuir isotherm parameter and is defined by the relationship:

$$R_L = 1/(1+bC_0) \quad \text{28}$$

where b is the Langmuir isotherm constant and  $C_0$  is the initial potassium concentration. The shape of an isotherm and the feasibility/favourability criteria of an adsorption process can be judged from the  $R_L$  values as described in Table 6.  $R_L$  values between 0 and 1 indicate favourable adsorption (Ahalya *et al.*, 2005; Horsfall and Spiff, 2005).

**Table 2. 6: Type of isotherm and favorability of adsorption processes for various  $R_L$  values.**

$R_L$	Type of isotherm/favorability
$R_L > 1$	unfavorable
$R_L = 0$	irreversible
$0 < R_L < 1$	favorable
$R_L = 1$	linear

Source: Ahalya *et al.*, 2005; Horsfall and Spiff, 2005

The Langmuir isotherm bears the following assumptions;

- The accessible sites on the adsorbent surface are fixed in number, and besides that, they have the same energy
- The adsorption process is reversible
- Its equilibrium is achieved when the rate of desorption of molecules from surface is the same as rate of adsorption of molecules onto the surface. More so, the adsorption rate is proportional to its driving force which is expressed as the difference between amount of material adsorbed at particular concentrations and the amount that can be adsorbed at the same concentration.

### 2.6.2 Zeolites

The zeolites are naturally occurring minerals, normally contained in volcanic rocks and sedimentary outcrops of ancient sea bed. They are composed of hydrous aluminium silicates of sodium, calcium, potassium or barium (Yetgin, 2006).

These are crystalline, hydrated aluminosilicates of alkali and alkaline earth metals with three dimensional atomic structures. They have the ability to exchange certain constituent atoms without major change of atomic structure. They also have a three dimensional framework of silicate ( $\text{SiO}_4^{4-}$ ) tetrahedral framework that bears open cavities in form of channels and cages (Ganrot, 2005).

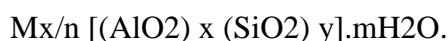
In zeolite structures, some  $\text{Si}^{4+}$  is replaced by  $\text{Al}^{3+}$ , resulting in deficiency of positive charge, which is balanced by presence of mono and divalent cations (Ganrot, 2005). They have large surface areas, with high cation exchangeable capacities, favourable hydraulic characteristics and are of low cost. They have a net negative structural charge which results from the isomorphic substitution of cations in crystal lattice. This negative charges explains the property of zeolites in ion exchange selectivity with cations (Faghihian and Bowman, 2005)

There are cavities within the zeolite framework connected by regular pores (channels) which the adsorbate molecule can penetrate. Their internal porosity is high and there is where most adsorption takes place. The channel size is determined by the number of atoms forming the cages (cavities) in the zeolites. For instance, the apertures may be constructed from rings of 8, 10 and 12 oxygen atoms together with same number of aluminium and, or silicon atoms. Cages with 6 atom apertures can admit the smallest molecules such as water and ammonium. The cages containing 8, 10 and 12 oxygen atoms have aperture sizes of 0.42, 0.7 and 0.74 nm respectively hence penetrable by molecules of increasing size (Crittenden and Thomas, 1998).

#### 2.6.2.1 Zeolite structures

The basic unit of a zeolitic structure is  $\text{TO}_4$  tetrahedron, where T is normally silicon or aluminium ion/atom (Rouquerol *et al.*, 1999).

The aluminosilicate zeolites have a general formula;



The framework is composed of  $[(\text{AlO}_2)_x (\text{SiO}_2)_y]$ , where M is a non-framework, exchangeable cation. The aluminosilicate framework, which is composed of  $(\text{AlO}_2)$  and

(SiO<sub>2</sub>)<sub>y</sub> is anionic, with net negative charge governed by number of aluminium atoms in T positions. Zeolites with a given Si/Al ratio have a certain number of exchangeable cations (Rouquerol *et al.*, 1999).

The ratio of combined silica to aluminium atom is equal to two, with each aluminium atom introducing a negative charge on the zeolite framework, to be balanced by an exchangeable cation. In the zeolite framework, the cations occupy positions depending on a number of cations per unit cell (Crittenden and Thomas, 1998).

The natural zeolite (clinoptilolite) used was sourced from *Landustrie B.V.*, in the Netherlands. It has characteristic silicon: aluminium ratio of 4, which is typical of clinoptilolite with a range of 4-5.5 (Erdem *et al.*, 2004).

Clinoptilolite is known for its abundance, and bears morphology of 8-10 rings. It also has a high affinity for ammonium ions over sodium and calcium, but not over potassium (Erdem *et al.*, 2004).

The SEM-EDX analysis of the zeolite shown in figure 4 has Silicon: Aluminium ratio of 4, with a 5% and 8% composition in atom and weight respectively.

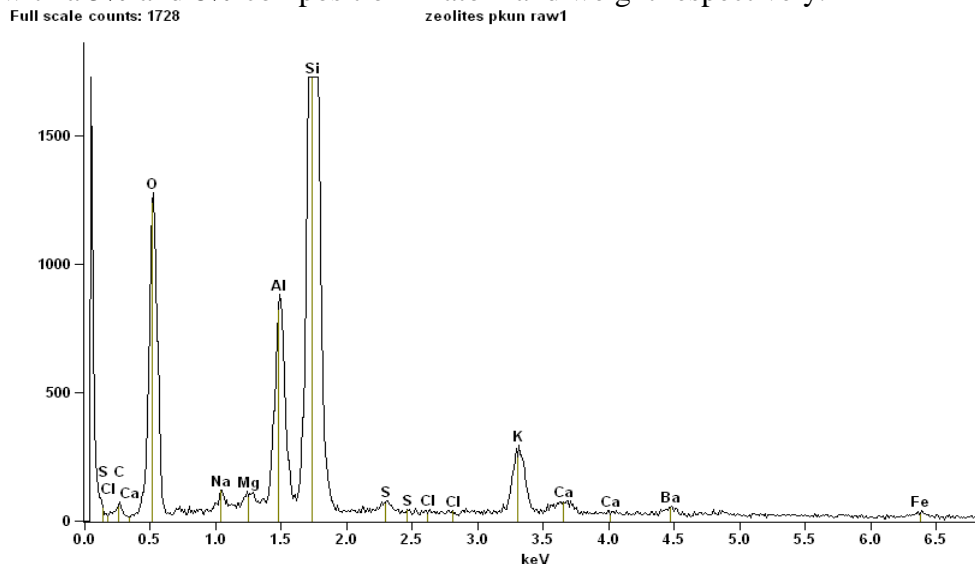


Figure 2.5 SEM EDX Analysis of Untreated zeolite

After treatment of the zeolites, the overall percentage of potassium reduces to 1.19% and 2.29% by composition in atom form and weight respectively.

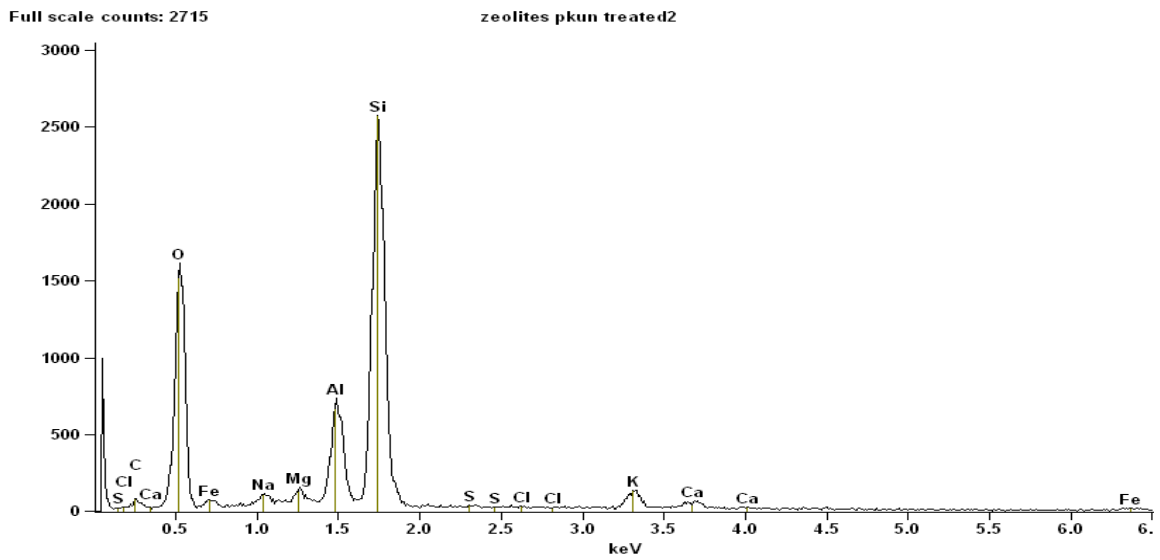


Figure 2.6 SEM EDX Analysis of treated zeolite

These zeolites are widely used in agriculture since they are non-toxic and affordable (Reháková, *et al.*, 2004).

## 3.0 MATERIALS AND METHODS

### Introduction

This section consists of laboratory experiments, divided mainly in three parts;

- 3.1 Derivation of synthetic urine recipes
- 3.2 The adsorption experiments
- 3.3 The precipitation experiments

#### 3.1) Derivation of Synthetic urine recipes

Griffiths et al.(1976) recipe was used to derive representative recipes for four urine treatment processes.

**Table 3.1 The formulation of synthetic urine by Griffith et al. (1976)**

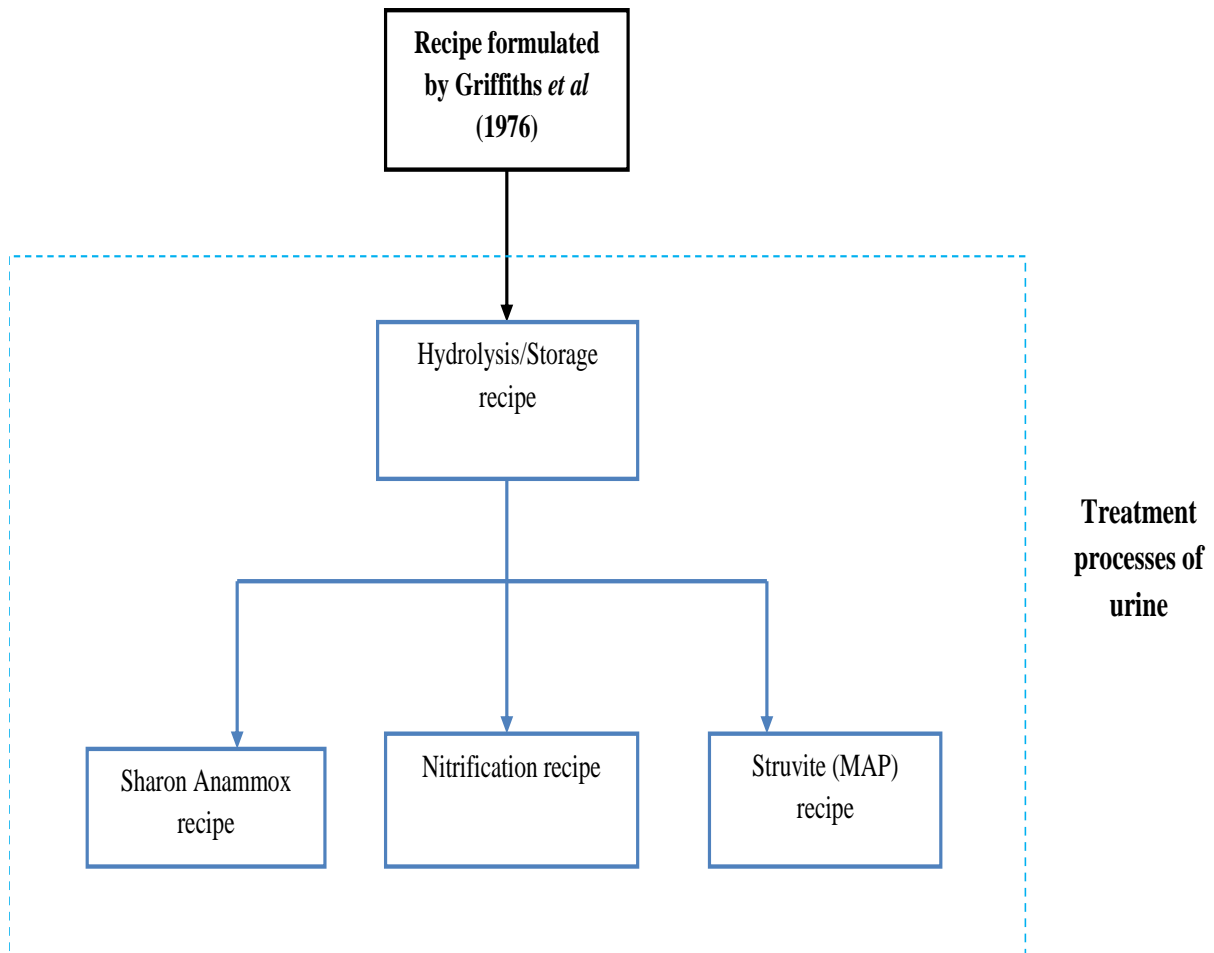
<i>Salt</i>		<i>Concentration(g/l)</i>	<i>mM</i>
Calcium chloride	$\text{CaCl}_2 \cdot 2\text{H}_2\text{O}$	0.65	4.4
Magnesium chloride	$\text{MgCl}_2 \cdot 6\text{H}_2\text{O}$	0.65	3.2
Sodium chloride	$\text{NaCl}$	4.6	78.7
Sodium sulphate	$\text{Na}_2\text{SO}_4$	2.3	16.2
Trisodium citrate	$\text{Na}_3\text{C}_6\text{H}_5\text{O}_7$	0.65	2.6
Urea	$\text{NH}_2\text{CONH}_2$	25	417
Creatinine	$\text{C}_4\text{H}_7\text{N}_3\text{O}$	1.1	9.7
Potassium chloride	$\text{KCl}$	1.6	21.5
Ammonium chloride	$\text{NH}_4\text{Cl}$	1	18.7
Sodium Oxalate	$\text{Na}_2\text{-(COO)}_2$	0.02	0.15
Potassium dihydrogen phosphate	$\text{KH}_2\text{PO}_4$	4.2	30.9

The individual ion concentrations from the Griffith's recipe are derived from equations 3.1a to 3.1o, in appendix 7. Thereafter, Table 3.3 summarizes the concentrations of fresh urine and the expected concentrations after the treatment processes.

The figure 3.1 shows the scheme of the treatment processes as they are derived from Griffiths *et al.*, (1976) recipe. Hydrolysis is the first treatment stage, also known as storage.

The three other recipes of sharon-anammox, nitrification and struvite (MAP) are derived from the hydrolysis/storage products.

**Figure 3.1 Derived treatment scheme of urine**



### 3.1.1 Hydrolysis (Storage)

This represents our first treatment process from which the other three; sharon-anammox, nitrification and struvite (MAP) are obtained. This also implies that all the urea in fresh urine is converted to bicarbonate ions, ammonium ions and ammonia gas depending on the pH of the urine (equation 8).

Due to the formation of hydroxylapatite during the hydrolysis, we assume a decrease in phosphate concentration by 2.64 mMole, according to the equation 11 and table 3.11 in appendix 7.

After hydrolysis, we also assume that all the magnesium is incorporated in struvite (Udert *et al*, 2006) according to the equation 20 and table 3.1n ,in appendix 7.

Therefore 3.2mM of  $Mg^{2+}$  reacts with an equivalent amount of ammonium and phosphate ions respectively to form struvite .This will reduce the concentrations of ammonium and

phosphates further by 3.2mM/litre respectively. In total, the phosphate ion concentration will reduce from 30.9mM to 25.06mM.

The sodium concentration increased in the recipe mainly because of unavailability of some chemical ingredients. Ammonium bicarbonate was replaced with sodium bicarbonate and hence increasing the concentration by 417 mM.

### **3.1.2 Sharon-anammox recipe**

The combination as a treatment process could then be used to remove ammonia from urine that has undergone hydrolysis and consequently produce nitrogen gas back to the atmosphere, according to the equations 12 and 13.

This follows that the ammonium and bicarbonate will be utilized completely from the hydrolysis process, and this is the reason for their exclusion in the sharon-anammox recipe.

### **3.1.3 Nitrification**

The nitrification process normally takes place according to equations 18 and 19. Given the concentration of ammonium ion, the expected concentration of the products will be as shown in Table 3.5 as per the equations. The stoichiometric reaction ratio is 1:1 in both stages, where it is expected that a similar amount of nitrite concentrations from the ammonium concentration

### **3.1.4 Struvite (MAP)**

During hydrolysis, precipitation of struvite is triggered by this pH and the concentrations of magnesium, calcium and phosphates (Udert *et al.*, 2003b). In derivation of struvite (MAP) recipe therefore, the initial magnesium and calcium in the urine before hydrolysis were excluded.

Besides that, there is still a large concentration of ammonium and a relatively lower concentration of phosphate ions prevail. The process of struvite formation can be stimulated again by addition of magnesium to the hydrolyzed urine (equation 20).

With the addition of 25.06 mM/l of Magnesium chloride, we expect a similar reduction in ammonium concentration and the depletion of phosphate in solution (i.e. from 849.5 to 824.44 mM/litre).

Sodium chloride was used to elevate the concentration of chloride ions in the assumption that, magnesium chloride was used for precipitation to recover the remaining phosphate in the urine after hydrolysis. The sodium concentration increased from 536.2 mM to 586.32 mM, as the chloride ions increased from 134 mM to 171.62 mM to cater for the chloride ions provided by the magnesium chloride.

**Table 3.2 Summary of chemicals used and their concentrations**

The table gives a summary of chemicals which provide the derived recipe and concentrations in table 4.1

	Chemical formula	Hydrolysis	Anammox	Struvite	Nitrification
Chemical ingredients		Concentration (mM/l)	Concentration (mM/l)	Concentration (mM/l)	Concentration (mM/l)
Potassium dihydrogen phosphate	$\text{KH}_2\text{PO}_4$	25.06	25.06	0	25.06
Potassium chloride	$\text{KCl}$	27.3	27.3	27.3	27.3
Sodium chloride	$\text{NaCl}$	78.7	78.7	128.82	78.7
Trisodium citrate	$\text{Na}_3\text{C}_6\text{H}_5\text{O}_7$	2.6	2.6	2.6	2.6
Sodium sulphate	$\text{Na}_2\text{SO}_4$	16.2	16.2	16.2	16.2
Sodium Oxalate	$\text{C}_2\text{Na}_2\text{O}_4$	0.15	0.15	0.15	0.15
Sodium bicarbonate	$\text{NaHCO}_3$	417	0	417	0
Ammonium chloride	$\text{NH}_4\text{Cl}$	15.5	0	15.5	0
Ammonium hydroxide	$\text{NH}_4\text{OH}$	834	0	808.94	0
Hydrochloric acid	$\text{HCl}$	0	15.5	0	15.5
Potassium hydroxide	$\text{KOH}$	0	0	25.06	0
Sodium nitrate	$\text{NaNO}_3$				849.5

## 3.2) Adsorption experiments

### 3.2.1 Preparation of adsorbents

The particle size of the zeolites used was of the range of 2-3.15 mm and 1-1.2 mm after performing a sieving analysis. The zeolites were washed with deionized water at 70°C for eight hours and dried overnight at 105°C. This was performed with the aim of removing impurities (Yetgin, 2006).



Figure 3.2 Zeolites (2-3.15) mm



Figure 3.3 Zeolites (1-1.2) mm

### 3.2.2 Batch experiment set up

The ion exchange of potassium was carried out using batch method. In this experiment, the adsorbent is contacted with the solution for a particular of time. There were three batch experiments performed;



Figure 3.4 Batch adsorption set up

#### 3.2.2.1 Batch experiment (1)

Batch adsorption experiments were conducted using dried prepared zeolites of size 2-3.15 mm. Different amounts of the dried zeolite were weighed using in the following range; 5, 10, 15, 20, 25, 30, 35 and 40 g. Each of the weighed zeolite was added to 100 ml of solution from each prepared synthetic urine solution in 250 ml plastic bottles.

The bottles containing the samples were agitated at 110 rpm on an orbital shaker for a maximum of 48 hours to attain adsorption equilibrium, where, 5 ml samples were drawn periodically from each bottle.

The samples were filtered using whatman filter (0.45 $\mu$ m) before measurement of Potassium concentration in duplicate using the atomic adsorption spectrophotometer (Model: Perkin-Elmer AAnalyst 200).

#### 3.2.2.2 Batch experiment (2)

Batch adsorption experiments were done using the synthetic urine concentrations with a dilution factor of three, and a pH range similar to the real solutions as shown in Table 3.3

**Table 3.3 The pH of diluted synthetic urine streams**

Stream solution	pH		Dilution	Source of literature values
	<i>In the prepared solutions</i>	<i>Literature values</i>		
Hydrolysis	8.62	9.0	About 4 times	Udert <i>et al.</i> (2003b)
		8.6	3 times	Gantenbein and Khadka(2009)
Nitrification	7.21	6.8-8.5	-	Gerardi(2006)
Sharon anammox	7.48	6.7-8.3	-	Young-Ho(2006)
		7.0-8.5	-	Jetten <i>et al.</i> (2001)
Struvite(MAP)	8.09	8.5	-	Bouropoulos and Koutsoukos(2000)
		7.4-9.4	-	Wilsenach <i>et al.</i> (2007)

The zeolites used were prepared and dried zeolites of 1-1.2 mm. Different amounts of the zeolite were measured: 1, 3, 5, and 10 g with 60 ml of solution from each prepared synthetic urine solution in 100 ml plastic bottles.

The bottles containing the samples were agitated at 110 rpm on an orbital shaker for a maximum of 72 hours to attain adsorption equilibrium, where, 5 ml samples were drawn periodically from each bottle.

The samples were filtered using whatman filter (0.45µm) before measurement of Potassium, Phosphate and Nitrates concentrations. Potassium concentration was analyzed in duplicate using the AES spectrometer (*Model: Perkin-Elmer AAnalyst 200*).

### 3.2.2.3 Batch experiment (3)

Batch adsorption experiments were conducted using dried prepared zeolites of size 2-3.15 mm. Different amounts of the dried zeolite were weighed using in the following range; 10, 20, 30 and 40 g. Each of the weighed zeolite was added to 100 ml of solution from each prepared synthetic urine solution in 250 ml plastic bottles.

The bottles containing the samples were agitated at 110 rpm on an orbital shaker for a maximum of 48 hours to attain adsorption equilibrium, where, 5 ml samples were drawn periodically from each bottle.

The samples were filtered using whatman filter (0.45µm) before measurement of Potassium concentration in duplicate using the ICP spectrometer (*Model ICP-OES, type Perkin Elmer Optima 5300 DV (Waltham), Massachusetts, USA*)



**Figure 3.5** Atomic emission spectrometer (Model: Perkin-Elmer AAnalyst 200)

### 3.3 Precipitation experiments

The characteristics of the four synthetic urine solutions prepared (nitrification, struvite (MAP), sharon-anammox and hydrolysis) were analysed as shown in table 3.4;

**Table 3.4** Characteristics of prepared synthetic urine streams

<i>Urine stream</i>	<i>Electrical conductivity(mS/cm)</i>	<i>Temperature (°C)</i>	<i>pH</i>	<i>Temperature (°C)</i>
Nitrification	78.9	24.3	4.24	24
Sharon-anammox	16.98	25	5.73	25
Struvite(MAP)	54.5	24.5	10.61	24
Hydrolysis	51.4	24.6	10.54	24

300 ml of each solution was used for the precipitation experiments. This contained 15.7 mM of potassium. It follows therefore that magnesium and phosphate should be in the

same amount as potassium in order to attain the 1:1:1 required ratio for the potassium struvite precipitation.

In all except the struvite stream, contained about 25.06 mM of phosphate after assuming precipitation of hydroxylapatite and struvite (MAP) with the trace amounts of magnesium and calcium as shown in Tables (3.3) and (3.4).

Therefore, in 300 ml of solution there should be about 7.52 mM of phosphate ions, which gives a deficiency of 8.19 mM to attain the required amount for a complete potassium recovery. In this case, the phosphate is added in form of sodium hydrogen phosphate. For struvite stream, the added phosphate was in the same ratio as magnesium and potassium in solution. The magnesium was absent in the solution streams and added in equal ratio as the equivalent of potassium in the form of magnesium chloride.



**Figure 3.6 Precipitation set-up**

There were three ratios that were developed for the addition of magnesium and phosphates as shown in table 3.5;

*i. Magnesium: Phosphate ratio of 1:1 (Mg: P=1:1)*

This ratio defines the equal concentrations of magnesium and phosphorus to the potassium concentration in the solution.

*ii. Magnesium: Phosphate ratio of 2:1 (Mg: P=2:1)*

This ratio had twice the concentration of magnesium added as the phosphate concentration was kept constant. The temperature was also maintained at room temperature of 25<sup>0</sup>C.

*iii. Magnesium: Phosphate ratio of 1:2 (Mg: P = 1:2)*

In this case, the phosphate concentration added was twice the concentration of magnesium, as the temperature was maintained at room temperature (25<sup>0</sup>C).

The batch precipitation experiments were performed with a magnetic stirrer with a stirring rate of 100 rpm for one hour.

During the experiment, the pH value was by addition of 1.0 molar sodium hydroxide or 2.0 hydrochloric acid solutions in order to optimize the precipitation process.

The precipitates formed were filtered using Whatman (GF/C) circles 125 mm filters and air dried except for the nitrification stream precipitate which was dried at temperature  $105^{\circ}\text{C}$  in the oven.

The filtrates after precipitation were analyzed for the presence of phosphates, magnesium and potassium using the phosphate ( $\text{PO}_4^{3-}$ ), and nitrate ( $\text{NO}_3^-$ ) concentrations were carried out using IC machine (Model: *Dionex ICS-1000 ION Chromatography system*) and ICP spectrometer (Model *ICP-OES, type Perkin Elmer Optima 5300 DV (Waltham), Massachusetts, USA*).

EDX analysis was performed on the precipitates, to determine the composition of the precipitates as the PHREEQC model results also were used to determine the key saturated species that are most likely to precipitate.



**Figure 3.7 IC Machine (Model: Dionex ICS-1000 ION Chromatography system).**

**Table 3.5 The ratios of magnesium chloride and sodium mono phosphate used for precipitation experiments in the four streams**

Ratios of magnesium and phosphate added	Stream	Magnesium Chloride		Sodium dihydrogen mono phosphate		
		Weight (g)	Millimoles (mM)	Deficit PO <sub>4</sub> <sup>3-</sup> for addition		Initial concentration of PO <sub>4</sub> <sup>3-</sup> in solution (mM)
				(g)	(mM)	
Magnesium: Phosphate ratio of 1:1 at 25°C	Hydrolysis	3.193	15.71	1.13	8.19	7.52
	Nitrification	3.193	15.71	1.13	8.19	7.52
	Struvite(MAP)	3.193	15.71	2.17	15.71	-
	Sharon-anammox	3.193	15.71	1.13	8.19	7.52
Magnesium: Phosphate ratio of 1:1 at 35°C	Hydrolysis	3.193	15.71	1.13	8.19	7.52
	Nitrification	3.193	15.71	1.13	8.19	7.52
	Struvite(MAP)	3.193	15.71	2.17	15.71	-
	Sharon-anammox	3.193	15.71	1.13	8.19	7.52
Magnesium :Phosphate ratio of 2:1	Hydrolysis	6.386	31.42	1.13	8.188	7.52
	Nitrification	6.386	31.42	1.13	8.188	7.52
	Struvite(MAP)	6.386	31.42	2.17	15.708	-
	Sharon-anammox	6.386	31.42	1.13	8.188	7.52
Magnesium :Phosphate ratio of 1:2	Hydrolysis	3.193	15.71	3.3	23.9	7.52
	Nitrification	3.193	15.71	3.3	23.9	7.52
	Struvite(MAP)	3.193	15.71	4.34	31.42	-
	Sharon-anammox	3.193	15.71	3.3	23.9	7.52

## 4.0 RESULTS AND DISCUSSION

### Introduction

This chapter presents the derived recipes and the respective constituents in concentration form, which were used in the adsorption and precipitation experiments. The results of the experiments are also presented, their analysis and brief discussion.

### 4.1 Constituent ions in the derived recipes

This is presented in table 4.1, where the elements in the recipe by Griffith *et al.*, (1976), were used to generate stoichiometric equations as shown in appendix 7.

**Table 4.1 The summary of expected concentrations of individual ions that are actively involved in the four treatment processes**

	<i>Fresh synthetic urine</i>	<i>Hydrolysis</i>	<i>SHARON-Anammox</i>	<i>Struvite MAP</i>	<i>Nitrification</i>
<i>Ion</i>	<i>Concentration (mM/l)</i>	<i>Concentration (mM/l)</i>	<i>Concentration (mM/l)</i>	<i>Concentration (mM/l)</i>	<i>Concentration (mM/l)</i>
Ca <sup>2+</sup>	4.4	0	0	0	0
Mg <sup>2+</sup>	3.2	0	0	0	0
Na <sup>+</sup>	119.2	536.2	119.2	586.32	968.7
Cl <sup>-</sup>	134.1	121.5	121.5	171.62	121.5
K <sup>+</sup>	52.4	52.36	52.36	52.36	52.36
PO <sub>4</sub> <sup>3-</sup>	30.9	25.06	25.06	0.00	25.06
NH <sub>4</sub> <sup>+</sup>	0	849.5	0	824.44	0
HCO <sub>3</sub> <sup>-</sup>	0	417	0	417.00	0
SO <sub>4</sub> <sup>2-</sup>	16.2	16.20	16.20	16.20	16.2
NO <sub>3</sub> <sup>-</sup>	0	0	0	0	849.5
(C <sub>6</sub> H <sub>5</sub> O <sub>7</sub> ) <sup>3-</sup>	2.6	2.6	2.6	2.6	2.6
(COO) <sub>2</sub>	0.15	0.15	0.15	0.15	0.15
Urea{NH <sub>2</sub> (CO)NH <sub>2</sub> }	417	0	0	0	0
pH	6.2	10.54	5.73	10.61	10.54

## 4.2. Adsorption results

The adsorption results for experiments (2) and (3) in 3.2.2.2 and 3.2.2.3 are presented in tables 4.2 and 4.3 respectively. The results for experiment 1 are presented in the appendix 4.

### 4.1.1 Results for batch adsorption experiments (1) using zeolites (2-3.15mm)

The analysis of this experiment showed some progress in adsorption, especially the sharon-anammox stream. However, during the analysis, the dilution factors used were very high (500 times) and therefore the results had some errors (Appendix 4).

### 4.1.2 Results for batch adsorption experiment (2) using zeolites (1-1.2mm)

The highest adsorption percentage was found in the 10 g zeolite mass for nitrification and sharon-anammox streams (Appendix 3), while the highest desorption percentages were found hydrolysis and struvite streams. Table 4.2 presents the concentration differences of 10 g zeolite masses, for 72 hours contact.

This experiment was carried out with using zeolites (2-3.15mm) at temperatures of 25°C ,as described in 3.2.2.3 with the diluted streams that had pH measurements as shown in Table 3.5.

There zeolites used were of smaller size than in exp 1 and 3.

**Table 4.2 Percentage adsorption and desorption for 10 g zeolite mass(1-1.2 mm) in experiment 2**

The table 4.2 below presents the difference in concentration during adsorption for a contact period of 72 hours ,at temperature 25°C

	$C_o$ (g/l)	$C_f$ (g/l)	$C_{diff}$ (g/l)	Percentage adsorption/desorption (%)
Hydrolysis	0.654	0.955	-0.301	-46
Struvite(MAP)	0.621	1.112	-0.491	-79
Nitrification	0.758	0.404	0.354	47
S/Anammox	0.653	0	0.653	100

Where  $C_o$  is initial concentration,  $C_f$  is final concentration after 72 hours contact time and  $C_{diff}$  is the concentration difference between the initial concentration ( $C_o$ ) and final concentration ( $C_f$ )

### 4.1.3 Results for adsorption batch experiment (3)

This experiment was a repeat of experiment 1, where the initial and final concentrations of potassium and sodium were determined for a period of 48 hours.

**Table 4.3 Potassium recovery from batch adsorption experiment (3) using zeolites of sizes 2-3.15 mm**

This table presents the average potassium recovery using four masses of zeolites for each urine stream at 25°C.

Amount of zeolites	Hydrolysis		Struvite		Nitrification		Sharon-anammox	
	Avg. conc. (g/l)	Potassium recovery (%)	Avg.conc. (g/l)	Potassium recovery (%)	Avg. conc. (g/l)	Potassium recovery (%)	Avg. conc (g/l)	Potassium recovery (%)
0g	<b>1.95</b>		<b>1.8</b>		<b>1.965</b>		<b>2.01</b>	
10 g	<b>1.4</b>	28.21	<b>1.245</b>	30.83	<b>1.46</b>	25.70	<b>0.906</b>	54.93
20 g	<b>1.075</b>	44.87	<b>0.959</b>	46.75	<b>1.195</b>	39.19	<b>0.4725</b>	76.49
30 g	<b>0.881</b>	54.82	<b>0.779</b>	56.75	<b>1.0025</b>	48.98	<b>0.3075</b>	84.70
40 g	<b>0.797</b>	59.13	<b>0.679</b>	62.31	<b>0.8675</b>	55.85	<b>0.234</b>	88.36

Where Avg.conc is the average concentration

## 4.2 Precipitation results

The table 4.3 below shows the summary of the batch experiment results together with their recovery rates and percentages in the precipitates respective precipitates. Both potassium and nitrogen were not very clearly visible in the EDX analysis spectrum of struvite and hydrolysis streams, and therefore more focus was on filtrate concentration changes.

**Table 4.4 The concentrations of potassium, phosphates and magnesium in the filtrates**

	Filtrate Concentration(mM/l)			Potassium recovery (%)	EDX Analysis (Percentage(%) by weight in Precipitate)		
	PO <sub>4</sub> <sup>3-</sup>	Mg <sup>2+</sup>	K <sup>+</sup>		PO <sub>4</sub> <sup>3-</sup>	Mg <sup>2+</sup>	K <sup>+</sup>
Initial concentration	52.36	52.38	59.85	-	-	-	-
Nitrification Mg:P= 1:2	15.26	0.00	23.90	60.07	18.66	13.83	7.37
Nitrification Mg:P= 2:1	17.58	0.00	27.69	53.73	19.05	22.29	9.71
Nitrification 25°C	0.71	3.28	27.44	54.16	21.79	17.47	9.78
Nitrification at 35°C	5.19	0.35	36.15	39.59	22.93	16.69	3.81
Initial concentration	52.36	52.38	55.45	-	-	-	-
Sharon anammox Mg:P=1:2	15.37	0.00	17.21	68.97	25.97	16.21	17.87
Sharon anammox Mg:P=2:1	0.00	1.46	24.92	55.05	21.52	24.41	11.26
Sharon anammox 25°C	1.44	0.00	22.13	60.09	22.35	16.68	15.96
Sharon anammox 35°C	0.55	0.63	21.77	60.74	20.24	17.4	12.68
Initial concentration	52.36	52.38	55.72	-	-	-	-
Struvite Mg:P=1:2	0.00	13.63	24.10	56.74	31.81	19.77	0
Struvite Mg:P=2:1	0.00	0.59	23.67	57.53	28.93	21.82	0.49
Struvite 25°C	1.09	13.79	53.59	3.82	22.87	29.76	0.53
Struvite 35°C	0.24	0.38	18.56	66.68	34.22	21.18	0
Initial concentration	52.36	52.38	57.89	-	-	-	-
Hydrolysis Mg:P=1:2	7.05	0.00	14.72	74.58	38.82	20.05	0
Hydrolysis Mg:P=2:1	0.00	22.21	37.95	34.45	22.63	28.89	0
Hydrolysis 25°C	0.65	0.47	59.23	0.00	29.92	22.86	0.39
Hydrolysis 35°C	0.09	0.45	18.95	67.27	30.72	21.39	0

--	--	--	--	--	--

In all the streams, the decrease of phosphates and magnesium concentrations was much higher than that of potassium. The highest potassium recovery was found in the hydrolysis sub-stream with magnesium-phosphates ratio of 1:2 with a 74% recovery. The lowest recovery was found on struvite 25°C and hydrolysis 35°C sub-streams with 3% and than 1% respectively.

There was also a considerable decrease in the concentration of the nitrates during the nitrification precipitation experiments as shown in table 4.5

**Table 4.5 The nitrate concentration recovery from nitrification stream**

	mMoles	Nitrate recovery (%)
Initial concentration	833.27	-
Nitrification Mg:P= 1:2	309.49	62.86
Nitrification Mg:P= 2:1	289.52	65.26
Nitrification at 25°C	344.57	58.65
Nitrification at 35°C	323.61	61.16

### 4.3 Analysis and Discussion

This section contains the analysis of batch adsorption and precipitation results. The adsorption experiments involved both 2-3.15 and 1-1.2 mm zeolites.

**Table 4.6 Combined Langmuir and Freundlich isotherms for experiments (1),(2) and (3)**

The table below shows the Langmuir and freundlich isotherms for the three experiments.

	Solution stream	Langmuir model data				Freundlich model data		
		R <sup>2</sup>	b (l/g)	q <sub>m</sub> (g/g)	R <sub>L</sub>	K	n	R <sup>2</sup>
Experiment 1 (2-3.15 mm zeolite sizes)	Hydrolysis	0.959	-0.12	-2.80E-02	1.31	3.90E-03	0.912	0.969
	Struvite	0.994	-0.12	-3.30E-02	1.27	4.40E-03	0.9	0.9962
	Sharon-Anammox	0.998	0.99	0.02	0.33	0.0121	1.51	0.990
	Nitrification	0.998	-0.11	-2.50E-02	1.28	3.20E-03	0.86	0.9957
Experiment 2 (1-1.2 mm zeolite size)	Hydrolysis	0.421	-1.57	-7.51E-04	-36.5	-	-	-
	Struvite	0.633	-1.75	-1.67E-03	-11.42	-	-	-
	Sharon-Anammox	0.999	10.83	0.016	0.12	0.018	2.85	0.940
	Nitrification	0.840	-0.57	-7.74E-03	1.76	7.5E-03	0.799	0.826
Experiment 3 (2-3.15 mm zeolite sizes)	Hydrolysis	0.3422	-0.97	5.93E-04	-0.926	1.90E-03	4.81	0.4254
	Struvite	0.5573	-0.76	1.75E-04	-2.1	5.30E-03	-0.29	0.6493
	Sharon-Anammox	0.7029	72.44	8.63E-03	6.03E-03	0.0095	7.41	0.6263
	Nitrification	0.884	-0.5	-3.38E-03	-8.16	3.90E-03	1.65	0.3821

#### 4.3.1 Batch adsorption experiment (2) using zeolites (1-1.2 mm)

This experiment gave more insight on effect of dilution to the four treatment streams. This is in comparison to the batch experiments (1) and (3) where there was no dilution in the solution with the aim of representing source separated urine.

Sharon-anammox still gave the best adsorption potential. Hydrolysis and Struvite streams had much of desorption than adsorption. This could be because of both; the use of smaller particles which increase the surface area for ammonia adsorption, and the difference in concentration gradient between the adsorbent and the solution.

The nitrification stream had shown a good trend and nearly all the masses had started approaching equilibrium concentration in less than ten hours. There was a steady decrease in potassium concentration with increase in contact time. This also indicates possible adsorption and desorption for masses of grams 1 and 5. For 1 g mass, there was no major effect as it probably stabilized at 50 hours of contact time with the solution.

The sharon-anammox on the other hand had a clearly significant decrease in Potassium concentration, especially in the highest amount of zeolite. Generally all the masses showed a steady decrease in Potassium concentration. This could be because of the lower ionic strength of this stream. This is shown in the kinetics of the each stream in figure 4.1.

The Langmuir and freundlich isotherms were only analysed for sharon-anammox and nitrification streams (figure 4.2) because there was adsorption as opposed to struvite and hydrolysis where there was desorption.

In the sharon-anammox stream, corresponding concentration to the 10 gram mass of zeolite was excluded because the concentration was below the limit of the analytical instrument used, and hence could not be used in comparison of both the Langmuir and Freundlich isotherm models.

The Langmuir model fitted well in this stream. It had a high correlation coefficient ( $R^2=0.9992$ ). It had also the highest monolayer adsorption capacity ( $q_m$ ) = 0.016 g/g. The separation factor ( $R_L$ ) was 0.13, which indicates favourable adsorption.

For nitrification stream, the Langmuir model had a good correlation coefficient ( $R^2=0.8404$ ). However adsorption capacity (adsorbate loading) ( $q_m = -7.74E-3$  g/g) and the equilibrium adsorption coefficient ( $K = -0.57$  l/g) was negative, possibly indicating the equilibrium concentration had not reached. The Langmuir separation factor ( $R_L$ ) was 1.76, which is also unfavourable for this model.

#### *4.3.1.1 Freundlich isotherms for experiment (2) using 1-1.2 mm zeolites*

The sharon-anammox stream had a higher equilibrium adsorption constant ( $K$ ) than that of nitrification stream.

The freundlich model had the equation =  $(0.0137) x^{0.1882}$ , with a strong correlation coefficient  $R^2=0.94$ . Similarly, this stream had the highest adsorption capacity ( $K=0.018$ ) and a favourable adsorption intensity ( $n=5.3$ ).

For the nitrification stream, the freundlich model equation, was  $q = (0.0075) x^{1.2516}$ , and had also a strong correlation coefficient ( $R^2=0.826$ ). The adsorption capacity,  $K$  was rather small (0.0075) with the adsorption intensity being unfavourable ( $n=0.799$ ). This implies that this stream is not favourable for this model.

The sharon-anammox stream therefore fits the freundlich model more than the nitrification stream.

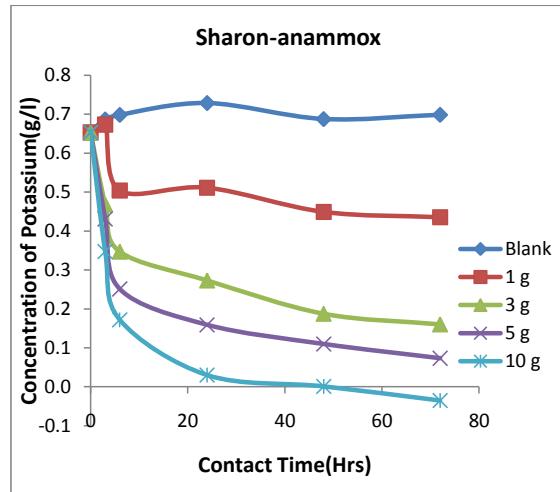
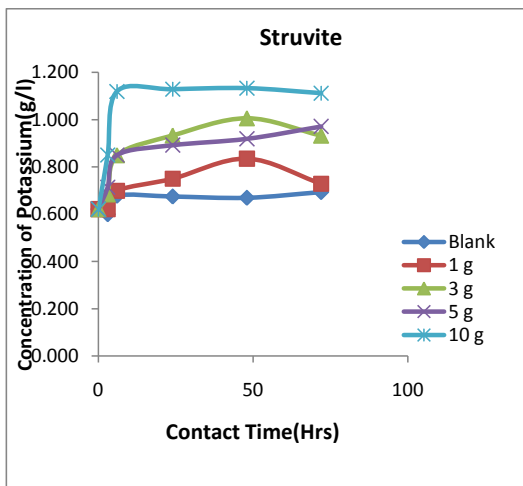
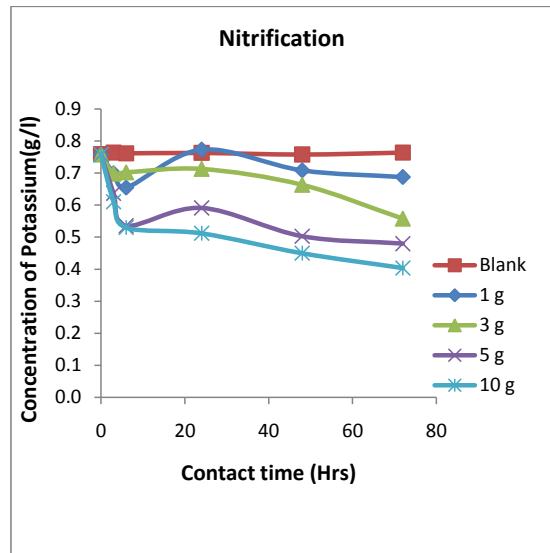
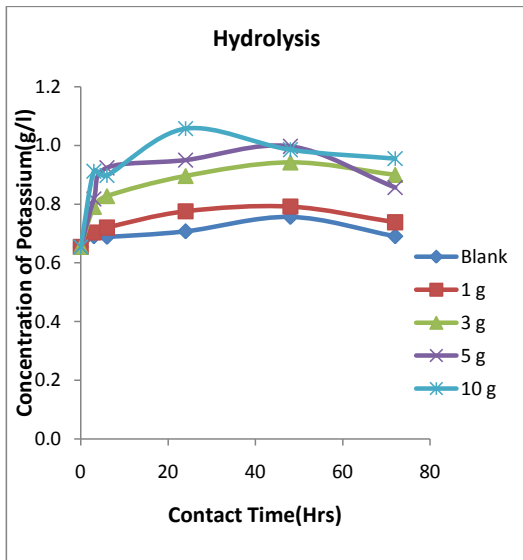
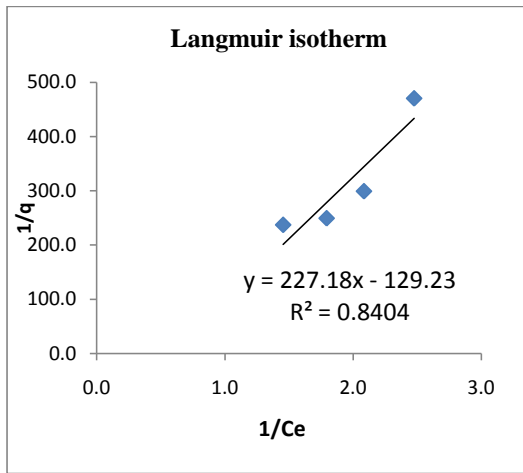
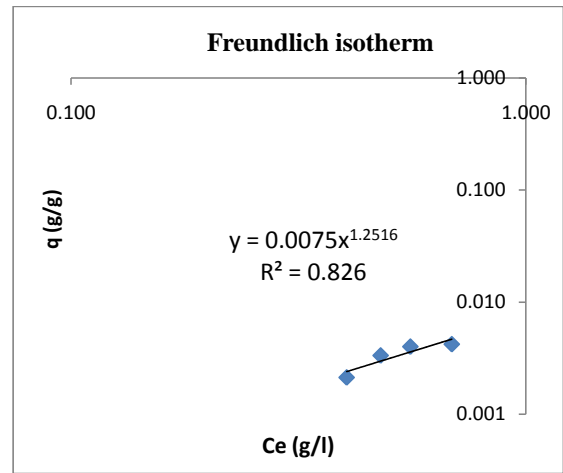


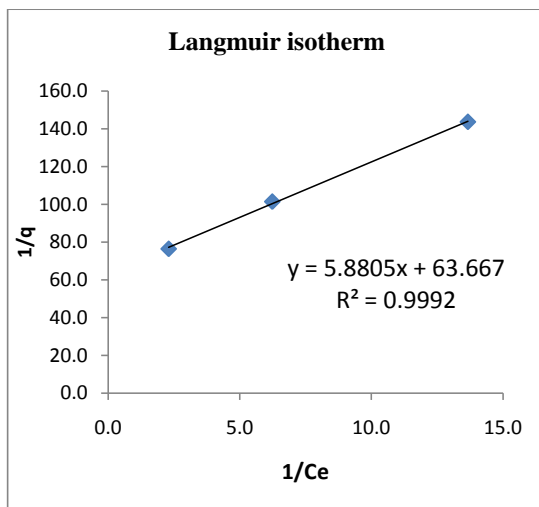
Figure 4.1 Adsorption kinetics for experiment 2 with zeolites (1-1.2mm)



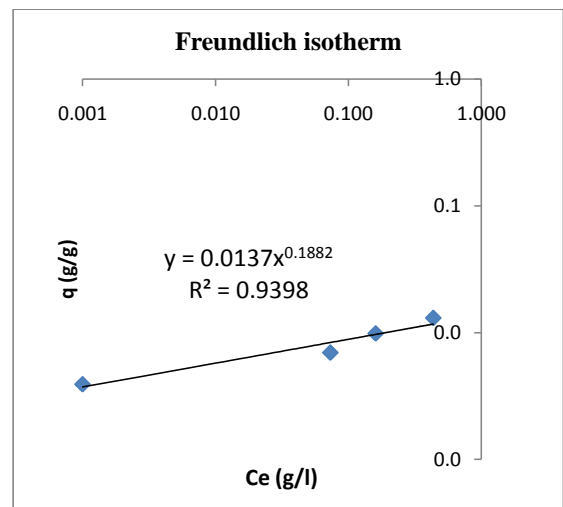
The Langmuir isotherm for the nitrification stream in experiment 2



The Freundlich isotherm for the nitrification stream in experiment 2



The Langmuir isotherm for the sharon anammox stream in experiment 2



The Freundlich isotherm for the sharon anammox stream in experiment 2

Figure 4.2 The Langmuir and Freundlich isotherm for experiment 2 (with 1-1.2 mm zeolites)

### 4.3.2 Batch adsorption for experiment (3) using zeolites (2-3.15mm)

The results for batch experiment (3) are presented in table 4.2. The zeolites of diameter between 2-3.15 mm were used. All the streams were exposed to a contact period of 48 hours.

The ICP spectrometer was used for analysis. The Langmuir and Freundlich adsorption isotherms were developed for each urine stream as shown in table 4.5.

#### 4.3.2.1 The Langmuir adsorption isotherms for batch adsorption experiment (3)

Adsorption in the hydrolysis stream was not favourable using the Langmuir adsorption model, although it had a strong correlation coefficient ( $R^2=0.9586$ ).

The equilibrium adsorption constant (b) was -0.12 l/g as the monolayer adsorption capacity ( $q_m$ ) was -0.028g/g of zeolite. The Langmuir separation factor ( $R_L$ ) was 1.31 which is beyond the favourable range. In this stream, the highest removal of potassium was 59.13% (40 g zeolite mass) while the lowest was 28.21% (10 g zeolite mass). Similarly, the struvite stream did not perform well using the 2-3.15 mm of zeolites. The Langmuir components had negative values. The equilibrium adsorption constant (b) was -0.118 l/g, and the monolayer adsorption capacity ( $q_m$ ) was -0.0033 g/g of zeolite. Also, the separation factor was 1.27 which indicates its unfavorability.

The highest removal of potassium was at 62.31%, with zeolite mass of 40 g, while the lowest was 30.83%.

The nitrification stream had the highest ionic strength (78.9 mS/cm) of the four, with high concentrations of nitrates. The adsorption process carried out using the 2-3.15mm zeolite was also not favourable using the Langmuir model. The Langmuir's equilibrium adsorption constant ( $b= -0.1$  l/g) was a negative value as well as the monolayer adsorption capacity ( $q_m = -0.025$  g/g of zeolite). The Langmuir separation factor ( $R_L$ ) was 1.28 which was beyond the favourable limit.

The sharon-anammox stream was the only stream that was favourable with the Langmuir adsorption model. The equilibrium adsorption coefficient (b) was highest, which was 0.99 l/g. The monolayer adsorption coefficient ( $q_m$ ) was 0.02 g/g of zeolite and separation factor ( $R_L$ ) as 0.33.

This stream had an average potassium removal of 76.12%. The highest removal was 88.36% (with 40g zeolite mass) and lowest removal was 54.93% (with 10 g zeolite mass). This stream also gave the best results for both the Langmuir and freundlich models.

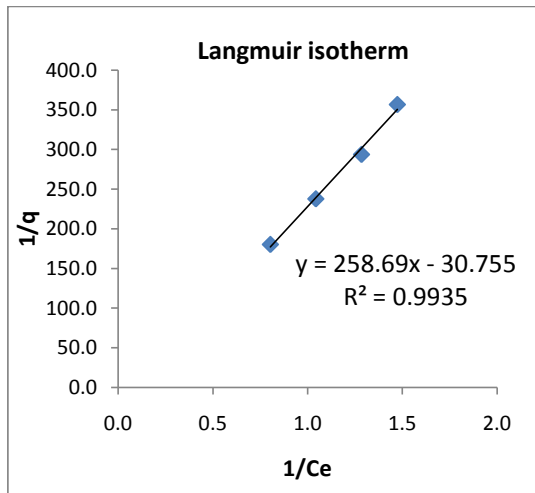
#### 4.3.2.2 The Freundlich isotherms for experiment (3) using zeolites (2-3.15mm)

This Sharon-anammox stream had the lowest ionic strength of the four and also gave the highest adsorption capacity (K) of 0.0121, as well as the adsorption intensity (n) of 1.51. The equation was  $q = 0.0121C^{0.6634}$ , where the adsorption capacity (K) was 0.012, adsorption intensity (n) = 1.51 and correlation coefficient ( $R^2$ ) being 0.99.

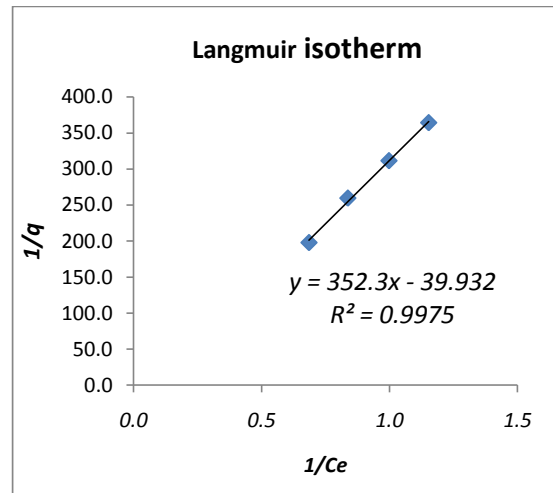
This was followed by the struvite stream which had an adsorption capacity (K) of 0.0044 and adsorption intensity (n) of 0.90. It also had a strong correlation coefficient ( $R^2 = 0.9962$ ). The equation was  $q = 0.0044x^{1.1054}$ . The adsorption capacity (K) was 0.0044, with an adsorption intensity constant (n=0.9).

The hydrolysis stream also fitted well in the Freundlich model with a strong correlation ( $R^2 = 0.969$ ). The adsorption capacity (K) was 0.0039, which was ranked third after Sharon-anammox and struvite streams. The adsorption intensity (n) was 0.91. The adsorption intensity (n) was found to be 0.91. The equation was  $q = 0.0039x^{1.0966}$ , where the adsorption capacity (K) as 0.0039.

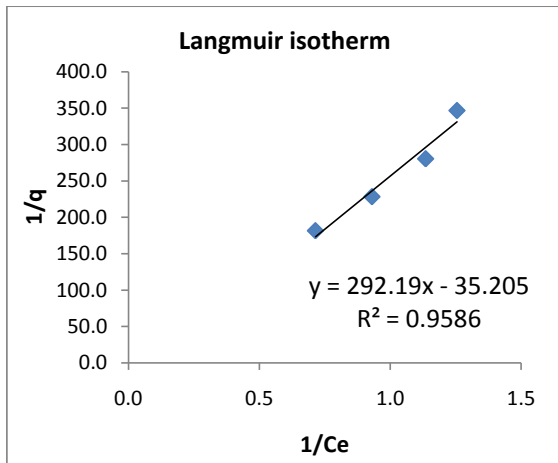
The nitrification stream was the least in performance. Its adsorption capacity (K) was 0.0032 and the intensity (n) was 0.86. The Freundlich equation isotherm equation was found to be  $q = 0.0032x^{1.1628}$ , with an adsorption intensity (n) of 0.86; adsorption capacity (K) of 0.0032 and coefficient correlation,  $R^2 = 0.9957$ .



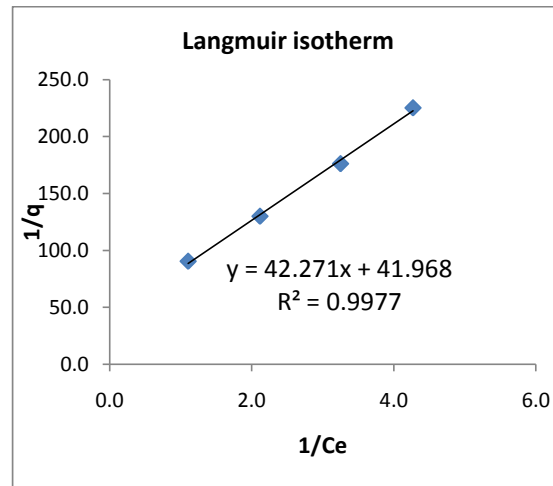
Langmuir isotherm for struvite stream in experiment 3



Langmuir isotherm for the nitrification stream in experiment 3

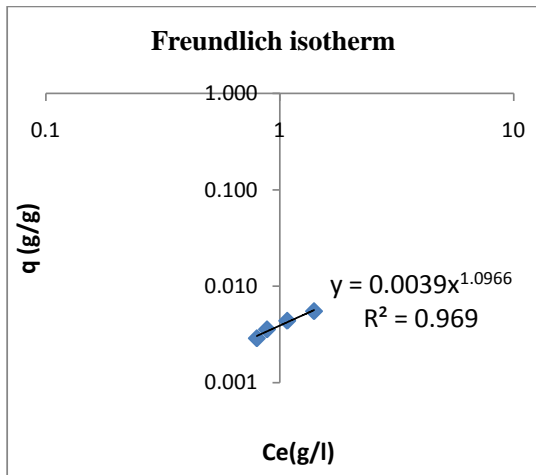


Langmuir isotherm for hydrolysis stream in experiment 3

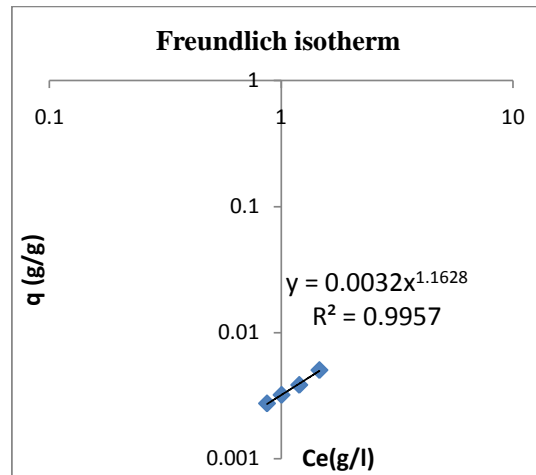


Langmuir isotherm for sharon-anammox stream in experiment 3

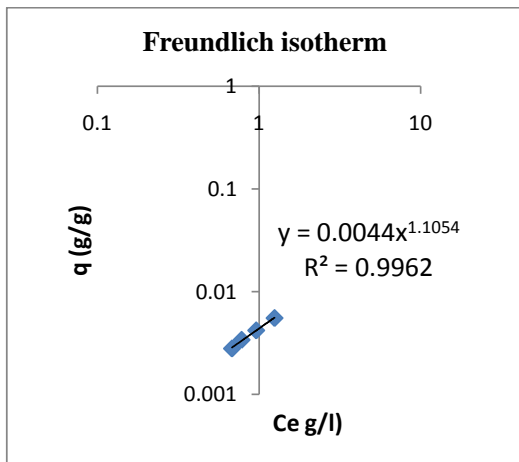
**Figure 4.3** The Langmuir isotherms for experiment 3 (using 2-3.15 mm of zeolite)



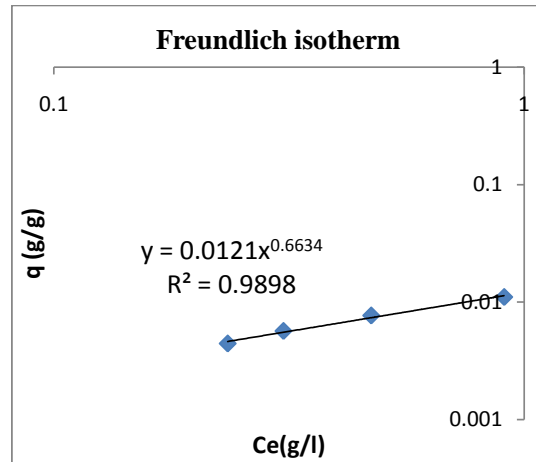
Freundlich isotherm for hydrolysis stream in experiment 3



Freundlich isotherm for nitrification stream in experiment 3



Freundlich isotherm for struvite stream in experiment 3



Freundlich isotherm for sharon-anammox stream in experiment 3

**Figure 4.4** The Freundlich isotherms for experiment 3 (using 1-1.2 mm of zeolite)

### 4.3.3 Precipitation

This section presents the initial concentrations of key ingredients before precipitation and after precipitation in the filtrates.

There were changes on both the electrical conductivity and pH using the 1.0 molar sodium hydroxide and 2.0 molar hydrochloric acid to determine the suitable range for precipitation.

**Table 4.7 The pH and Electrical conductivity of the solution streams**

Urine stream	Initial		Final		Duration(mins)
	pH	EC(mS/cm)	pH	EC(mS/cm)	
Hydrolysis	10.54	51.4	10.36	56.9	45
Struvite(MAP)	10.61	54.5	10.32	61.8	45
Sharon-anammox	5.73	16.98	12.03	23.4	45
Nitrification	4.24	78.9	9.85	72.1	45

### 4.3.3.1 Nitrification

There was a high concentration of nitrate ions in this stream. The nitrate ions are known to be inert are non-complexing (Dzombak and Morel, 1990) and therefore not expected to interfere with precipitation process greatly. However, there was considerable removal of nitrates from the sub streams, where the highest recovery was in the sub-stream of nitrification (Mg:P-2:1) with a recovery of 65%. This shows the possible formation of magnesium nitrate which was incorporated in the precipitate.

For potassium recovery, there was a clear decrease in the three ingredients in all the urine streams. The nitrification (Mg: P=1:2) gave the highest recovery in this stream with 60.07%, while nitrification 35 gave the lowest with 39.59%.

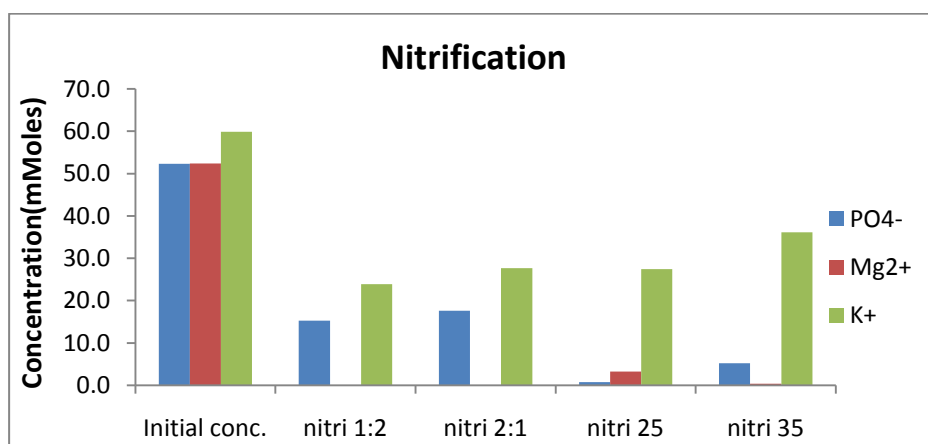


**Figure 4.5 The concentration of potassium, phosphates and magnesium in the nitrification filtrate stream**

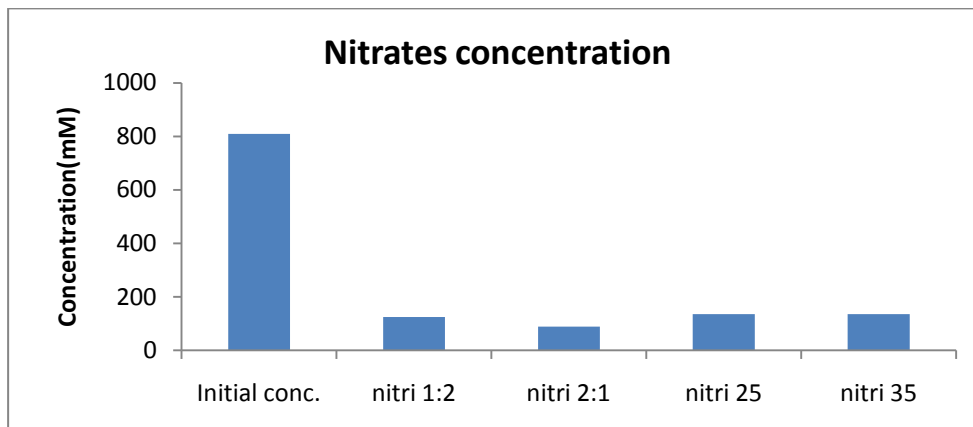


**Figure 4.6** The concentration of nitrates in the filtrate of nitrification stream

The highest potassium removal was found out from the sub-stream of Nitrification (Mg: P-1:2), with a 60% recovery, but a low 7.37% potassium recovery by weight (3.94% by atom) in the precipitates. The filtrates had the lowest amount of potassium concentration which indicates that this precipitation stream gave the highest potassium removal (60.07%). The PHREEQC model predicted the highest precipitation potential of potassium struvite (SI=1.26) in this stream.

The lowest potassium recovery was found in the sub-stream, nitrification 35<sup>0</sup>C with 39 % recovery.

There was a 3.81% potassium recovery by weight (2.04% by atom). Considering the concentrations in the filtrates, the potassium removal was lowest in this case (39.59%). This indicates poor recovery in this precipitation stream. The PHREEQC model predicts the precipitation of potassium struvite (SI=1.13), but at a lower potential than the nitrification stream at 25<sup>0</sup>C. The model also predicts the existence of potassium ion in solution in the form of complexes with the phosphates and hydroxyl ions.

In the case of nitrification 25<sup>0</sup>C sub stream, there was a higher recovery than nitrification 35<sup>0</sup>C sub-stream. A 9.78% potassium recovery by weight (5.21% by atom) was realised. However; the PHREEQC model predicted a considerable amount of potassium in solution, forming complexes with the hydrogen phosphate and dihydrogen phosphate ions. This could account for the high concentration of potassium in the filtrate.

In the nitrification (Mg: P-1:2) sub-stream, 63% of nitrates were recovered from the solution. Besides that, the magnesium was depleted. In comparison to the nitrification (Mg: P-2:1) sub-stream, where 53% of potassium was recovered, a 65% recovery of the nitrates was achieved. Similarly, like the nitrification (Mg: P-1:2) sub-stream, the magnesium was also depleted from the solution. But the fraction of phosphates recovered was almost similar to the nitrification (Mg: P-1:2) sub-stream given that both had different amounts of phosphorus and magnesium. This implies a possible formation of magnesium nitrate which is incorporated in the precipitate. Considering the EDX spectrum analysis, 7% and 9% of potassium were recovered in the precipitates of nitrification Mg: P- 1:2 and nitrification Mg: P - 2:1 sub streams respectively. This confirms the presence of potassium struvite in the precipitates.

There was a higher potassium removal from nitrification 25<sup>0</sup>C sub-stream than nitrification 35<sup>0</sup>C sub-stream. This could be due to the increase in temperature in the latter which could have led to increase in solubility of struvite thus a lower recovery (Le Corre, 2006).

#### 4.3.3.2 Sharon-anammox

This stream had the highest potential in recovery since it had the lowest ionic strength. Ammonium as the main competitor for potassium was absolutely absent as is expected in the real sharon-anammox process. All the precipitates from this stream had some potassium, and also the overall potassium removal was the highest.

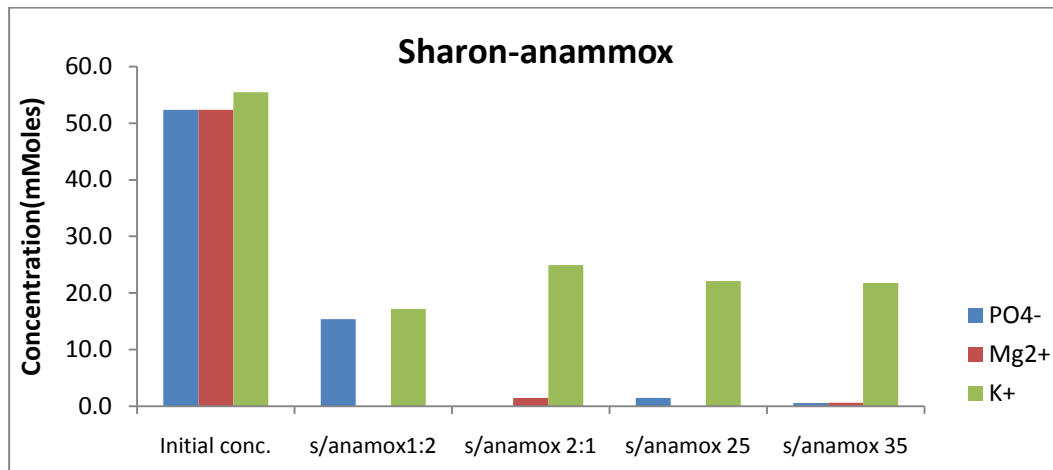


Figure 4.7 The concentration of potassium, phosphates, and magnesium in the filtrate

The Sharon-anammox stream had a low pH (5.73) apart from the low ionic strength, which was adjusted to 7.5. Generally, in all the sub-streams generated from the nitrification main stream, there was a reduction in pH during the formation of precipitates. This is similar to Wilsenach *et al.* (2007) findings, where they reported more participation of hydrogen phosphate than phosphate ion in potassium struvite formation, hence liberating a proton which reduces the pH. Generally in this stream, the PHREEQC model predicts low saturation indices for potassium struvite. This could be due to increased potential of precipitation of potassium struvite which lowers the pH significantly and the ionic strength. The highest potassium recovery was in the sub-stream sharon-anammox (Mg: P-1:2) with a 68% recovery, while the lowest was in the sub-stream sharon-anammox (Mg: P-2:1) with a recovery of 55%. This could be due to the roles of both phosphate and magnesium ions; where with reduction of pH due to potassium struvite protons are liberated in solution. This would increase the net positive charged ions in solution more than the available anions and hence reduce the potential of the sub-stream.

The sharon-anammox (25°C) and (35°C) streams both gave a similar recovery percentage. Also the depletion of the constituent components decreased almost with the same concentration. In addition, the percentage recovery of potassium in the precipitate was also similar.

The Sharon-anammox (25°C) involved precipitation at 25°C, with the precipitation ingredients (Magnesium and phosphorus) added in the same molar ratio as the potassium

in the solution. The EDX analysis shows similar amounts of magnesium and phosphorus in the precipitate. There is also presence of potassium, which indicates potassium struvite, although has a very low precipitation potential predicted by the PHREEQC model (SI=0.74). The potassium recovery was 15.96% by weight (9.15% by atom) while that of sharon-anammox (35<sup>0</sup>C) had a potassium recovery of 12.68% by weight (7% by atom).

The sharon-anammox (35<sup>0</sup>C) sub-stream had the same conditions with sharon-anammox (25<sup>0</sup>C) except the temperature was elevated in this case. There was also a considerable amount of potassium in solution, although both magnesium and phosphates were almost depleted indicating possible formation of other complexes. The precipitation potential was predicted at a lower saturation index (SI=0.66) than the sharon-anammox stream at 25<sup>0</sup>C, but both had the same removal rate of potassium from the solution (65%).

Sharon-anammox Mg: P=1:2 had the lowest peaks in the EDX analysis compared to other Sharon anammox precipitation sub-streams. There was presence of potassium struvite in the precipitate, with a potassium recovery of 17.87% by weight (10.61% by atom) and also with the highest potassium removal in the precipitate (72.8%). The PHREEQC model predicted saturation of potassium struvite (SI= 1.02).

As for the sharon-anammox Mg: P=2:1 sub-stream, there was an increased magnesium peak in the precipitate as compared to phosphorus and potassium because the increased magnesium concentration. The precipitation of potassium struvite was predicted by the PHREEQC model (SI=1.21), as it is also in the precipitate. The potassium recovery was 55% from the stream and constituted 11.26% by weight (6.38% by atom) in the precipitate.

#### 4.3.3.3 Struvite

This stream has a high concentration of ammonium ions, which favour the formation of the struvite MAP. In the precipitation processes, the struvite 25<sup>0</sup>C sub-stream had the lowest removal of potassium, while struvite 35<sup>0</sup>C stream had the highest removal as per the concentrations in the filtrates. This is owed to the presence of very high concentrations of ammonium which act as a competitor to potassium (Wilsenach *et al*, 2007). Therefore; the potassium recovery was poor in this stream. The nitrogen component, which represents the ammonium component in struvite MAP, was equally low because of volatilization during drying at 105<sup>0</sup>C (Tettenborn *et al.*, 2007).

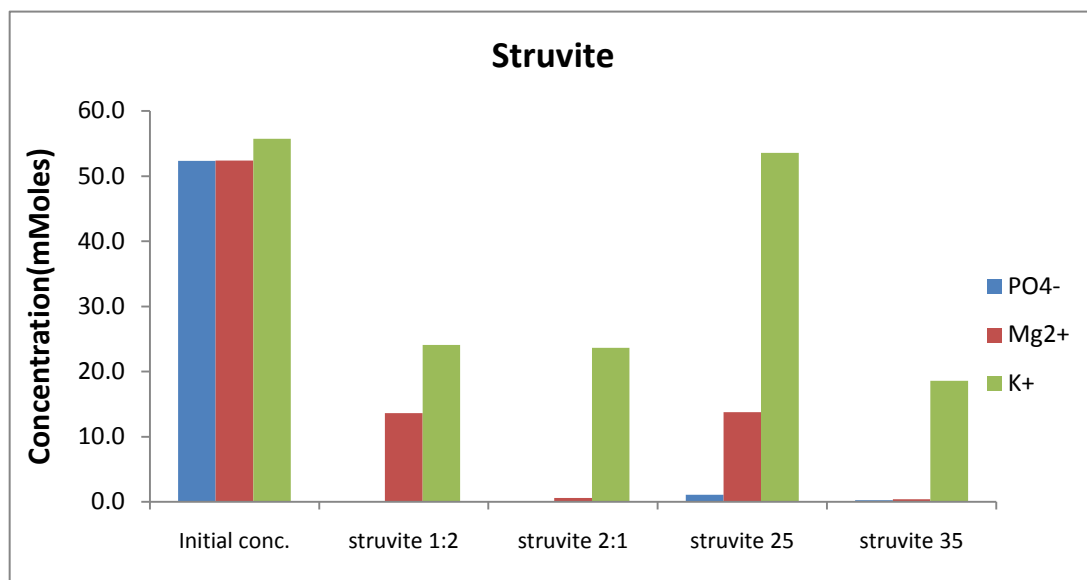


**Figure 4.8** The concentration of phosphates, magnesium and potassium in precipitation filtrate

The stream also had a high alkalinity (pH = 10.61) and ionic strength (54.5 mS/cm). This required the reduction of the pH to about 8.5 using 2 molar hydrochloric acid, in order to monitor an appropriate range suitable for a real stream that has undergone struvite recovery, before potassium is recovered. This was done in order to prevent the reduction of magnesium concentration by forming magnesium hydroxide (Du, *et al.*, 2005), since the ammonium concentration was too high to achieve any significant impact at that pH value. Secondly, this is also because struvite formation reduces the pH gradually (Tettenborn *et al.*, 2007), which is expected in a urine stream that has undergone struvite recovery.

Lastly, to allow manipulation of pH within the range 8.5 to 9.5 using 1.0 molar sodium hydroxide in this case. This is reported by Le Corre (2006) as the optimum pH for struvite recovery.

The different ratios of magnesium and phosphates applied were aimed at determining the limiting element in the precipitation process. In struvite (Mg: P-1:2) sub-stream, phosphate amount added was twice the concentration of magnesium and potassium in solution. During the precipitation, the phosphate component was depleted, as the concentration of both magnesium and potassium still remained considerably high. This implies possible formation of ammonium phosphate and other sodium related compounds like; sodium phosphate and disodium hydrogen phosphate.

The reduction in phosphates was confirmed from the EDX analysis where phosphates gave a higher peak than magnesium. The potassium recovery was 56.74% in the precipitate. The PHREEQC model predicted both the precipitation of struvite MAP (SI= 4.53) and potassium struvite (SI= 1.09). This could imply a precipitation of both struvite MAP and potassium struvite.

Similarly, in the other sub-stream of struvite (Mg: P-2:1), the phosphates were depleted in solution. In this stream the phosphates were the limiting component. The magnesium concentration was added as twice as both the phosphorus and potassium in solution. Potassium recovery was realised in EDX analysis results of the precipitate. More so, the

filtrate also had a considerable lower potassium concentration. This indicates a low percentage of potassium struvite being incorporated in the precipitate together with struvite MAP, which covered the large option. The PHREEQC model also predicted precipitation of struvite MAP (SI=4.43), and potassium struvite (SI=1.16). This could possibly be because of ammonia loss during drying as the oven was maintained at 105<sup>0</sup>C .

The Struvite (25<sup>0</sup>C) sub-stream had the lowest recovery compared to struvite (35<sup>0</sup>C), although there was presence of trace potassium in the precipitate indicating a small proportion of potassium struvite. But the peaks of nitrogen species in the EDX analysis implied that struvite MAP was largely formed .This was also predicted by the phreeqc model, with struvite MAP (SI = 4.32) being potentially formed at higher proportion than potassium struvite (SI = 0.97).The low amount of potassium in the precipitate could be justified by the presence of high potassium concentration in the filtrates.

The struvite 35<sup>0</sup>C stream was expected to precipitate a higher amount of potassium struvite than struvite (25<sup>0</sup>C) sub-stream, because of the heat energy at elevated temperatures that will reduce the concentration of ammonium through volatilization. The potassium recovery was high at 66.68%.The PHREEQC model predicted both struvite MAP (SI = 4.28) and potassium struvite (SI = 0.84) to be precipitated which implies both struvite MAP and potassium struvite could be incorporated in the precipitate.

In summary, the struvite 35<sup>0</sup>C sub-stream gave the highest potassium recovery with 66%, while the lowest was struvite 25<sup>0</sup>C sub-stream with 3.8% recovery. This could be due to ammonium volatilization at increased temperatures (Tettenborn *et al.*,2007).For the struvite 25<sup>0</sup>C stream, the high concentration of ammonium ions could have inhibited the formation of potassium struvite, instead of struvite MAP (Wilsenach *et al.*,2007).

#### **4.3.3.4 Hydrolysis**

This stream had a high ionic strength (51.4 mS/cm). Figure 4.9 below shows the variation potassium concentration, together with the phosphate and magnesium in the filtrates of four different precipitation conditions. The hydrolysis stream at 25<sup>0</sup>C had no potassium removal, while the highest potassium removal was in the hydrolysis (Magnesium: Phosphorus stream with the ratio of 1:2) with 74.58%.

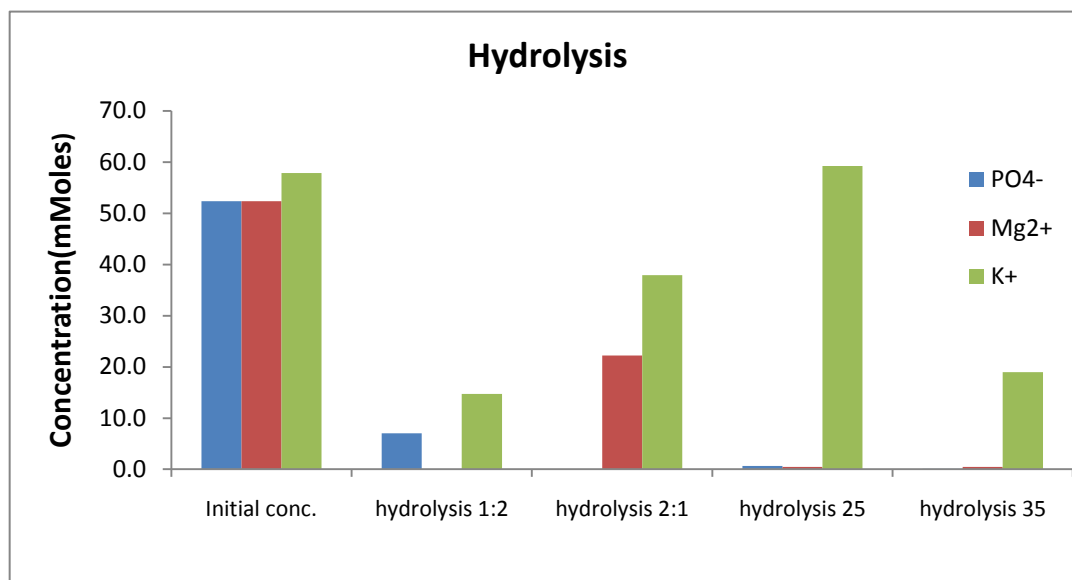


**Figure 4.9** The concentration of potassium, phosphates and magnesium in the filtrate

The concentration of bicarbonate and ammonia is also high which increases the pH (10.54). This pH was reduced also to about 9.27 using 2.0 M hydrochloric acid before starting the experiment.

This was done with the aim of attaining a pH value similar to the real hydrolyzed urine, with a pH of 9.1 (Udert *et al.*, 2006). Moreover, this was also done to prevent magnesium from forming Magnesium hydroxide thus reducing the available magnesium for precipitation (Song *et al.*, 2007).

The highest potassium recovery was the sub-stream of hydrolysis (Mg: P-1:2) with a 74% removal, while the lowest was the sub-stream of Hydrolysis 25°C with less than one percent.

The hydrolysis (Mg: P-1:2) stream had almost all both magnesium and phosphate depletion with a considerable decrease in potassium. This stream consisted of twice the concentration of phosphorus, as compared to magnesium. In the filtrates the magnesium was depleted, and both potassium and phosphates had low concentrations. Although both struvite MAP (SI=4.52) and Potassium struvite (SI=1.09) are predicted to precipitate in the PHREEQC model, struvite MAP would be the major precipitation component. The potassium still could be low in the precipitate. This would largely be a mixture of both struvite MAP and potassium struvite.

For hydrolysis (Mg: P-2:1), there was a complete depletion of phosphates but a high concentration of magnesium and potassium. The PHREEQC model predicted a higher saturation index for struvite MAP (SI= 4.42) than for potassium struvite (SI=1.16). There was a 34.45% potassium recovery, which implies unsuitability of this stream for precipitation of potassium struvite. This recovery percentage signifies the competition for phosphate ions between the cations in solution. This also implies the formation of different complexes with both potassium and magnesium (Abbona *et al.*, 1988). For hydrolysis 25°C stream, the high concentration of ammonium inhibited the formation of potassium struvite (Wilsenach *et al.*, 2007) and predominantly struvite MAP was formed.

The hydrolysis 35°C stream had much higher potassium recovery than hydrolysis 25°C, which could be attributed to more of ammonium volatilization with increase in

temperature (Tettenborn *et al.*, 2007) than increase in solubility of potassium struvite with the same (Le Corre, 2006). However, this was not clearly reflected in the EDX analysis spectrum.

The hydrolysis 25<sup>0</sup>C sub-stream EDX analysis shows low concentration of potassium in the precipitate, and presence of nitrogen. This implies struvite MAP was largely formed as opposed to potassium struvite. It also shows high magnesium and phosphorus concentrations. The PHREEQC model predicts a high saturation index for struvite MAP, than for potassium struvite. More so; the filtrate contains a high concentration of potassium, as magnesium and phosphates are almost used up. This implies that this precipitation stream is not conducive for potassium struvite.

For the hydrolysis (35<sup>0</sup>C) sub-stream, there were lower concentration peaks of magnesium and phosphates than hydrolysis (25<sup>0</sup>C). There were no traces of potassium that were detected, but the nitrogen component was present indicating presence of struvite MAP. More so, The PHREEQC model predicted both precipitation of struvite MAP (SI=4.27) and potassium struvite (SI=0.84), although the former has a higher saturation index. The filtrates also show a low concentration of potassium with 67.27% removal. This is also attributed to the volatility of ammonium at increased temperatures which acts as a competitor to potassium (Tettenborn *et al.*, 2007).

#### **4.3.4 Summary of discussion**

This section gives a summary of this chapter together with the influence of sodium in adsorption

##### *4.3.4.1 Recovery of potassium through zeolites*

The zeolite sizes used in this experiments were of sizes (2-3.15 mm) and (1-1.2 mm). The adsorption process increased with the increase in amount of zeolite. This can be seen in the concentration changes in the higher masses of zeolite in Tables 4.2 and 4.3.

The other major factor involved in the process is ionic strength which is determined the concentration of ions. This could be partly the reason that increased adsorption potential in the sharon-anammox stream. In addition to that, the sundstrom and Klei (1979) as mentioned in section 2.6.1, say that adsorption decreases with increasing ionic strength.

The high ionic strength of recipes nitrification, hydrolysis and struvite MAP had a much lower adsorption potential compared to sharon anammox stream. The main difference is the absence of bicarbonates and ammonium which increases the ionic strength as well acts as a competitor to potassium. This implies that elimination of nitrogen from urine can enhance better adsorption of potassium using zeolites.

The smaller sized zeolites (1-1.2mm) were used in a diluted recipe which resembles average dilution of urine from different sources as shown in table 3.5.

These zeolites were used in place of the previous large sizes because of the low adsorption capacity in their smaller quantities as seen in experiment 1 (appendix 4). The sharon anammox stream had also the best adsorption of the four streams. On the contrary, struvite and hydrolysis streams had complete desorption of potassium. This is due to the presence of ammonium as a competitor for adsorption sites. Ammonium is also favoured by the increase in concentration relative to potassium. The presence of other ions also could have affected the desorption process (Rezaei and Naeni, 2009).

Therefore, in summary the zeolites had a better adsorption in the absence of ammonia and in the low ionic strength stream, sharon anammox. This implies that hydrolyzed urine has to undergo treatment for the removal of ammonia before adsorption using zeolites.

#### *4.3.4.2 Recovery of potassium through potassium struvite precipitation*

Potassium struvite can be obtained in the absence of ammonium. This could be the reason for a higher potassium recovery in sharon anammox and nitrification streams than struvite and hydrolysis streams. Moreover, the increase in the concentrations of magnesium or phosphates increased the recovery percentage. This can be seen in table 4.4 for all the streams with magnesium-phosphorus ratio 2:1 and 1:2.

More so, the increase of temperature in both struvite and hydrolysis streams, where the precipitation was carried out at elevated temperature of 35°C, the potassium recovery increased. This implies the reduction of ammonia through volatilization. However, this experiment was carried out in a fume chamber and the ammonium concentration was not measured.

At normal room temperature of 25°C the hydrolysis and struvite streams had very low recovery rates. The ammonium concentration was high and this hindered potassium struvite precipitation. Therefore largely ammonium magnesium phosphate was precipitated. The sharon-anammox and the nitrification streams had a high potassium struvite recovery than struvite (MAP) and hydrolysis streams. This is mainly because of the absence of ammonium in sharon anammox and nitrification streams. In addition, sharon anammox had also a much lower ionic strength than the other three streams.

The nitrification streams also had a high concentration of nitrate. But during the KMP precipitation considerable reduction of nitrate was also observed (Table 4.3). Furthermore, the EDX analysis showed a small percentage of nitrogen in the spectrum.

#### *4.3.4.3 Exclusion of micro pollutants*

The micropollutants are capable of causing adverse environmental effects on the human health and environment (Pronk *et al.*, 2006). Nitrification process is known to degrade micro pollutants as mentioned in nitrification process (2.5.4) and struvite precipitation is known for separation of micro pollutants (Maurer *et al.*, 2006).

The combination of nitrification followed by potassium struvite precipitation or adsorption using zeolites can be a good scheme for recovery of potassium without the presence of micro pollutants.

This is because nitrification stream had considerably good potassium recovery percentages as seen on table 4.3, especially where the ratios of magnesium and phosphates were varied. The results showed a potassium recovery potential of at least 50%, where the other fraction can be recovered by adsorption using zeolites.

The sharon-anammox is not yet known to degrade micro pollutants, and it therefore requires artificial treatment using technologies like electro dialysis, nanofiltration and ozonation. These technologies are expensive and therefore not feasible in particular places like the developing world.

The hydrolysis process on the other hand, also does not degrade the micro pollutants but can reduce the pathogens significantly. This is because of the increased pH after hydrolysis of urea.

#### 4.3.4.4 Potassium recovery versus removal

As mentioned in section 1.3, potassium is not a pollutant on the surface waters as compared to the effects of nitrogenous and phosphorus compounds. Therefore potassium removal has not raised concerns in the environmental scale. However, recovery is an important component of sustainable management of natural resources. As mentioned in section 1.2, extraction of potassium could possibly affect biodiversity and also contaminate the water resources.

In addition to that, the growing human population also means increase in food demand. This also translates into growth in fertilizer demand which necessitates increased mining activities for the mineral to satisfy the demand. Recovery of potassium through potassium struvite precipitation provides three ingredients; magnesium, phosphorus and potassium, which are necessary for agricultural activities.

The recovery of potassium through adsorption also enables re-use of the zeolites in agricultural sector. The zeolites have been used as slow releasing carriers of nutrients. They also used in improving water balance in the soil by their capacity for hydration and dehydration. In other agricultural applications, they have also been used as feed additives in animal feed mixtures (Reháková, *et al.*, 2004)

The potassium struvite also is used as a fertilizer. Wilsenach (2005) reported the production of potassium struvite as fertilizer from a calf manure treatment at Putten, the Netherlands which is distributed to the local farmers in Netherlands. The biggest challenge with potassium struvite precipitation is the source of magnesium and phosphates.

The magnesium and phosphorus sources used in this study were analytical grade, and as such commercial products. Magnesium chloride presents the best characteristics than the other salts used, such as magnesium sulphate, magnesium oxide and magnesium hydroxide because of its high solubility although less content of magnesium.

Therefore, with the use of magnesium chloride as a magnesium salt, we would expect good precipitation results. Sea water acts as a potential source for the recovery of magnesium chloride (Etter, 2009) with a composition of about 1350 ppm (Snoeyink and Jenkins, 1980).

#### 4.3.4.5 Comparison of Sodium and Potassium adsorption in the Batch adsorption experiment (3) for 2-3.15 mm zeolites

There was considerable interference by increased sodium concentrations in the recipes. There was some adsorption of sodium in all the four streams. The highest adsorption was in struvite stream, while the lowest was in sharon-anammox. This is agreement with Cooney *et al* (1999) who reported that co-existing ions which include sodium, calcium and magnesium, in solutions that contain potassium and ammonium, possibly affect adsorption or desorption on clinoptilolite. Some of the concentrations of magnesium and calcium were below the detection limit of the ICP machine (Model ICP-OES, type Perkin Elmer Optima 5300 DV (Waltham), Massachusetts, USA), and hence could not be analyzed.

Table 4.8 shows changes in concentration for sodium within a period of 48 hours, during the potassium adsorption experiment at Wetsus using 2-3.15 mm zeolites. The concentration changes were determined by the difference between initial and the final concentrations (Appendix 4).

Sodium and potassium are both members of alkali metals (group 1A). Sodium has a smaller ionic radii (95 pm) while potassium has a higher ionic radii (133 pm). Therefore with the increased concentration, it could gather more access to adsorption sites besides the obvious effect on their concentration gradients (House and House, 2010).

**Table 4.8 Changes in concentration of Potassium and Sodium during the adsorption in experiment 3 with zeolites (2-3.15mm)**

<i>Mass of Zeolite</i>		<i>Change in concentration(g/l)</i>			
		10 g	20 g	30 g	40 g
<i>S/Anammox</i>	Sodium	-0.01	0.05	0.25	0.355
	Potassium	1.104	1.538	1.703	1.776
<i>Nitrification</i>	Sodium	0.5	0.7	1.1	1.55
	Potassium	0.505	0.77	0.963	1.098
<i>Struvite</i>	Sodium	0.45	0.65	1.45	1.7
	Potassium	0.555	0.842	1.022	1.122
<i>Hydrolysis</i>	Sodium	0.25	0.9	1.55	1.4
	Potassium	0.55	0.875	1.069	1.153

The amounts of sodium in the solution compared to potassium were very high, and any change could not be represented in the form of percentages. The highest change in sodium concentration was found in the struvite stream (for the 40 g zeolite), at 1.7 g/l, while the lowest was in the sharon-anammox stream at 0.355 g/l (for the 40 g stream).

It was not possible to add in the same amount of sodium in nitrification, for instance, in other streams with the aim of lowering the effect of high concentration. This is because, other streams, precisely struvite (MAP) and hydrolysis, had already high concentrations of sodium and this could increase the ionic strength beyond comparable levels with the streams represented.

The sharon-anammox stream had sodium concentrations as expected in the recipe. On the contrary, the nitrification stream had the highest concentration of sodium, because sodium nitrate was used to provide the nitrate ions. In the struvite stream, sodium was elevated in providing both bicarbonate and chloride ions. Lastly, in the hydrolysis stream elevation of sodium was similarly done through the addition of hydrogen carbonate ions.

#### **4.3.5 Limitations encountered in the experiments**

Most of the objectives in this experiment were met, although there were limitations;

- i. The use of sodium hydrogen carbonate as an ingredient in recipes of hydrolysis and struvite streams, and sodium nitrate in nitrification streams, elevated the sodium concentrations beyond the expected recipe concentrations. This resulted in interference with the adsorption and precipitation process.
- ii. Lack of monitoring facilities that can determine the concentration changes of constituent elements during the precipitation process.
- iii. The PHREEQC (Version 2) was designed for aqueous solutions which are suitable for low ionic solutions (Parkhurst and Appelo, 1999). Apart from the sharon anammox solution stream, the other three streams; hydrolysis, struvite MAP and nitrification, had a relatively high ionic strength. Parkhurst and Appelo (1999) further point out, that solutions with high concentration of sodium chloride, the model reliability increases.

## 5.0 RECOMMENDATIONS AND CONCLUSION

The main purpose of this study was to determine the composition of four urine treatment streams and their respective potassium recovery potential. Therefore, the specific conclusions derived from this study are;

- i. The sharon-anammox stream was the best stream for potassium recovery using both adsorption and precipitation processes respectively.
- ii. Urine solutions with low ionic strength would increase the recovery potential of potassium in both adsorption and precipitation processes.
- iii. The complete removal of ammonia in a urine solution would also increase the potassium recovery potential. This implies that potassium could be best recovered in the absence of ammonium in the hydrolysis and struvite MAP streams. This could be the reason for low recovery in the hydrolysis and struvite streams.
- iv. The adsorption process performed better than precipitation in terms of potassium recovery;  
This is because precipitation required addition of magnesium and phosphates in order to recover potassium. The highest percentage recovery(74%) was the hydrolysis sub-stream(Mg:P-1:2) with twice the concentration of phosphorus as compared to magnesium and potassium in solution. The zeolites on the other hand, are low cost and the adsorption increases with increase in surface area and mass.

Based on the conclusions, following recommendations are proposed;

- i. The experiment should be carried out using real urine streams that have undergone sharon-anammox, struvite MAP precipitation, nitrification and hydrolysis processes.
- ii. Real urine contains both organic and inorganic compounds. The four treatment processes could be quantitatively analyzed on their recovery potential given treatment measures like degradation of micro pollutants and organic compounds.
- iii. The contact period of adsorption to be investigated further in determination of an appropriate equilibrium concentration;  
This factor should be investigated further in order to determine adsorptive and desorptive characteristics of the zeolite used. This will also determine the suitable quantity and particle size for efficient in the real urine streams.
- iv. The suitability of alternative non-commercial sources of phosphates and magnesium should be investigated on their performance with precipitation .The economic and qualitative application of sea water and sewage sludge for the supply of magnesium and phosphorus in potassium struvite recovery should also be investigated.
- v. A combination of both precipitation and adsorption to be investigated to determine their combined potassium recovery potential, with possible application of the recovered products. The recovery potential from this study could provide guidance

towards a suitable combination of treatment processes that can possibly optimize the safe recovery of potassium.

Precipitation process enhances complete separation of the solid phase with the liquid. This enables qualitative and quantitative analysis of both the precipitate and the filtrate.

Based on this study, the nitrification stream is capable of 50 % recovery of potassium and 60 % recovery of nitrates through precipitation. Similarly, according to Gujer (2010) and Pronk and Kone (2009), nitrification is capable of completely eliminating micro pollutants.

This could be used in combination with zeolite to increase the potassium recovery potential to more than 90%.

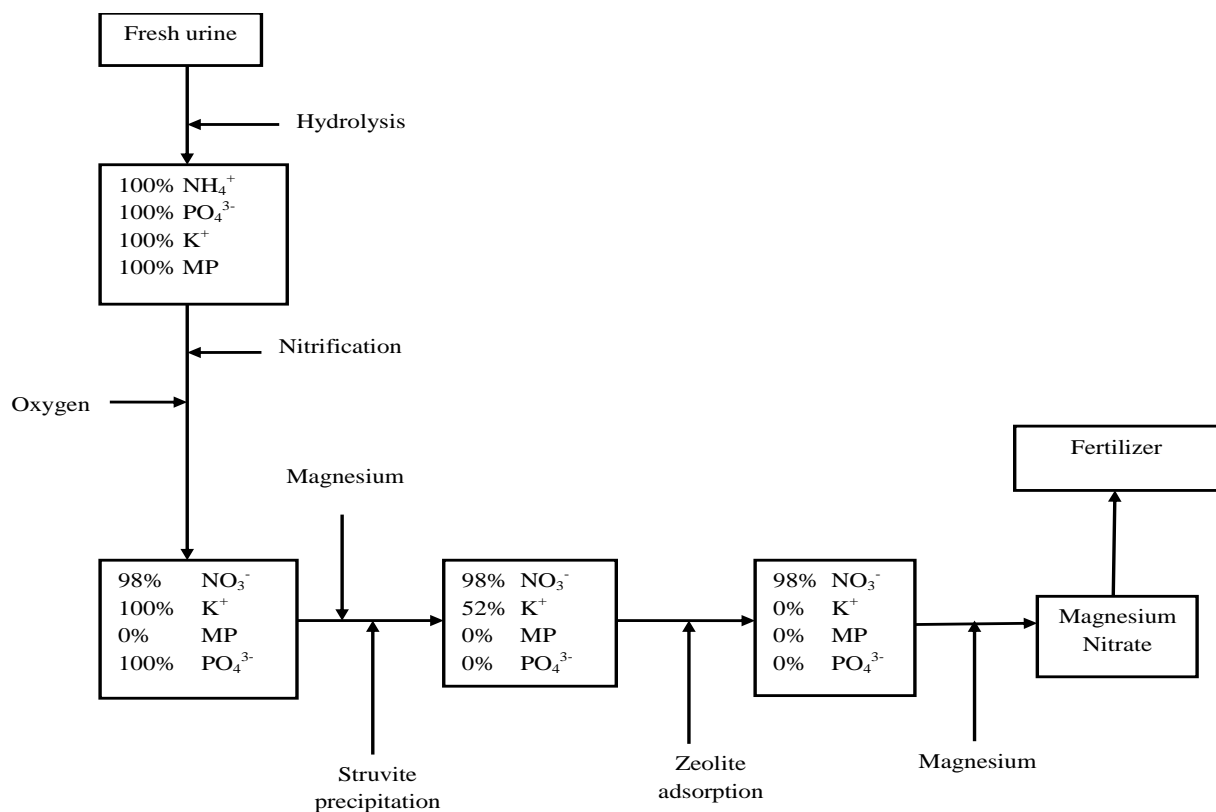


Figure 5.1 Proposed scheme for adsorption and precipitation

## REFERENCE

- Abbona, F., Madsen, H.E.L., Boistelle, R., 1988. The final phases of calcium and magnesium phosphates, struvite and newberyite-effect of pH and concentration. *J. Cryst. Growth*, 57(1), 6-14.
- Abeling, U., Seyfried, C.F. (1992). Anaerobic-aerobic treatment of high strength ammonium wastewater-nitrogen removal via nitrite. *Water Science & Technology*, 26(5-6), 1007-1015.
- Ahalya, N., Kanamadi, R.D., Ramachandra, T.V (2005) Biosorption of chromium (VI) from aqueous solutions by the husk of Bengal gram (*Cicer arientinum*). *Journal of Biotechnology*, 8 (3).
- Ames, L.L (1960) The cation sieve properties of clinoptilolite, *Am. Mineral.* 45. pp 689-670.
- Asano, T., Burton, F.L., Leverenz, H.L., Tsuchihashi, R., Tchobanoglous, G. 2007. *Water reuse : issues, technologies, and applications*. Metcalf & Eddy, Inc.
- APHA (2005). *Standard methods for the examination of water and wastewater*, 21st edition, American public health association
- Booker N.A., Cooney E.L. and Priestley A.J. (1996). Ammonia removal from sewage using natural Australian zeolite. *Wat. Sci. Tech.*, 34, 17–24.
- Bouropoulos NC, Koutsoukos PG (2000) Spontaneous precipitation of struvite from aqueous solutions. *Journal of Crystal Growth* 213: 381-388
- Balmer, P. (2004). Phosphorus recovery-an overview of potentials and possibilities. *Water science and technology*. 49 (10), 185-190.
- Bhuyian, M.I.H., Mavinic, D.S., Beckie, R.D (2007). A solubility and thermodynamic study of struvite. *Environ. Technol.* 28. (2007)1015
- Bouropoulos NC, Koutsoukos PG (2000) Spontaneous precipitation of struvite from aqueous solutions. *Journal of Crystal Growth* 213: 381-388
- Buchanan J.R., Mote C.R. and Robinson R.B. (1994) Thermodynamics of struvite formation. *Trans. ASAE*, 37, 617-621.
- Celenza, G.J. (2000). *Specialized treatment systems (Volume 3)* Technomic Publishing, U.S.A.
- Crittenden, B., Thomas W.J., (1998) *Adsorption technology and design*. Reed educational and professional publishing Limited
- Cooney E.L., Booker N.A. (1999). Ammonia removal from wastewater using natural Australian zeolite. I. Characterization of the zeolite. *Separation Sci. and Tech.*, 34, 2307–2327.
- Demir A., Gunay A. and Debik E. (2002). Ammonium removal from aqueous solution by ion exchange using packed bed natural zeolite. *Water SA.*, 28, 329–336.
- Dong X, Tollner, E.W (2003) .Evaluation of Anammox and denitrification during anaerobic digestion of poultry manure. *Bioresource Technology* 86: 139-145
- Dorfner K. (1991). *Ion Exchangers*. Walter de Gruyter & Co., Berlin, Germany.
- Doyle JD, Parsons S.A (2002) Struvite formation, control and recovery. *Water Research* 36: 3925-3940
- Du Q, Liu S, Cao Z, Wang Y (2005) Ammonia removal from aqueous solution using natural Chinese clinoptilolite. *Separation and Purification Technology* 44: 229-234
- Dzombak ,D.A. and Morel, F.M.M. (1990) *Surface complexation modelling-Hydrous Ferric oxides*. John Wiley and Sons Inc., USA

- Eatock, W.H., (1985).Advances in Potassium mining and refining. In:"Potassium in Agriculture"(R.D.Munson, ed.).pp.29-48.ASA/CSSA/SSSA,Madison,WI.
- Erdem E, Karapinar N, Donat R (2004) The removal of heavy metal cations by natural zeolites. *Journal of Colloid and Interface Science* 280: 309-314
- Esrey,S.A.,Anderson,I.,Hillers,A.,Sawyer,R.,2001.Closing the Loop-Ecological Sanitation for food security, A Publication of Swedish International Development Cooperation Agency.
- Etter,B. (2009) .Process optimization of low cost struvite recovery .An MSc. thesis E P F L – ENA C – SIE – LCE ,Eawag – Sandec – STUN ,UN - Habitat Nepal
- Fux,C,2003.Biological nitrogen elimination of ammonium-rich sludge digester liquids.A dissertation submitted to Swiss Federal institute of Technology,Zurich
- Galbraith S.C,Schneider,P.A.2009. A review of struvite nucleation studies.A presentation at the International conference on nutrient recovery from wastewater streams.IWA publishing.
- Gantenbein,B,Khadka,R(2009).Struvite recovery from urine at community scale in nepal.Swiss federal institute of aquatic science and technology
- Ganrot, Z., 2005, Urine processing for efficient recovery and reuse in Agriculture, PhD thesis, Goteborg University, Sweden.
- Ganrot Z, Dave G, Nilsson E (2007) Recovery of N and P from human urine by freezing, struvite precipitation and adsorption to zeolite and active carbon. *Bioresource Technology* 98: 3112-3121
- Gerardi M.H.(2006).Wastewater bacteria. John Wiley and sons Inc., New Jersey
- Graeser,S.,Postl,W,Bojar,H, Berlepsch, P, Armbruster,T , Raber, T, Ettinger,K ,Walter, F (2008) Struvite-(K),  $\text{KMgPO}_4 \cdot 6\text{H}_2\text{O}$ , the potassium equivalent of struvite; a new mineral *European Journal of Mineralogy* (August 2008), 20(4):629-633
- Griffith, D.P., Musher, D.M., Itin, C., 1976. The primary cause of infection induced urinary stones. *Invest. Urol.* 13 (5), 347–350.
- Hedstrom A. (2001). Ion exchange of ammonium in zeolites: A literature review. *J. Env. Eng.*, **127** (8), 673 – 681.
- Hellinga C, Schellen A.A.J.C, Mulder, J.W, van Loosdrechet, M.C.M, Heijnen J. J (1998) The SHARON process: an innovative method for nitrogen removal from ammonia-rich wastewater. *Water Science and Technology*, 37:135-142.
- Henze, M., Somlyody, L., Schilling, W.,(1997).Sustainable sanitation. Selected papers on the concept of sustainability in sanitation and water and waste water management
- Hoglund, C. (2001).Evaluation of microbial health risks associated with the re-use of source separated human urine, PhD Thesis, Royal Institute of Technology, Department of Biotechnology
- Horsfall, M, Spiff, A. I (2005) Equilibrium sorption study of  $\text{Al}^{3+}$ ,  $\text{Co}^{2+}$ , and  $\text{Ag}^+$  in aqueous solutions by fluted pumpkin (*Telfairia Occidentalis* HOOK f) waste biomass. *Act Chim.Slov*, **52: pp** 175 - 181.
- House J.E., House, K.A., Descriptive inorganic chemistry (2010).Second edition. Elsevier Inc.pp 169-172.
- Faghihian H, Bowman RS (2005) Adsorption of chromate by clinoptilolite exchanged with various metal cations. *Water Research* 39: 1099-1104
- Ferro,R.,Saccone,A.2008.Intermetallic chemistry.First edition.Elsevier Ltd/Pergamon materials series.
- Jetten, M.S.M., Horn, S.J. , Van Loosdrecht, M.C.M. (1997). Towards a more sustainable wastewater treatment system. *Water Science & Technology*, **35**(9), 171-180.

- Jetten MSM, Wagner M, Fuerst J, van Loosdrecht M, Kuenen G, Strous M (2001) Microbiology and application of the anaerobic ammonium oxidation ('*n*-anammox') process. *Current Opinion in Biotechnology* 12: 283-288
- Jetten M, Strous M, Pas Schoonen K, Schalk J, Dongen U, Graaf A, Logemann S, Muyzer G, Loosdrecht M, Kuenen J (1998) The anaerobic oxidation of ammonium. *FEMS Microbiology Reviews* 22: 421-437
- Jones, A.G (2002). Crystallization process system. Butterworth /Heinemann, London.UK.
- Kentucky Office of Energy policy (2006).*Kentucky Energy Watch*.7 (22)
- King, B.R. (1995).Inorganic chemistry of Main group elements.VCH Publishers, Inc.
- Koutsoukos, P.G., Kofina, A.N. and Klepetsanis, P.G. (2003).Exploration of alternatives for phosphate recovery from waste water by crystallization.Wasic Workshop, Istanbul (Turkey).
- Krebs, R.E. 2006.The history and use of our Earth's chemical elements: A reference guide, Second edition. Green wood publishing group, Inc.U.S.A.
- Larsen, T.A., Gujer, W., 1996.Separate management of anthropogenic nutrient solutions (Human urine).*Water Science and Technology*.34 (3-4), 87-94.
- Le Corre, K.S. (2006).Understanding struvite crystallization and Recovery. A PhD.thesis for the doctor of philosophy, Cranfield University.
- Lentner, C., Wink, A.,(1981). Units of Measurement, Body Fluids, Composition of the Body, Nutrition. Geigy Scientific Tables. CIBA-GEIGY Ltd, Basle, Switzerland.
- Liberti L, Petruzzelli D, De Florio L (2001) REM NUT ion exchange plus struvite precipitation process. *Environmental technology* 22: 1313-1324
- Liberti L, Boari G, Petruzzelli D, Passino R (1981) Nutrient removal and recovery from wastewater by ion exchange. *Water Research* 15: 337-342
- Lind, B.-B., Ban, Z. and Byde'n, S. (2000). Nutrient recovery from human urine by struvite crystallization with ammonia adsorption on zeolite and wollastonite. *Bioresource Technology*, **73**, 169–174.
- Lind B-B, Ban Z, Byde'n S (2001) Volume reduction and concentration of nutrients in human urine. *Ecological Engineering* **16**: 561-566
- Liu Z, Zhao Q, Wang K, Lee D, Qiu W, Wang J (2008) Urea hydrolysis and recovery of nitrogen and phosphorous as MAP from stale human urine. *Journal of Environmental Sciences* 20: 1018-1024
- Massey,A.G.(2000).Main group chemistry .John wiley and Company England.
- Main group chemistry, 2nd edition.A.G Massey.2000.John Wiley & sons Ltd., England
- Maurer, M., P. Schwegler, T.A. Larsen (2003) Nutrients in urine: energetic aspects of removal and recovery. *Water Science and Technology* 48(1): 37-46.
- Maurer M, Pronk W, Larsen T (2006) Treatment processes for source-separated urine. *Water Research* 40: 3151-3166
- Mobley H L T, Hausinger R P, 1989. Microbial ureases: significance, regulation, and molecular characterization. *Microbiol Rev*, 53(1): 85–108.
- Mullin, J.W.1993.*Crystallization*, Oxford, Butterworth-Heinemann.
- Ohlinger, K.N., Young, T.M. and Schroeder, E.D.(1999).Kinetic effects on preferential struvite accumulation in waste water. *Journal of environmental engineering*.**125**, 730-737.

- Parkhurst, D.L., Appelo, C.A.J. (1999). User's guide to PHREEQC (Version 2)-A computer program for speciation, batch reaction, one dimensional transport, and inverse geochemical calculations. The United States Department of Interior, Denver, USA.
- Pronk W, Koné D (2009) Options for urine treatment in developing countries. *Desalination* 248: 360-368
- Pronk W, Palmquist H, Biebow M, Boller M (2006) Nanofiltration for the separation of pharmaceuticals from nutrients in source-separated urine. *Water Research* 40: 1405-1412
- Rangel, Y.A., 2008. Quantifying Mineral Sources of Potassium in Agricultural Soils. A PhD Thesis, Swedish University of Agricultural Sciences
- Regy, S., Mangin, D., Klein, J.P., Lieto, J. (2001). Phosphate recovery by struvite precipitation in a stirred reactor. *Phosphate recovery in waste water by crystallization*. LAGEP, CEEP.
- Reháková M, Cuvanová S, Dzivák M, Rimár J, Gaval'ová Z (2004) Agricultural and agrochemical uses of natural zeolite of the clinoptilolite type. *Current Opinion in Solid State and Materials Science* 8: 397-404
- Rezaei, M.; Naeini, S. A. R. M. (2009) Kinetics of Potassium Desorption from the Loess Soil, Soil Mixed with Zeolite and the Clinoptilolite Zeolite as Influenced by Calcium and Ammonium. Volume: 9 | Issue: 18 | Page No.: 3335-3342. *Journal of Applied Sciences* Vol. 9 No. 18 pp. 3335-3342
- Robertson, W.G., Peacock, M., Nordin, B.E. (1968). Activity products in stone forming and non-stone forming urine. *Clin. Sci.* 34 (3). pp 579-594.
- Ronteltap M., Maurer M., Gujer W. (2007). The behaviour of pharmaceuticals and heavy metals during struvite precipitation in urine. *Water research* 2007;41(9):1859-68.
- Roosa, S.A., 2008. Sustainable development handbook, Fairmont Press, Inc.
- Rouquerol, F., Rouquerol, J., Sing K. (1999). Adsorption by powders and porous solids (principles, methodology and applications) Academic press, UK
- Rousseau, R.W. 1987. Handbook of separation process Technology. John Wiley and Sons.
- Song Y, Yuan P, Zheng B, Peng J, Yuan F, Gao Y (2007) Nutrients removal and recovery by crystallization of magnesium ammonium phosphate from synthetic swine wastewater. *Chemosphere* 69: 319-324
- Stratful I, Scrimshaw MD, Lester JN (2001) Conditions influencing the precipitation of magnesium ammonium phosphate. *Water Research* 35: 4191-4199
- Schönning, C. and Stenström, T-A. 2004. Guidelines for the safe Use of Urine and Faeces in Ecological Sanitation. Report 2004-1. Ecosanres, SEI. Sweden. Available at: [www.ecosanres.org](http://www.ecosanres.org).
- Schuling, R.D. and Andrade, A. (1999). Recovery of struvite from calf manure. *Environmental Technology*, 20(7), 765-768.
- Sharma, K.S (2001). Adsorptive Iron removal from ground water. PhD dissertation at UNESCO-IHE and Wageningen University.
- Snoeyink, V.L., Jenkins, D. (1980). *Water Chemistry*. John Wiley and Sons Inc. Canada.
- Snoeyink, V.L., Summers (1999), "Adsorption of Organic compounds," *Water quality and treatment: A handbook of community water supplies*, 5<sup>th</sup> edition, AWWA, McGraw-Hill New York.
- Sundstrom, D.W., Klei, H.E. (1979). *Wastewater Treatment*. Prentice-Hall Inc., Eagle-Woods.

- Stefan G, Postl W, Bojar H, Peter B, Thomas A, Raber T, Karl E, Franz W (2008) Struvite-(K),  $\text{KMgPO}_4 \cdot 6\text{H}_2\text{O}$ , the potassium equivalent of struvite—a new mineral. *European Journal of Mineralogy* 20: 629-633
- Stratful I, Scrimshaw MD, Lester JN (2001) Conditions influencing the precipitation of magnesium ammonium phosphate. *Water Research* 35: 4191-4199
- Stumm W., Morgan, J., Aquatic chemistry-chemical equilibria and rates in natural waters.1996.3rd edition. A Wiley interscience publication (John-Wiley and sons Inc.)
- Surampalli RY, Tyagi RD, Scheible OK, Heidman JA (1997) Nitrification, denitrification and phosphorus removal in sequential batch reactors. *Bioresource Technology* 61: 151-157
- Sustainable sanitation practice, 2010. *Use of Urine*, Ecosan Club, Issue 3
- Tettenborn, F. Behrendt, J., Otterpohl, R.(2007).Resource recovery and removal of pharmaceutical residues Treatment of separate collected urine .A report for the demonstration project “Sanitation Concepts for Separate Treatment of Urine, Faeces and Greywater “ (SCST).University of Hamburg and Institute of wastewater management and water protection
- Tilley, E. (2006).The effects of urine storage conditions on struvite recovery. A thesis submitted for the degree of master of applied science. University of British Columbia.
- Tsushima I, Ogasawara Y, Kindaichi T, Satoh H, Okabe S (2007) Development of high-rate anaerobic ammonium-oxidizing (anammox) biofilm reactors. *Water Research* 41: 1623-1634
- Udert,K.M.,Larsen,T.A.,Biebow M,Gujer W(2003a).Urea hydrolysis and precipitation dynamics in a urine-collecting system.*Water Res*,37(11):2571-2582
- Udert, K.M., Larsen, T.A. and Gujer, W. (2003b). Biologically induced precipitation in urine-collecting systems. *Water Science and Technology: Water Supply*, 3(3), 71–78.
- Udert, K.M., Larsen, T.A., Gujer, W. (2006) Fate of major compounds in source-separated urine. *Water Sci. Technol.* 54, 11-12, 413-420.
- UN, 2002.United Nations, Johannesburg Summit. [Http://www.johannesburgsummit.org](http://www.johannesburgsummit.org)
- UNEP, IFA (2001), Environmental aspects of phosphate and potash mining, UN publications.
- Van Dongen, U., Jetten, M.S.M. & van Loosdrecht, M.C.M. (2001a). *The combined SHARON/Anammox process*. IWA Publishing, London, UK.
- Van Dongen, U., Jetten, M.S.M., Van Loosdrecht, M.C.M. (2001b). The SHARON® Anammox® process for treatment of ammonium rich wastewater. *Water Science & Technology*, 44(1), 153-160. Vangheluwe, H., Claeys, F. & Vansteenkiste
- Vinnerås, B. (2001). Faecal separation and urine diversion for nutrient management of household biodegradable waste and wastewater. Swedish University of Agricultural Sciences. Report 244. Licentiate Thesis.
- WHO, (2006). Guidelines for the safe use of wastewater, excreta and greywater. Volume 4. Excreta and greywater use in agriculture
- Wellmer F, Becker-Platen J (2002) Sustainable development and the exploitation of mineral and energy resources: a review. *International Journal of Earth Sciences* 91: 723-745
- Wilsenach JA, Schuurbiers CAH, van Loosdrecht MCM (2007) Phosphate and potassium recovery from source separated urine through struvite precipitation. *Water Research* 41: 458-466
- Wilsenach JA, Van Loosdrecht,M. (2003) Impact of separate urine collection on wastewater treatment systems. *Water Science and Technology* 48: 103-110
- Wilsenach J (2005).DESAR-Options for separate treatment of urine.Published by STOWA ,The Netherlands.
- Wypych, G.2001.Handbook of Solvents.Chem Tec Publishing

Yetgin S. (2006).Investigation of fuel oxygenate adsorption on clinoptilolite rich natural zeolite, A thesis for the Master of science in Chemical engineering, Izmir institute of Technology

Young-Ho Ahn. (2006) Sustainable nitrogen elimination biotechnologies: A review, Process Biochemistry, Volume 41, Issue 8, August, Pages 1709-1721.

# APPENDICES

## Appendix 1

Table 1.1 Compiled PHREEQC (Version 2) model output results of precipitation of Potassium struvite, Ammonium struvite and ammonia gas in the urine streams

	Saturation index (SI)		
	Potassium struvite	Struvite MAP	Ammonia gas
Nitri Mg:P=1:2	1.26	-	-
Nitri Mg:P=2:1	1.22	-	-
Nitri 25°C	1.18	-	-
Nitri 35°C	1.13	-	-
S/anammox Mg : P= 1:2	1.02	-	-
S/anammox Mg : P= 2:1	1.21	-	-
S/anammox 25 °C	0.74	-	-
S/anammox 35 °C	0.66	-	-
Hydrolysis Mg : P= 1:2	1.09	4.52	2.01
Hydrolysis Mg : P= 2:1	1.16	4.42	2.11
Hydrolysis 25 °C	1.15	3.85	2.21
Hydrolysis 35 °C	0.84	4.27	1.96
Struvite Mg : P= 1:2	1.09	4.53	2.0
Struvite Mg : P= 2:1	1.16	4.43	2.10
Struvite 25 °C	0.97	4.32	2.06
Struvite 35 °C	0.84	4.28	1.95

## Appendix 2 Langmuir and Freundlich components for batch adsorption experiments (2) using zeolites (1-1.2mm)

Where;

$C_e$ -Potassium equilibrium concentration as at 72 hours of contact time

M- Mass of adsorbent (g)

V- Volume of solution = 0.06 liters

X - Amount of potassium adsorbed =  $(C_0 - C_e) * V$

q- Amount of potassium adsorbed per amount of zeolite used =  $X/M$

## Hydrolysis

Table 2.1 below shows the changes in potassium concentration in hydrolysis stream, after 72 hours contact time with four different masses of zeolite: 1g, 3g, 5g and 10g

*Table A 2.1 The changes in concentration of Potassium in the adsorption process for hydrolysis stream in experiment 3*

Contact Time (Hrs)	Concentration of Potassium(g/l)				
	Blank	1g	3g	5g	10g
0	0.654	0.654	0.654	0.654	0.654
3	0.690	0.704	0.791	0.818	0.912
6	0.688	0.720	0.828	0.924	0.898
24	0.707	0.776	0.896	0.950	1.057
48	0.756	0.792	0.942	0.997	0.986
72	0.690	0.738	0.900	0.856	0.955

*Table A 2.2 The Langmuir and Freundlich isotherm components for Hydrolysis stream*

Amount of zeolite (g)	Ce(g/l)	(Co-Ce) (g)	(Co-Ce)*V=X (g)	q=X/M (g/g)	1/Ce	1/qe	Potassium recovery (%)
1	0.738	-0.084	-0.005	-0.005	1.355	-198.934	-12.80
3	0.900	-0.245	-0.015	-0.005	1.111	-203.691	-37.51
5	0.856	-0.202	-0.012	-0.002	1.168	-412.439	-30.88
10	0.955	-0.301	-0.018	-0.002	1.047	-554.115	-45.96

Where;

Co - Initial potassium concentration in the solution = 0.654 g/l

## Sharon-anammox

Table 2.3 below shows the changes in potassium concentration in sharon-anammox stream, after 72 hours contact time with four different masses of zeolite: 1g, 3g, 5g and 10g

*Table A2.3 The changes in concentration of Potassium in the adsorption process for Sharon anammox stream*

Contact Time (Hrs)	Concentration of Potassium(g/l)				
	Blank	1g	3g	5g	10g
0	0.653	0.653	0.653	0.653	0.653
3	0.687	0.673	0.468	0.431	0.347

6	0.698	0.504	0.347	0.251	0.172
24	0.729	0.511	0.273	0.159	0.030
48	0.688	0.449	0.188	0.110	0.001
72	0.699	0.435	0.160	0.073	0.00

Table A2.4 The Langmuir and Freundlich isotherm components for Sharon-anammox stream

Amount of zeolite (g)	Ce (g/l)	(Co-Ce) (g/l)	(Co-Ce)*V=X (g)	q=X/M (g/g)	1/Ce	1/qe	log Ce	log q	Potassium recovery (%)
1	0.435	0.218	0.013	0.013	2.297	76.453	-0.361	-1.883	33.37
3	0.160	0.493	0.030	0.010	6.234	101.434	-0.795	-2.006	75.45
5	0.073	0.580	0.035	0.007	13.665	143.641	-1.136	-2.157	88.80
10	0.001	0.652	0.039	0.004	1000.000	255.494	-3.000	-2.407	99.85

Where;

Co - Initial potassium concentration in the solution = 0.653g/l

### Nitrification

Table 2.5 below shows the changes in potassium concentration in nitrification stream, after 72 hours contact time with four different masses of zeolite: 1g, 3g, 5g and 10g

Table A2.5 The changes in concentration of Potassium in the adsorption process for nitrification stream

Contact Time (Hrs)	Concentration of Potassium(g/l)				
	Blank	1g	3g	5g	10g
0	0.759	0.758	0.758	0.758	0.758
3	0.764	0.699	0.698	0.637	0.610
6	0.762	0.655	0.702	0.535	0.530
24	0.763	0.773	0.713	0.591	0.512
48	0.758	0.709	0.663	0.503	0.450
72	0.764	0.688	0.558	0.480	0.404

Table A2.6 The Langmuir and Freundlich isotherm components for Nitrification

Amount of zeolite (g)	Ce(g/l)	(Co-Ce) (g/l)	(Co-Ce)*V=X (g)	q=X/M	1/Ce	1/q	log Ce	log q	Potassium recovery (%)
1	0.688	0.070	0.004	0.004	1.454	237.417	-0.163	-2.376	9.26
3	0.558	0.200	0.012	0.004	1.793	249.576	-0.254	-2.397	26.43
5	0.480	0.278	0.017	0.003	2.085	299.426	-0.319	-2.476	36.72
10	0.404	0.354	0.021	0.002	2.476	470.597	-0.394	-2.673	46.72

Where;

Co - Initial potassium concentration in the solution = 0.758 g/l

### Struvite

Table 2.7 below shows the changes in potassium concentration in struvite stream, after 72 hours contact time with four different masses of zeolite: 1g, 3g, 5g and 10g

Table A 2.7 The changes in concentration of Potassium in the adsorption process for struvite stream

Contact Time (Hrs)	Concentration of Potassium(g/l)				
	Blank	1g	3g	5g	10g
0	0.621	0.621	0.621	0.621	0.621
3	0.600	0.621	0.684	0.714	0.851
6	0.678	0.699	0.850	0.850	1.119
24	0.675	0.750	0.933	0.892	1.129
48	0.670	0.835	1.006	0.919	1.133
72	0.694	0.729	0.933	0.972	1.112

Table A 2.8 The Langmuir and Freundlich isotherm components for Struvite stream

Amount of zeolite (g)	Ce(g/l)	(Co-Ce) (g/l)	(Co-Ce)*V=X (g)	q=X/M (g/g)	1/Ce	1/qe	Potassium recovery (%)
-----------------------	---------	---------------	-----------------	-------------	------	------	------------------------

1	0.729	-0.107	-0.006	-0.006	1.372	-155.531	-17.24
3	0.933	-0.311	-0.019	-0.006	1.072	-160.751	-50.05
5	0.972	-0.350	-0.021	-0.004	1.029	-238.061	-56.33
10	1.112	-0.491	-0.029	-0.003	0.899	-339.72	-78.94

Where;

Co - Initial potassium concentration in the solution = 0.621 g/l

### Appendix 3 Langmuir and Freundlich components for batch adsorption experiments (3) using zeolites (2-3.15mm)

Where;

C<sub>0</sub> - Potassium initial concentration (g/l)

C<sub>e</sub>-Potassium equilibrium concentration as at 48 hours of contact time (g/l)

M- Mass of adsorbent (g)

V- Volume of solution = 0.1liters

X - Amount of potassium adsorbed = (C<sub>0</sub>-C<sub>e</sub>)\*V

q- Amount of potassium adsorbed per amount of zeolite used =X/M

$$\text{Recovery (\%)} = \frac{(C_0 - C_e)}{C_e} * 100$$

$$\text{Percentage adsorption (\%)} = \frac{(C_0 - C_f)}{C_0} * 100$$

#### Sharon-anammox

Table A3.1 below shows the average change in concentration after 48 hours of contact time for the sharon anammox stream using four different masses of zeolite: 10g, 20g, 30g and 40g.

Table A3.1 Final concentrations of Potassium in 48 hour contact period

Amount of zeolites (g)	Concentration of Potassium (g/l)			Percentage Potassium recovery (%)
	Analysis 1 (g/l)	Analysis 2 (g/l)	Average concentration (g/l)	
0	2.02	2	<b>2.01</b>	
10	0.896	0.916	<b>0.906</b>	54.93
20	0.47	0.475	<b>0.4725</b>	76.49
30	0.308	0.307	<b>0.3075</b>	84.70
40	0.235	0.233	<b>0.234</b>	88.36

Table A3.2 The Langmuir and Freundlich isotherm components for Sharon-anammox stream

Amount of zeolites(g)	Ce (g/l)	(Co-Ce) (g/l)	(Co-Ce)*V=X (g)	q=X/M (g/g)	1/Ce	1/q	log Ce	log q
10	0.906	1.104	0.110	0.0110	1.104	90.580	-0.043	-1.957
20	0.473	1.538	0.154	0.0077	2.116	130.081	-0.326	-2.114
30	0.308	1.703	0.170	0.0057	3.252	176.211	-0.512	-2.246
40	0.234	1.776	0.178	0.0044	4.274	225.225	-0.631	-2.353

Where;

Co - Initial potassium concentration in the solution = 2.01 g/l

### Nitrification

The table below shows the average change in concentrations after 48 hours of contact for the nitrification stream using four different masses of zeolite: 10g, 20g, 30g and 40g.

Table A 3.3 Final concentrations of Potassium in 48 hour contact period

Amount of zeolites (g)	Concentration of Potassium (g/l)		Average concentration (g/l)	Percentage Potassium recovery (%)
	Analysis 1 (g/l)	Analysis 2 (g/l)		
0	1.96	1.97	<b>1.965</b>	
10	1.46	1.46	<b>1.46</b>	25.70
20	1.18	1.21	<b>1.195</b>	39.19
30	0.995	1.01	<b>1.0025</b>	48.98
40	0.867	0.868	<b>0.8675</b>	55.85

Table A3.4 The Langmuir and Freundlich isotherm components for Nitrification stream

Amount of zeolites(g)	Ce (g/l)	(Co-Ce) (g/l)	(Co-Ce)*V=X (g)	q=X/M (g/g)	1/Ce	1/q	log Ce	log q
10	1.46	0.505	0.0505	0.0051	0.685	198.020	0.164	-2.297

20	1.195	0.77	0.077	0.0039	0.837	259.740	0.077	-2.415
30	1.003	0.963	0.096	0.0032	0.998	311.688	0.001	-2.494
40	0.868	1.098	0.110	0.0027	1.153	364.465	-0.062	-2.562

Where;

Co - Initial potassium concentration in the solution = 1.965 g/l

## Hydrolysis

The table A3.5 below shows the average change in concentrations after 48 hours of contact for the hydrolysis stream using four different masses of zeolite: 10g, 20g, 30g and 40g.

Table A3.5 Final concentrations of Potassium in 48 hour contact period

Amount of zeolites(g)	Concentration of Potassium (g/l)			Percentage Potassium recovery (%)
	Analysis 1 (g/l)	Analysis 2 (g/l)	Average concentration (g/l)	
0	1.99	1.91	<b>1.95</b>	
10	1.41	1.39	<b>1.4</b>	28.21
20	1.06	1.09	<b>1.075</b>	44.87
30	0.886	0.876	<b>0.881</b>	54.82
40	0.801	0.793	<b>0.797</b>	59.13

Table A3.6 The Langmuir and Freundlich isotherm components for Hydrolysis stream

Amount of zeolites(g)	Ce (g/l)	(Co-Ce) (g/l)	(Co-Ce)*V=X (g)	q=X/M (g/g)	1/Ce	1/q	log Ce	log q
10	1.4	0.55	0.055	0.0055	0.714	181.818	0.146	-2.260
20	1.075	0.875	0.0875	0.0044	0.930	228.571	0.031	-2.359
30	0.881	1.069	0.107	0.0036	1.135	280.636	-0.055	-2.448
40	0.797	1.153	0.115	0.0029	1.255	346.921	-0.099	-2.540

Where;

Co - Initial potassium concentration in the solution = 1.95 g/l

## Struvite

The table A3.7 below shows the average change in concentrations after 48 hours of contact for the struvite stream

Table A3.7 Final concentrations of Potassium in 48 hour contact period

Amount of zeolites (g)	Concentration of Potassium (g/l)			Percentage Potassium recovery (%)
	Analysis 1 (g/l)	Analysis 2 (g/l)	Average concentration (g/l)	
0	1.8	1.8	<b>1.8</b>	
10	1.26	1.23	<b>1.245</b>	30.83
20	0.962	0.955	<b>0.959</b>	46.75
30	0.782	0.775	<b>0.779</b>	56.75
40	0.678	0.679	<b>0.679</b>	62.31

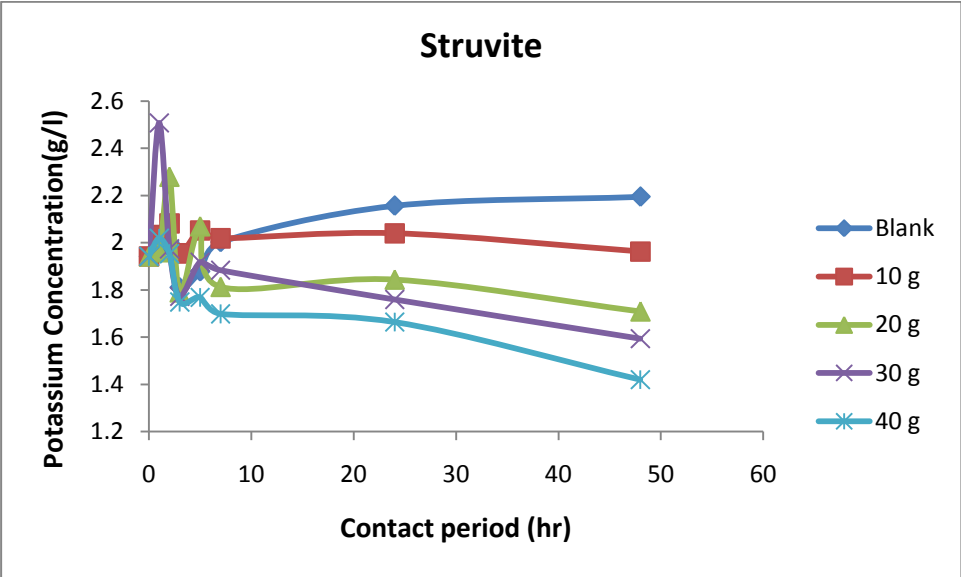
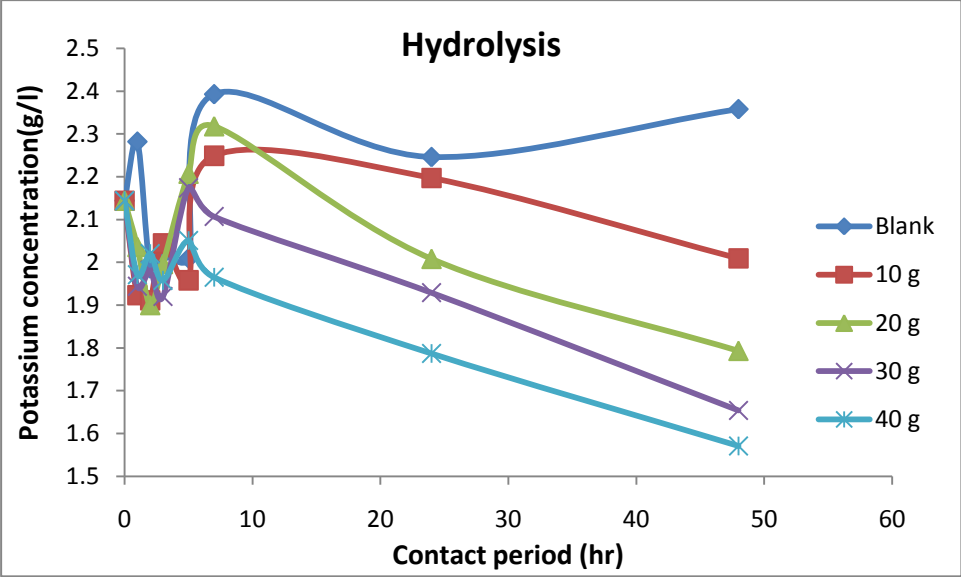
Table A3.8 The Langmuir and Freundlich isotherm components for Struvite stream

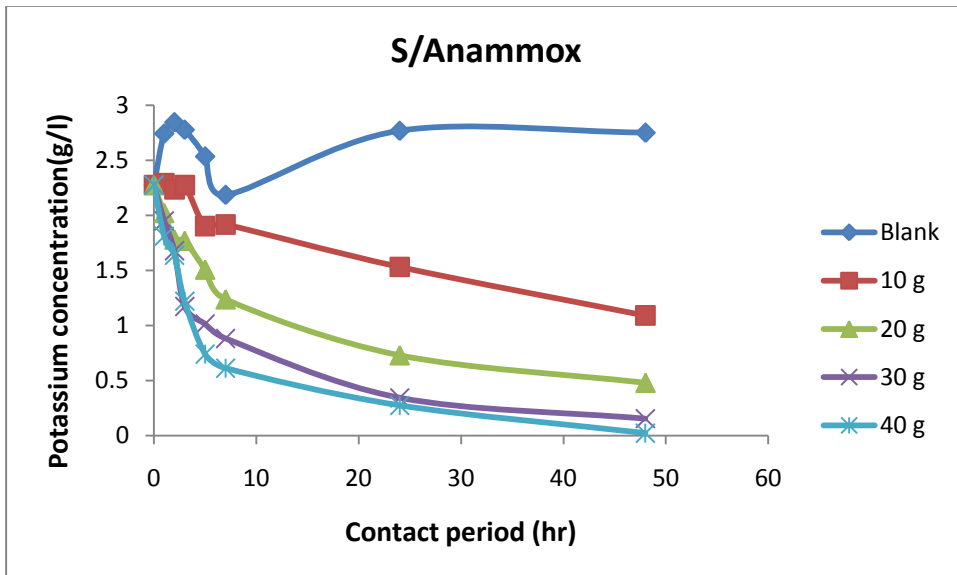
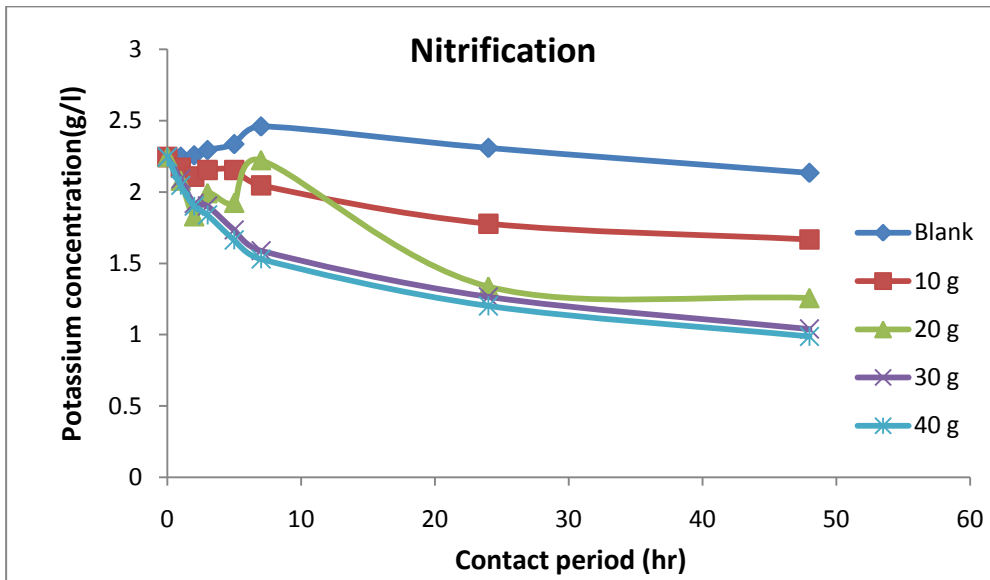
Amount of zeolites(g)	Ce (g/l)	(Co-Ce) (g/l)	(Co-Ce)*V=X (g)	q=X/M (g/g)	1/Ce	1/q	log Ce	log q
10	1.245	0.555	0.056	0.0056	0.80	180.18	0.095	-2.26
20	0.959	0.842	0.084	0.0042	1.04	237.67	-0.018	-2.38
30	0.779	1.022	0.102	0.0034	1.28	293.69	-0.109	-2.47
40	0.679	1.122	0.112	0.0028	1.47	356.67	-0.168	-2.55

Where;

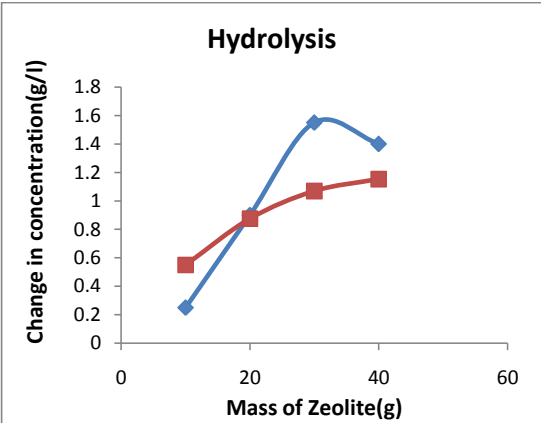
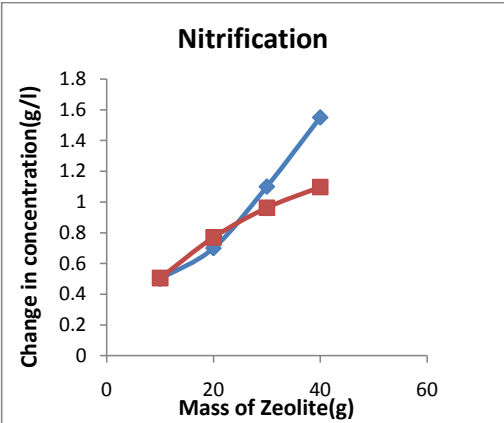
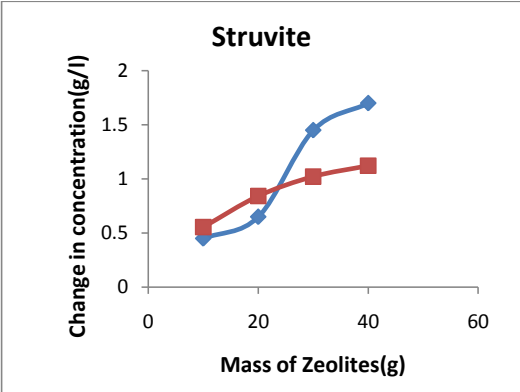
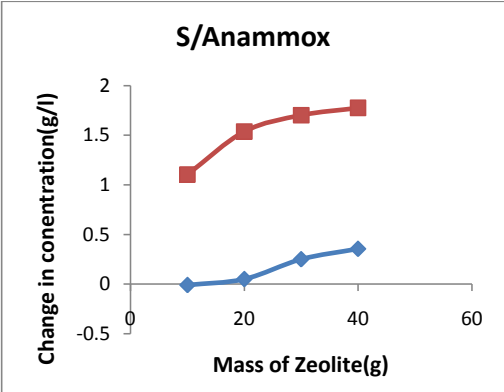
Co - Initial potassium concentration in the solution = 1.80 g/l

**Appendix 4 The Kinetic results of urine streams for batch adsorption experiment (1) using Zeolites (2-3.15mm)**





**Appendix 5 The comparison of changes in concentration of potassium with sodium in the batch experiment 3 for (2-3.15 mm zeolites)**



**Key**  
 Sodium ———  
 Potassium ———

## Appendix 6 Codes used in the synthetic urine treatment schemes

<i>Treatment stream</i>	<i>Code</i>	<i>Magnesium: Phosphorus ratio</i>	<i>Temperature (°C)</i>
Nitrification	Nitri 1:2	1:2	25
	Nitri 2:1	2:1	25
	Nitri 25	1:1	25
	Nitri 35	1:1	35
Sharon-Anammox	S/Anammox 1:2	1:2	25
	S/Anammox 2:1	2:1	25
	S/Anammox 25	1:1	25
	S/Anammox 35	1:1	35
Struvite (MAP)	Struvite 1:2	1:2	25
	Struvite 2:1	2:1	25
	Struvite 25	1:1	25
	Struvite 35	1:1	35
Hydrolysis	Hydrolysis 1:2	1:2	25
	Hydrolysis 2:1	2:1	25
	Hydrolysis 25	1:1	25
	Hydrolysis 35	1:1	35

## Appendix 7 The stoichiometric equations from Griffith et al., (1976) recipe

### *Calcium chloride*

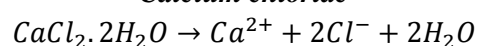


**Table 3.1a**

	$CaCl_2 \cdot 2H_2O$	$Ca^{2+}$	$2Cl^-$
Concentration(mM/l)	4.4	4.4	8.8

### *Magnesium chloride*

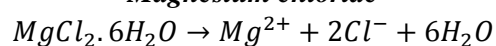


**Table 3.1b**

	$MgCl_2 \cdot 6H_2O$	$Mg^{2+}$	$2Cl^-$	$6H_2O$
Concentration(mM/l)	3.2	3.2	6.4	19.2

**Sodium chloride**  
 $NaCl \rightarrow Na^+ + Cl^-$

**Table 3.1c**

	$NaCl$	$Na^+$	$Cl^-$
Concentration(mM/l)	78.7	78.7	78.7

**Sodium sulphate**  
 $Na_2SO_4 \rightarrow 2Na^+ + SO_4^{2-}$

**Table 3.1d**

	$Na_2SO_4$	$2Na^+$	$SO_4^{2-}$
Concentration(mM/l)	16.2	32.4	16.2

**Trisodium citrate**  
 $Na_3C_6H_5O_7 \rightarrow 3Na^+ + C_6H_5O_7^{3-}$

**Table 3.1e**

	$Na_3C_6H_5O_7$	$3Na^+$	$C_6H_5O_7^{3-}$
Concentration(mM/l)	2.6	7.8	2.6

**Urea**  
 $NH_2(CO)NH_2 + 3H_2O \rightarrow 2NH_4^+ + OH^- + HCO_3^-$

**Table 3.1f**

	$NH_2(CO)NH_2$	$2NH_4^+$	$OH^-$	$HCO_3^-$
Concentration(mM/l)	417	834	417	417

**Potassium chloride**  
 $KCl \rightarrow K^+ + Cl^-$

**Table 3.1g**

	$KCl$	$K^+$	$Cl^-$
Concentration(mM/l)	21.5	21.5	21.5

**Ammonium chloride**  
 $NH_4Cl \rightarrow NH_4^+ + Cl^-$

**Table 3.1h**

	$NH_4Cl$	$NH_4^+$	$Cl^-$
Concentration(mM/l)	18.7	18.7	18.7

**Sodium oxalate**  
 $Na_2 - (COO)_2 \rightarrow 2Na^+ + 2COO^-$

**Table 3.1i**

	$Na_2 - (COO)_2$	$2Na^+$	$2COO^-$
Concentration(mM/l)	0.15	0.3	0.3

**Potassium dihydrogen phosphate**

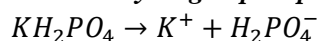


**Table 3.1j**

	$KH_2PO_4$	$K^+$	$H_2PO_4^-$
Concentration(mM/l)	30.9	30.9	30.9

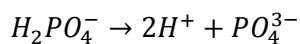


**Table 3.1k**

	$H_2PO_4^-$	$2H^+$	$PO_4^{3-}$
Concentration(mM/l)	30.9	61.8	30.9

**Table 3.1l Formation of Hydroxylapatite**

	$5Ca^{2+}$	$3PO_4^{3-}$	$OH^-$	$Ca_5(PO_4)_3OH_{(s)}$
Concentration(mM/l)	4.4	2.64	0.88	0.88

**Table 3.1m concentrations of ammonium, nitrite and nitrate under nitrification process**

	$NH_4^+$	$NO_2^-$	$NO_3^-$
Concentration(mM/l)	849.5	849.5	849.5

**Table 3.1n Struvite component species in hydrolyzed urine**

	$Mg^{2+}$	$NH_4^+$	$PO_4^{3-}$	$6H_2O$	$MgNH_4PO_4 \cdot 6H_2O$
Concentration(mM/l)	3.2	3.2	3.2	19.2	3.2

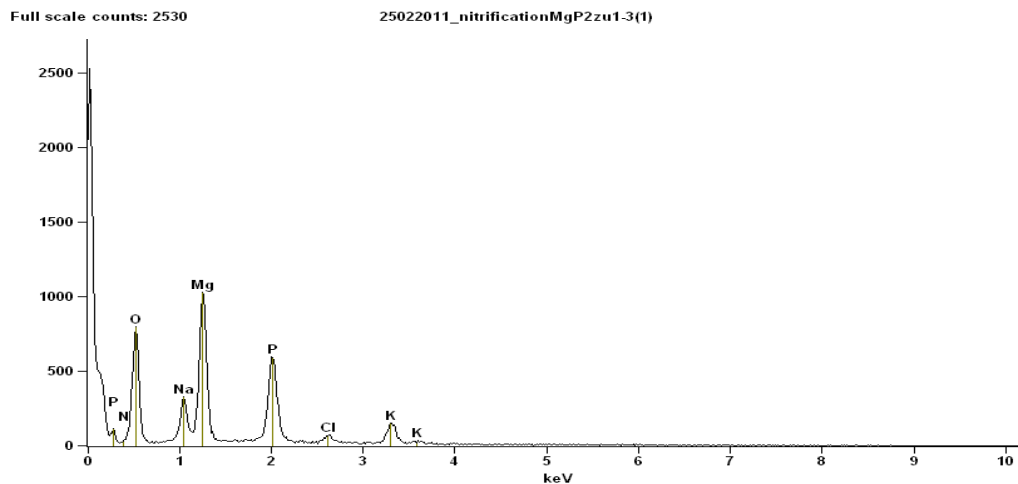
**Table 3.1o Constituent of Struvite MAP**

	$Mg^{2+}$	$NH_4^+$	$PO_4^{3-}$	$6H_2O$	$MgNH_4PO_4 \cdot 6H_2O$
Concentration(mM/l)	25.06	25.06	25.06	150.36	25.06

## Appendix 8 EDX Analysis Tables

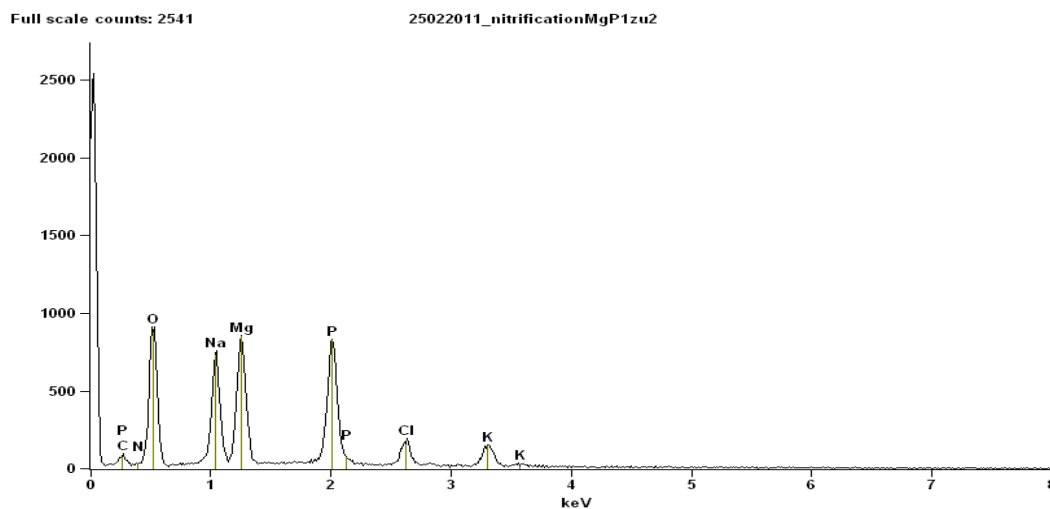
### Nitrification

#### Nitrification Mg: P =2:1



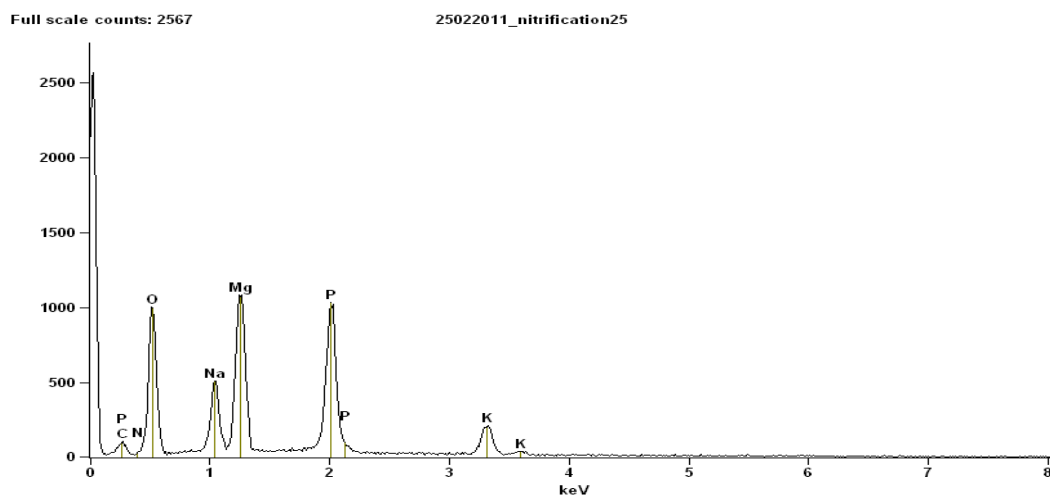
<i>Element Line</i>	<i>Net Counts</i>	<i>Weight %</i>	<i>Atom %</i>
<i>N K</i>	0	0.00	0.00
<i>O K</i>	5652	39.97	54.01
<i>Na K</i>	2213	6.14	5.77
<i>Mg K</i>	8899	22.29	19.82
<i>P K</i>	6972	19.05	13.30
<i>Cl K</i>	680	2.84	1.73
<i>Cl L</i>	1938	---	---
<i>K K</i>	1716	9.71	5.37
<i>K L</i>	0	---	---
<b>Total</b>		100.00	100.00

#### Nitrification Mg: P =1:2



<i>Element Line</i>	<i>Net Counts</i>	<i>Weight %</i>	<i>Atom %</i>
<i>C K</i>	434	3.83	6.67
<i>N K</i>	0	0.00	0.00
<i>O K</i>	6982	38.40	50.25
<i>Na K</i>	5961	12.56	11.44
<i>Mg K</i>	6933	13.83	11.92
<i>P K</i>	9062	18.66	12.61
<i>Cl K</i>	1692	5.36	3.16
<i>Cl L</i>	0	---	---
<i>K K</i>	1708	7.37	3.94
<i>K L</i>	0	---	---
<i>Total</i>		100.00	100.00

### Nitrification 25<sup>0</sup>C

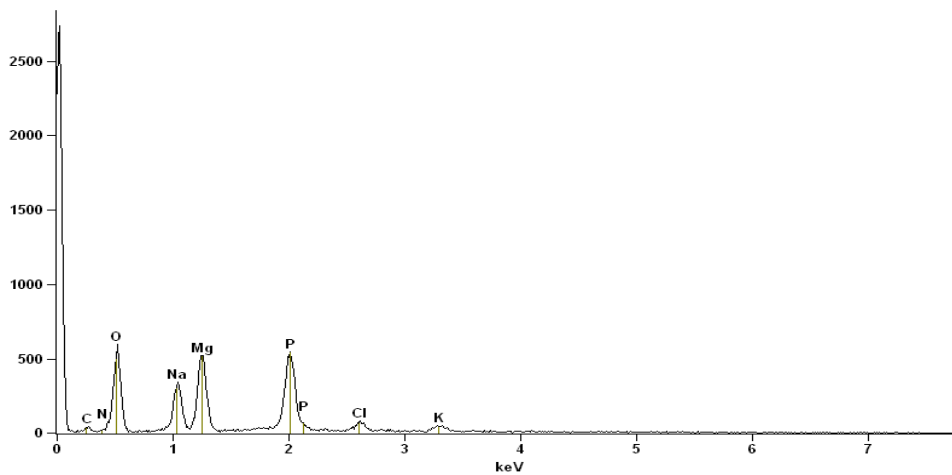


<i>Element Line</i>	<i>Net Counts</i>	<i>Weight %</i>	<i>Atom %</i>
<i>C K</i>	578	4.35	7.56
<i>N K</i>	0	0.00	0.00
<i>O K</i>	7503	38.69	50.40
<i>Na K</i>	4054	7.93	7.19
<i>Mg K</i>	9766	17.47	14.98
<i>P K</i>	11408	21.79	14.66
<i>K K</i>	2458	9.78	5.21
<i>K L</i>	0	---	---
<i>Total</i>		100.00	100.00

# Nitrification 35<sup>0</sup>C

Full scale counts: 2737

25022011\_nitrification35



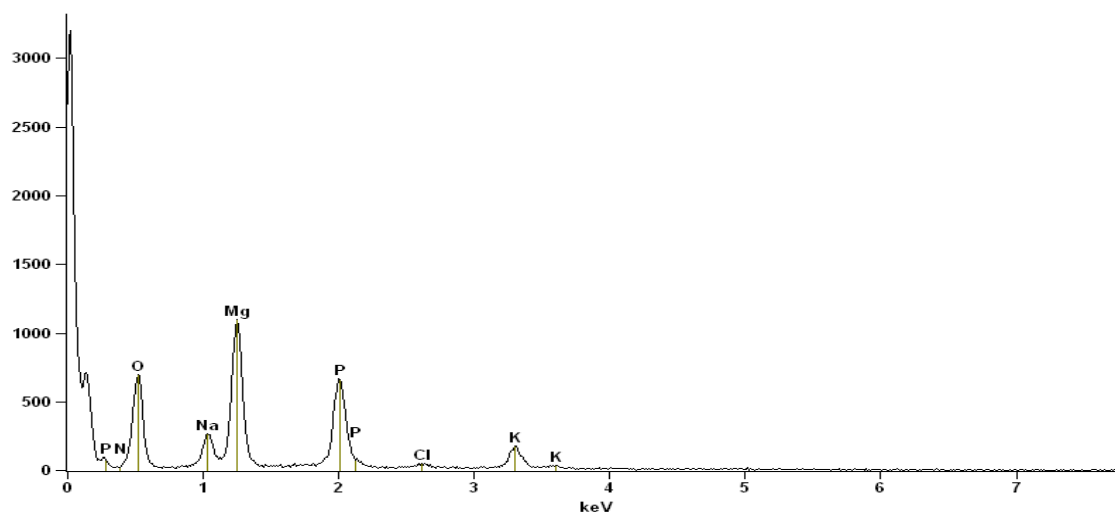
<i>Element Line</i>	<i>Net Counts</i>	<i>Weight %</i>	<i>Atom %</i>
<i>C K</i>	160	2.94	5.12
<i>N K</i>	0	0.00	0.00
<i>O K</i>	3947	39.12	51.13
<i>Na K</i>	2651	10.40	9.46
<i>Mg K</i>	4554	16.69	14.36
<i>P K</i>	5946	22.93	15.48
<i>Cl K</i>	686	4.10	2.42
<i>Cl L</i>	0	---	---
<i>K K</i>	472	3.81	2.04
<i>K L</i>	0	---	---
<i>Total</i>		100.00	100.00

# Sharon Anammox

## Sharon-anammox Mg:P=2:1

Full scale counts: 3201

25022011\_SAMgP2zu1

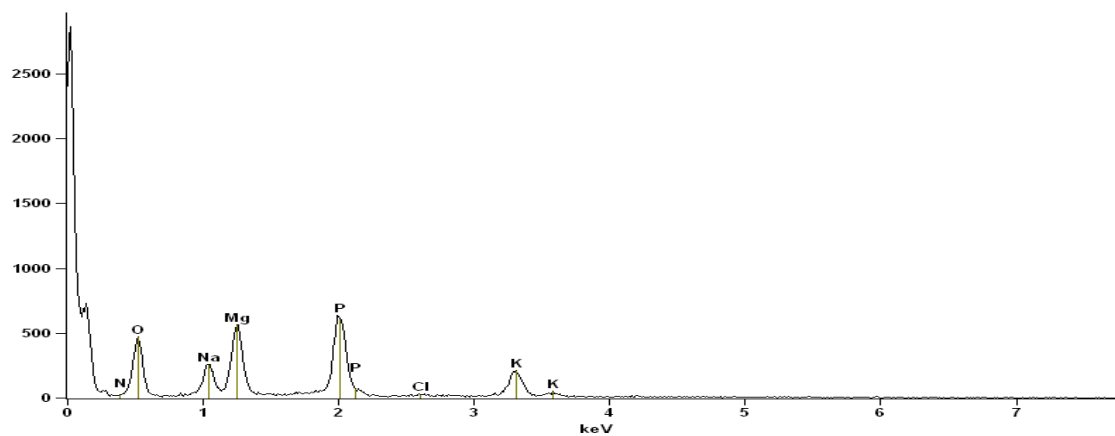


<i>Element Line</i>	<i>Net Counts</i>	<i>Weight %</i>	<i>Atom %</i>
<i>N K</i>	2	0.03	0.05
<i>O K</i>	4675	36.21	50.08
<i>Na K</i>	1838	5.27	5.08
<i>Mg K</i>	9435	24.41	22.23
<i>P K</i>	7497	21.52	15.38
<i>Cl K</i>	294	1.29	0.81
<i>Cl L</i>	610	---	---
<i>K K</i>	1896	11.26	6.38
<i>K L</i>	0	---	---
<b>Total</b>		100.00	100.00

## Sharon-anammox Mg:P=1:2

Full scale counts: 2860

25022011\_SAMgP1zu2

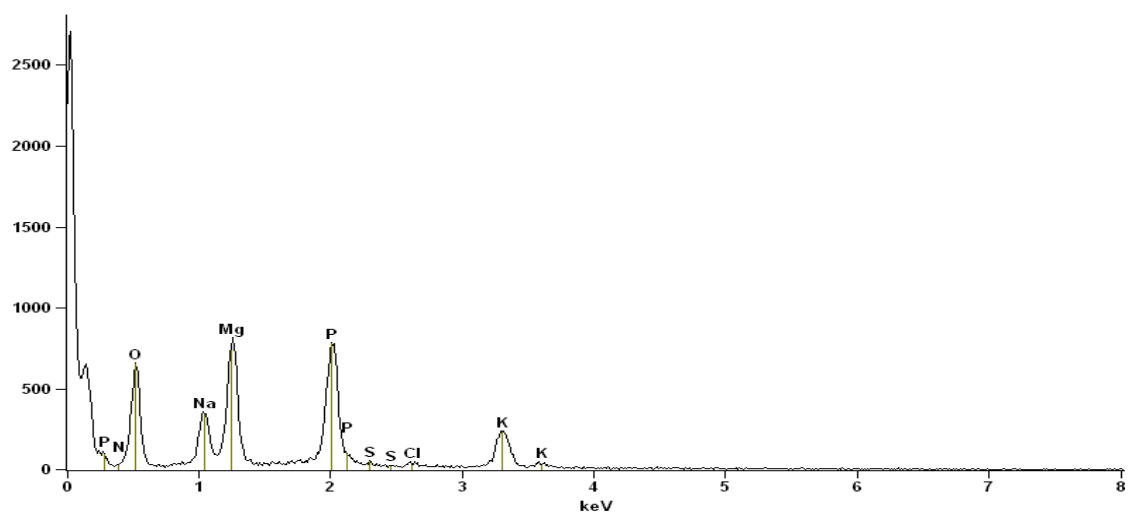


<i>Element Line</i>	<i>Net Counts</i>	<i>Weight %</i>	<i>Atom %</i>
<i>N K</i>	1	0.04	0.07
<i>O K</i>	2896	32.41	47.01
<i>Na K</i>	1896	6.94	7.01
<i>Mg K</i>	4883	16.21	15.48
<i>P K</i>	7333	25.97	19.46
<i>Cl K</i>	102	0.56	0.37
<i>Cl L</i>	730	---	---
<i>K K</i>	2393	17.87	10.61
<i>K L</i>	0	---	---
<b>Total</b>		100.00	100.00

### Sharon-anammox 25<sup>0</sup>C

Full scale counts: 2706

25022011\_SA25-1

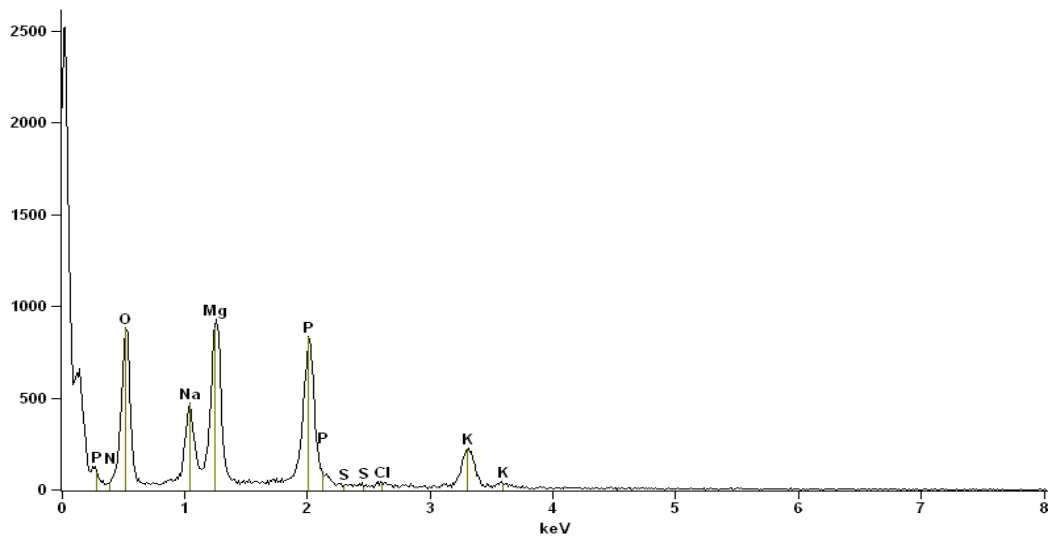


<i>Element Line</i>	<i>Net Counts</i>	<i>Weight %</i>	<i>Atom %</i>
<i>N K</i>	0	0.00	0.00
<i>O K</i>	4955	36.92	51.74
<i>Na K</i>	2685	7.06	6.89
<i>Mg K</i>	7012	16.68	15.38
<i>P K</i>	8846	22.35	16.18
<i>S K</i>	27	0.08	0.06
<i>S L</i>	2288	---	---
<i>Cl K</i>	245	0.96	0.60
<i>Cl L</i>	0	---	---
<i>K K</i>	3017	15.96	9.15
<i>K L</i>	0	---	---
<b>Total</b>		100.00	100.00

# Sharon-anammox 35<sup>0</sup>C

Full scale counts: 2518

25022011\_SA35



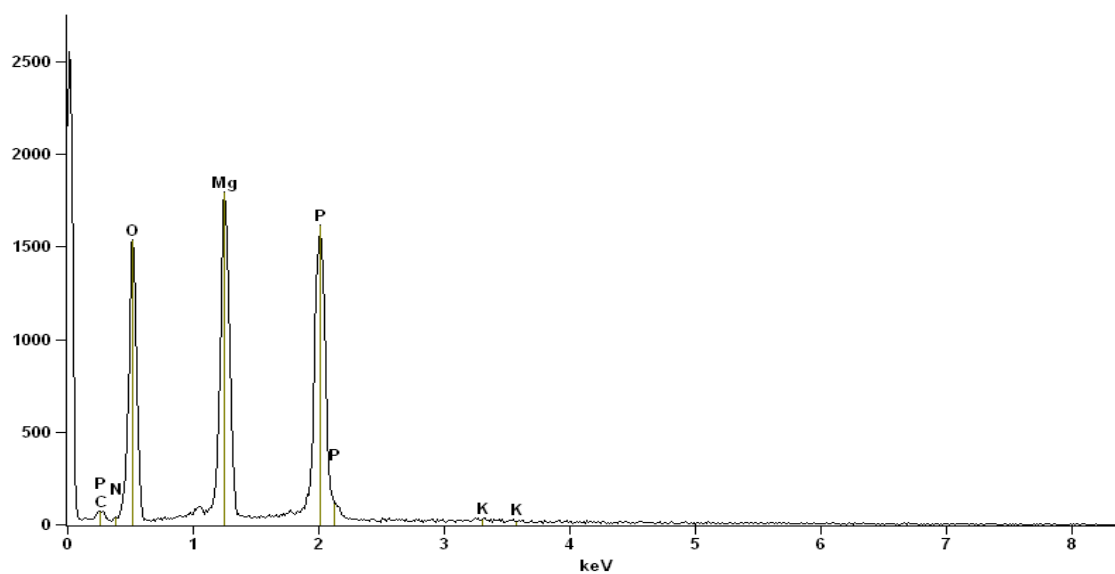
<i>Element Line</i>	<i>Net Counts</i>	<i>Weight %</i>	<i>Atom %</i>
<i>N K</i>	0	0.00	0.00
<i>O K</i>	6800	41.41	55.89
<i>Na K</i>	3226	7.61	7.15
<i>Mg K</i>	8134	17.40	15.45
<i>P K</i>	8938	20.24	14.11
<i>S K</i>	0	0.00	0.00
<i>S L</i>	1998	---	---
<i>Cl K</i>	189	0.66	0.40
<i>Cl L</i>	0	---	---
<i>K K</i>	2694	12.68	7.00
<i>K L</i>	0	---	---
<b>Total</b>		100.00	100.00

# Hydrolysis

## Hydrolysis 25<sup>0</sup>C

Full scale counts: 2550

25022011\_hydrolysis25

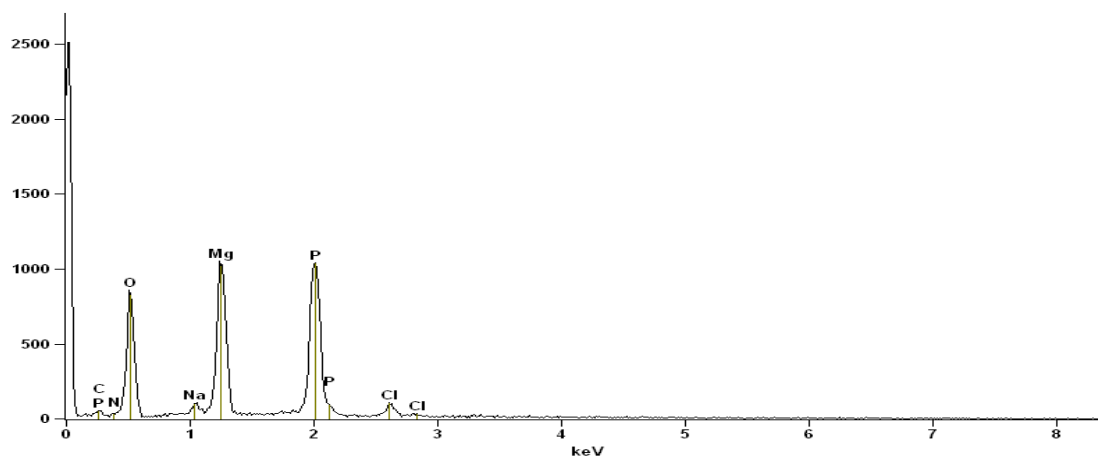


<i>Element Line</i>	<i>Net Counts</i>	<i>Weight %</i>	<i>Atom %</i>
<i>C K</i>	311	2.56	4.36
<i>N K</i>	0	0.00	0.00
<i>O K</i>	10795	44.26	56.49
<i>Mg K</i>	14874	22.86	19.21
<i>P K</i>	17163	29.92	19.73
<i>K K</i>	106	0.39	0.20
<i>K L</i>	0	---	---
<b>Total</b>		100.00	100.00

## Hydrolysis 35<sup>0</sup>C

Full scale counts: 2508

25022011\_hydrolysis35

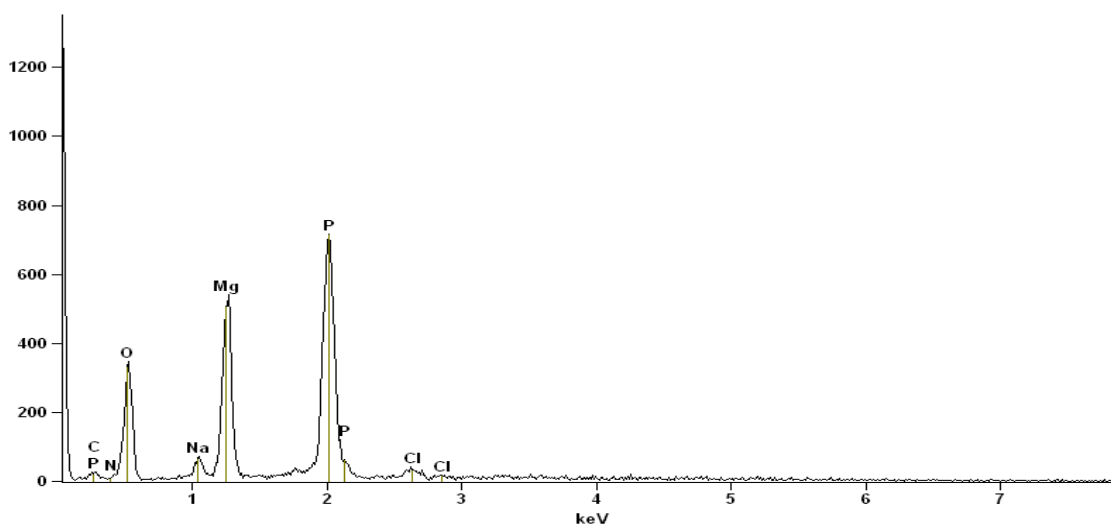


<i>Element Line</i>	<i>Net Counts</i>	<i>Weight %</i>	<i>Atom %</i>
<i>C K</i>	211	2.93	5.10
<i>N K</i>	0	0.00	0.00
<i>O K</i>	6043	40.45	52.80
<i>Na K</i>	407	1.11	1.00
<i>Mg K</i>	9014	21.39	18.38
<i>P K</i>	11480	30.72	20.71
<i>Cl K</i>	799	3.39	2.00
<i>Cl L</i>	7	---	---
<b>Total</b>		100.00	100.00

### Hydrolysis Mg:P=1:2

Full scale counts: 1254

25022011\_hydrolysisMGP1zu2

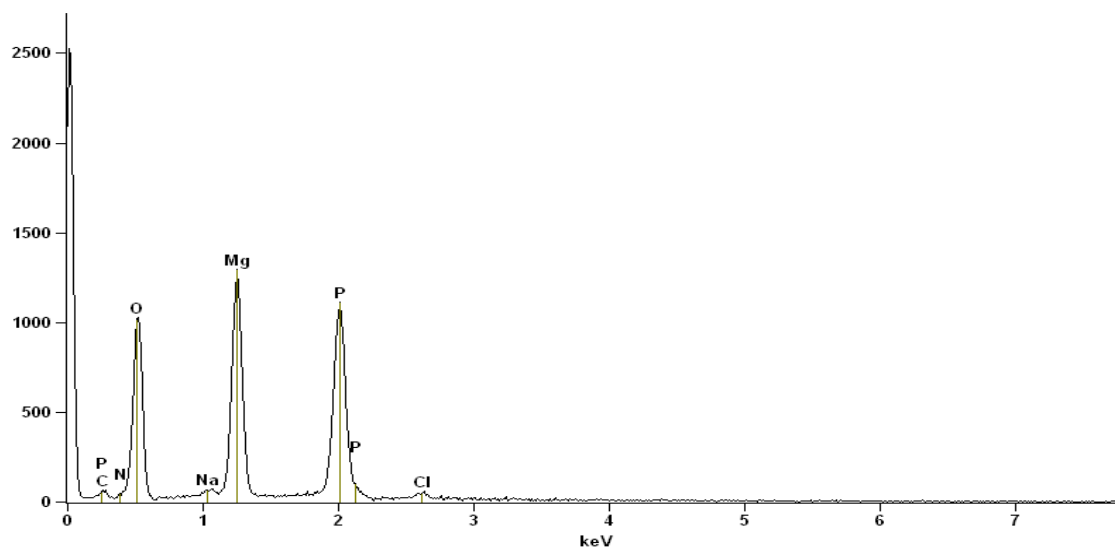


<i>Element Line</i>	<i>Net Counts</i>	<i>Weight %</i>	<i>Atom %</i>
<i>C K</i>	140	4.22	7.65
<i>N K</i>	0	0.00	0.00
<i>O K</i>	2253	31.75	43.18
<i>Na K</i>	472	2.38	2.25
<i>Mg K</i>	4476	20.05	17.94
<i>P K</i>	7647	38.82	27.27
<i>Cl K</i>	338	2.79	1.71
<i>Cl L</i>	0	---	---
<b>Total</b>		100.00	100.00

## Hydrolysis Mg: P=2:1

Full scale counts: 2524

25022011\_hydrolysisMGP2zu1



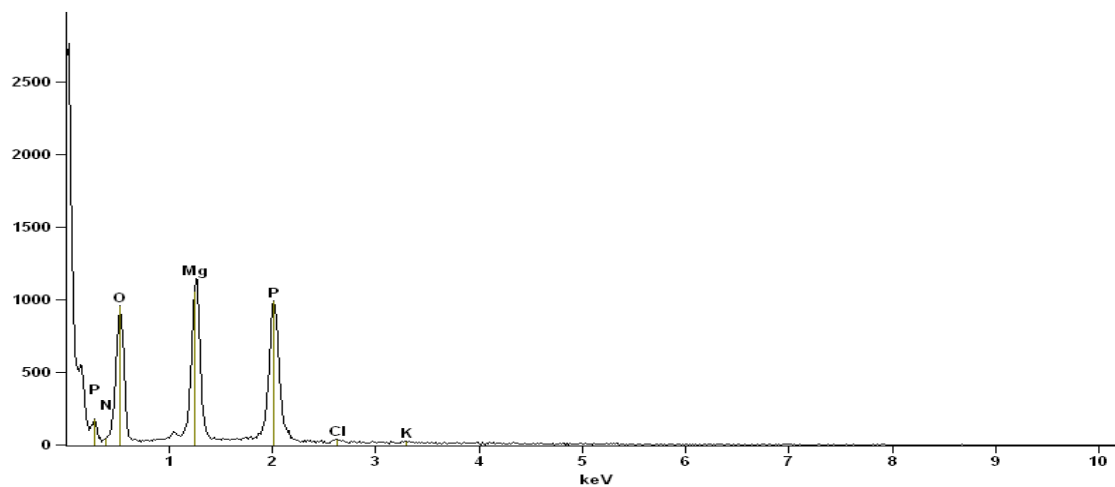
<i>Element Line</i>	<i>Net Counts</i>	<i>Weight %</i>	<i>Atom %</i>
<i>C K</i>	262	3.00	5.11
<i>N K</i>	0	0.00	0.00
<i>O K</i>	7702	43.43	55.45
<i>Na K</i>	242	0.58	0.52
<i>Mg K</i>	10811	22.63	19.02
<i>P K</i>	12213	28.89	19.06
<i>Cl K</i>	390	1.46	0.84
<i>Cl L</i>	0	---	---
<i>Total</i>		100.00	100.00

# Struvite (MAP)

## Struvite 25°C

Full scale counts: 2764

25022011\_map25

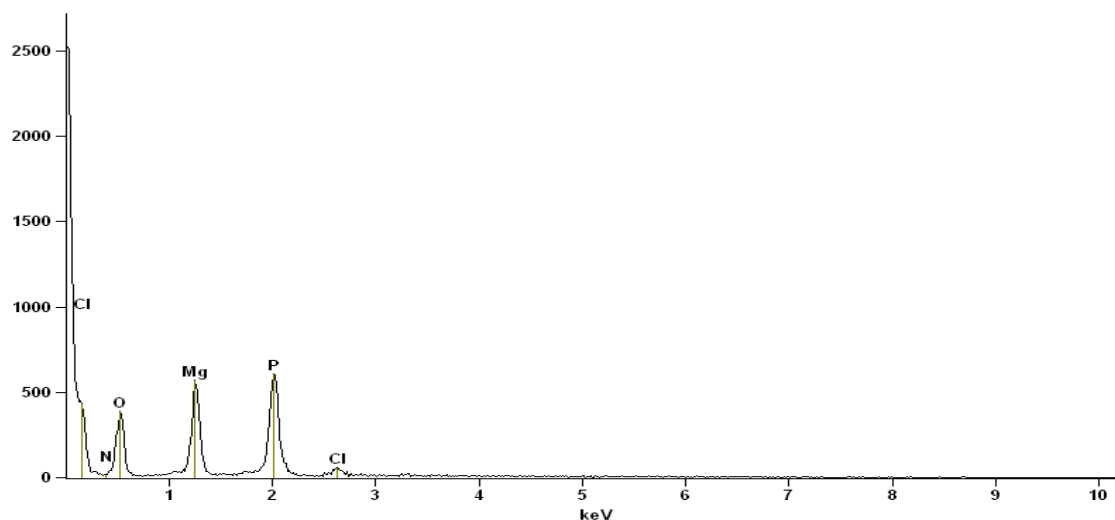


Element Line	Net Counts	Weight %	Atom %
N K	0	0.00	0.00
O K	7665	46.02	59.74
Mg K	9944	22.87	19.54
P K	11463	29.76	19.95
Cl K	201	0.82	0.48
Cl L	0	---	---
K K	97	0.53	0.28
K L	0	---	---
<b>Total</b>		<b>100.00</b>	<b>100.00</b>

## Struvite 35°C

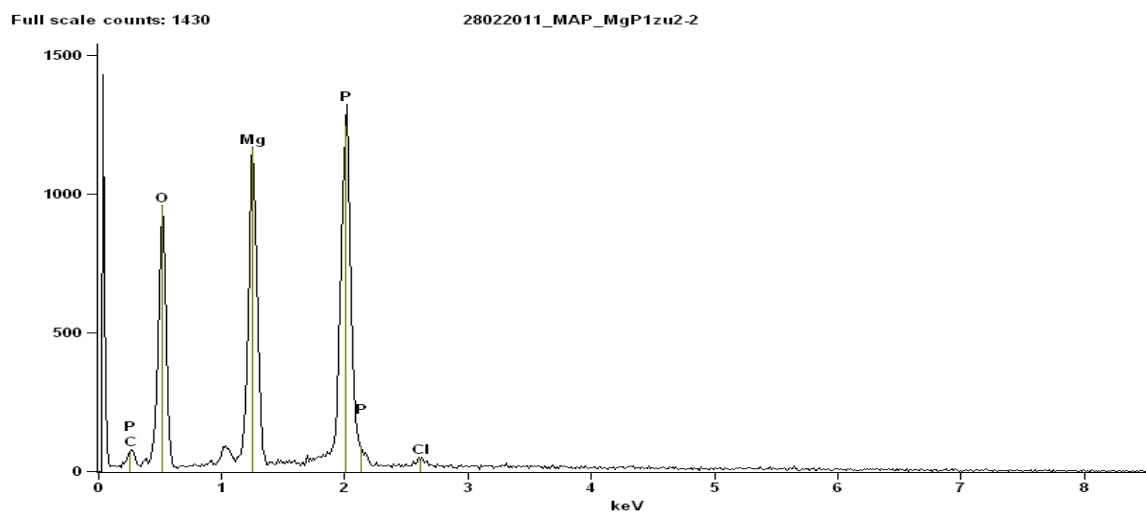
Full scale counts: 2520

25022011\_map35



<i>Element Line</i>	<i>Net Counts</i>	<i>Weight %</i>	<i>Atom %</i>
<i>N K</i>	0	0.00	0.00
<i>O K</i>	3121	39.97	54.25
<i>Mg K</i>	4772	21.18	18.92
<i>P K</i>	6810	34.22	23.99
<i>Cl K</i>	574	4.63	2.83
<i>Cl L</i>	565	---	---
<b>Total</b>		100.00	100.00

### Struvite Mg:P=1:2

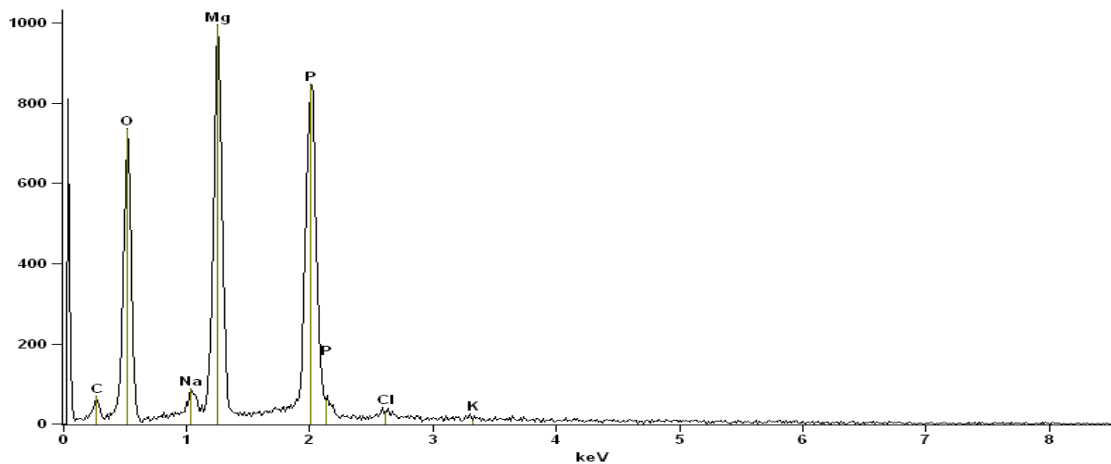


<i>Element Line</i>	<i>Net Counts</i>	<i>Weight %</i>	<i>Atom %</i>
<i>C K</i>	516	6.20	10.41
<i>O K</i>	6632	41.19	51.90
<i>Mg K</i>	9154	19.77	16.40
<i>P K</i>	13081	31.81	20.71
<i>Cl K</i>	263	1.02	0.58
<i>Cl L</i>	0	---	---
<b>Total</b>		100.00	100.00

## Struvite Mg:P=2:1

Full scale counts: 995

28022011\_MAP\_MgP2zu1



<i>Element Line</i>	<i>Net Counts</i>	<i>Weight %</i>	<i>Atom %</i>
<i>C K</i>	389	5.83	9.81
<i>O K</i>	5184	40.58	51.20
<i>Na K</i>	430	1.36	1.20
<i>Mg K</i>	7874	21.82	18.13
<i>P K</i>	9270	28.93	18.86
<i>Cl K</i>	198	0.98	0.56
<i>Cl L</i>	0	---	---
<i>K K</i>	75	0.49	0.25
<i>K L</i>	0	---	---
<i>Total</i>		100.00	100.00

## Untreated Zeolite

Quantitative Results    zeolites pkun raw1			
<i>Element Line</i>	<i>Net Counts</i>	<i>Weight %</i>	<i>Atom %</i>
<i>C K</i>	0	0.00	0.00
<i>O K</i>	7768	31.76	49.25
<i>Na K</i>	404	0.67	0.72
<i>Mg K</i>	367	0.52	0.53
<i>Al K</i>	6445	8.49	7.81
<i>Si K</i>	25349	35.31	31.18
<i>S K</i>	306	0.57	0.44
<i>S L</i>	0	---	---
<i>Cl K</i>	19	0.04	0.03
<i>Cl L</i>	0	---	---
<i>K K</i>	2638	8.02	5.09
<i>K L</i>	0	---	---
<i>Ca K</i>	448	1.64	1.01
<i>Ca L</i>	0	---	---
<i>Fe K</i>	246	6.03	2.68
<i>Fe L</i>	144	---	---
<i>Ba L</i>	641	6.95	1.26
<i>Ba M</i>	0	---	---
<i>Total</i>		100.00	100.00

### Treated zeolite

<i>Element Line</i>	<i>Net Counts</i>	<i>Weight %</i>	<i>Atom %</i>
<i>C K</i>	0	0.00	0.00
<i>O K</i>	11352	43.62	59.35
<i>Na K</i>	500	0.86	0.81
<i>Mg K</i>	591	0.86	0.77
<i>Al K</i>	5890	8.05	6.49
<i>Si K</i>	23788	34.61	26.82
<i>S K</i>	124	0.24	0.17
<i>S L</i>	0	---	---
<i>Cl K</i>	12	0.03	0.02
<i>Cl L</i>	0	---	---
<i>K K</i>	1266	4.12	2.30
<i>K L</i>	0	---	---
<i>Ca K</i>	508	1.99	1.08
<i>Ca L</i>	0	---	---
<i>Fe K</i>	212	5.63	2.19
<i>Fe L</i>	642	---	---
<i>Total</i>		100.00	100.00

